Thermal Regeneration of Metallic Fibrous Particulate Filter

by

Chau Man Wai

A thesis submitted to The Hong Kong Polytechnic University
in accordance with the regulations for the Degree of Master of Philosophy

Department of Mechanical Engineering
The Hong Kong Polytechnic University

2003

Abstract of thesis entitled 'Thermal Regeneration of Metallic Fibrous Particulate Filter'

submitted by Chau Man Wai

for the degree of Master of Philosophy in Mechanical Engineering

at The Hong Kong Polytechnic University in August 2002.

Diesel particulate emitted from diesel vehicles is carcinogenic and a major air pollutant in a big city. The problem can be solved effectively by installing suitable after-treatment devices to the vehicle-tailpipes. A diesel particulate filter using stainless steel fibres as the filtering elements, has been developed by The Hong Kong Polytechnic University for application to light-duty diesel vehicles for such purpose. It has been found to be a very effective device, however, it should be cleaned regularly to recover its usefulness once it has been over-accumulated with particulates. Thermal regeneration, a process to burn off the accumulated particulate, has been suggested to be a possible method to clean up the filter. Literatures on experimental and numerical simulation studies on the thermal regeneration of ceramic wall-flow particulate filter are available, but those on metallic fibrous filter were rare. The present study, which is conducting to fill the gap, contains two integrated parts: an experimental investigation and a numerical simulation study.

In the experimental study, an experimental rig had been designed and built to simulate the regeneration process in the metallic fibrous particulate filter. A gas burner was used to heat up the diluted air to ignite the particulate in the filter. The experimental study involved different configurations of the filter including length of the filter cartridge, and packing densities of the filter element, and different particulate loading conditions. The

effects of different conditions of the heated air mixture including its temperature, oxygen concentration, and volume flow rate were studied. Temperature distributions along the particulate filter before, during and after the regeneration process were measured by twelve K-type thermocouples inserted along the length of the particulate filter. The present experimental study provided very comprehensive data under different operation conditions. It was found that the temperature increased sharply during the regeneration process throughout the entire length of the filter. Thermal regeneration proceeded from the upstream to the downstream regions and excessive heat might accumulate at the downstream region leading to local melting of the filtering element.

A mathematical model had also been developed to simulate the thermal regeneration process of the filter. The model consisted of two parts, with one part concerning with the particulates oxidation in the filter and the other part concerning with the heat transfer processes. The model included the conduction heat transfer within the solid phase, the change in internal energy of the gas and solid phases inside the filter, and the heat released during the oxidation of particulate. The particulate oxidation was controlled by the kinetic reaction rate of oxygen and carbon, thus the particulate consumption rate, which cannot be obtained experimentally, can be simulated and provide insights into the regeneration process. Numerical simulations were performed to obtain the filter temperatures at different locations along the filter at different time steps. The thermal regeneration characteristics with respect to the same parameters of the experimental study had been simulated. It was found that the simulated results were in good agreement with the experimental results with an acceptable degree of deviation. The deviation was small in the heating up and cooling down periods and was relatively large in the heat release period.

A significant contribution of the present study is to achieve a better understanding of the thermal regeneration process of a metallic fibrous particulate filter, which is a very important process to maintain its best performance on a continuous basis.

ACKNOWNLEDGEMENTS

I would like to acknowledge The Hong Kong Polytechnic University for the financial support of this study.

I would like to give my great thanks to those people who gave me advices, ideas, information and support in every stage of this project.

It is a pleasure to me to have Prof. C. W. Leung and Dr. C. S. Cheung to be my chief and co-supervisor of the research project. They have taught me a lot of knowledge relating to the project like Combustion and Heat Transfer. I also learned much skill in thesis writing.

Many thanks are also due to Dr. C. S. Tse in the Combustion and Heat Transfer Laboratory for the technical support and advice.

Last but not least, I would like to thank my parents for their encouragement and steadfast supports in the period of the study.

TABLE OF CONTENTS

LIST OF FIGURES

LIST OF TABLES

NOMENCLATURE

Letter symbols

a_{conv}	specific area for convection, m^{-1}
A	frequency factor, m^3/s-kg
A_c	particulate surface area, m^2
b	number of independent valuables
$c_{p,a}$	specific heat capacity of air, kJ/kg-K
$c_{p,f}$	specific heat capacity of steel fibres, kJ/kg-K
$c_{p,p}$	specific heat capacity of particulate, kJ/kg-K
$c_{p,s}$	specific heat capacity of solid-phase, kJ/kg-K
C	carbon
C_1	constant for equation (5.20)
CO	carbon monoxide
CO_2	carbon dioxide
d	diameter of fibre, m
E	activation energy, kJ/kg-mol
$E(j)$	change in internal energy at the j^{th} zone, kJ
$\dot{E}(j)$	rate of change in internal energy at the j^{th} zone, kJ/s
$E(t)$	instantaneous heat energy released, kJ
E_{total}	total heat energy released during regeneration, kJ
h	average heat-transfer coefficient for flow across cylinders, kW/m^2-^oC
$h_{a,ex}$	enthalpy of air at the outlet, kJ/kg

$h_{a,in}$	enthalpy of air at the inlet end, kJ/kg
$h_{a(i,j)}$	enthalpy of air at the i^{th} time-step and the j^{th} zone, kJ/kg
h_{conv}	convective heat transfer coefficient, kW/m^2-^{o}C
h_w	wall heat transfer coefficient, kW/m^2-^{o}C
$h(T_{a,in})_{exp}$	enthalpy of air according to the experimental inlet air temperature, kJ/kg
H	half of the channel height, m
H_2	hydrogen
H_2O	water
$\dot{H}_{comb}$	rate of heat released due to combustion of the particulate, kJ/s
$\dot{H}_{comb,j}$	rate of heat released due to combustion of particulate at the j^{th} zone, kJ/s
i	i^{th} time-step
j	j^{th} zone
k_f	thermal conductivity of air at film temperature, kW/m-^{o}C
$k_{f,eff}$	effective fluid conductivity, kW/mK
k_s	conductivity of stainless steel fibre, kW/m-^{o}C
K	rate coefficient, 1/s
K_h	hydrodynamic factor
m_a	mass of air inside the filter, kg
m_{aj}	mass of air at the j^{th} zone, kg
$\dot{m}_a$	mean value of $\dot{m}_{a,in}$ and $\dot{m}_{a,ex}$, kg/s
$\dot{m}_{a,ex}$	mass flow rate of air at the outlet of the filter, kg/s
$\dot{m}_{a,in}$	mass flow rate of air at the inlet of the filter, kg/s

m_c	mass of carbon, g
m_f	mass of stainless steel fibre, kg
m_{fj}	mass of stainless steel fibre at the j^{th} zone, kg
$m_{filter,c}$	mass of a filter after filtration, kg
$m_{filter,o}$	mass of a filter after regeneration, kg
$m_{filter,i}$	mass of a filter before filtration, kg
m_p	mass of particulate in a zone, kg
m_{pj}	mass of particulate at the j^{th} zone, kg
m_{p0}	initial mass of particulate in the filter, kg
$m_{p(0,j)}$	initial mass of particulate in any zone, kg
$\dot{m}_p$	rate of oxidation of diesel particulate, kg/s
$\dot{m}_{p,(j)}$	rate of oxidation of diesel particulate at the j^{th} zone, kg/s
M	a calculated value
M_p	total mass of particulate in a entire filter, kg
n	number of zones of a filter
Nu	Nusselt number
Nu_f	Nusselt number of air at film temperature
O_2	oxygen
p	constant for equation (5.20)
P_{Ox}	oxygen partial pressure, atm
Pe	Peclet number
Pr_f	Prandlt number of air at film temperature

q	reaction order with respect to oxygen
$q_{a,ex}$	volume flow rate of air at the outlet of the filter, m^3/s
$q_{a,in}$	volume flow rate of air at the inlet of the filter, m^3/s
R	reaction rate, 1/s
R_u	universal gas constant, 8.314 kJ/kgmole-K
Re_f	Reynolds number of air at film temperature base on diameter of cylinder
R_{inter}	interception parameter
Stk	Stokes number
t	time, s
T	temperature of filter, °C
$T_{(i,j)}$	temperature of filter at the i^{th} time-step and the j^{th} zone, °C
$T_{(i)}$	temperature of filter at the i^{th} time-step, °C
$T_{(0,j)}$	initial temperature of filter at any zone, °C
T_a	temperature of air, °C
T_{aj}	local temperature of air at the j^{th} zone, °C
T_{fj}	local temperature of stainless steel fibre at the j^{th} zone, °C
T_f	temperature of stainless steel fibre at the j^{th} zone, °C
$T_{in,air}$	temperature of inlet hot air, °C
T_j	local temperature of the filter at the j^{th} zone, °C
T_{pj}	local temperature of particulate at the j^{th} zone, °C
T_s	temperature of solid-phase, °C
$\overline{T_a}$	mean temperature of the air inside the filter, °C

$\overline{T_f}$	mean temperature of the stainless steel fibre inside the filter, °C
$\overline{T_p}$	mean temperature of the particulate inside the filter, °C
u_a	velocity of air, m/s
u_∞	free stream velocity of air, m/s
U	calorific value of carbon particle, kJ/kg
v_{filter}	volume of a discrete zone of a filter, m^3
V_{filter}	volume of the entire filter, m^3
w_b	estimated uncertainty of the independent variable b, %
$w_{\dot{H}_{comb}}$	estimated uncertainty of the rate of heat release due to combustion, %
w_i	estimated uncertainty of the independent variable i, %
$w_{\dot{m}_{a,in}}$	estimated uncertainty of the mass flow rate of air at inlet end, %
$w_{\dot{m}_{a,ex}}$	estimated uncertainty of the mass flow rate of air at outlet end, %
w_{m_f}	estimated uncertainty of the mass of stainless steel fibre, %
w_{m_p}	estimated uncertainty of the mass of particulate, %
$w_{q_{a,in}}$	estimated uncertainty of the volume flow rate of air at inlet end, %
$w_{q_{a,ex}}$	estimated uncertainty of the volume flow rate of air at outlet end, %
w_M	estimated uncertainty of the calculated value, %
$w_{\frac{\partial T}{\partial t}}$	estimated uncertainty of the rate of change of temperature, %
x	axial displacement, m
y_b	b^{th} independent variable
y_i	i^{th} independent variable

Greek symbols

α	packing density of the filter matrix, %
Δx	thickness of a zone, m
Δt	duration of a time-step, s
Δh_a	change in enthalpy of air, kJ/kg
η_{diff}	single-fibre efficiency due to diffusion, %
η_{inter}	single-fibre efficiency due to interception, %
η_{imp}	single-fibre efficiency due to impaction, %
η_{reg}	regeneration efficiency, %
η_{sf}	single-fibre efficiency, %
ν_f	kinematic viscosity of air at film temperature, m^2/s
ρ_a	density of air, kg/m^3
$\rho_{a,ex}$	density of air at the outlet end, kg/m^3
$\rho_{a,in}$	density of air at the inlet end, kg/m^3
ρ_f	density of stainless steel fibre, kg/m^3
ρ_{O_2}	density of oxygen, kg/m^3
ρ_s	bulk density of solid-phase, kg/m^3
ϕ	porosity of the filter matrix, %

Others

$[O_2]$	volume concentration of oxygen, %
$[O_2]_{(i,1)}$	volume concentration of oxygen at the first zone at any time, %

$[O_2]_{input\ value}$	input value of volume concentration of oxygen, %
$[O_2]'$	molar concentration of oxygen, kmol/kg

CHAPTER 1 INTRODUCTION

1.1 Emissions from motor vehicles

Outdoor air quality is becoming worse nowadays in many big cities over the world mainly due to emissions from motor vehicles, Hong Kong is no exception. Major pollutants emitted from motor vehicles can be classified in two main categories: gaseous pollutants and solid pollutants. The gaseous pollutants contain mainly carbon monoxide (CO), nitrogen oxides (NO_x) and unburned hydrocarbon (HC) whereas the solid pollutants are essentially particulate matters. Vehicular pollutants are harmful, in particular particulate matters emitted from diesel vehicles are considered carcinogenic. Hence vehicular emissions are regulated. New vehicles are required to meet increasingly stringent emissions standards. Stringent controls are also exercised on emissions from existing vehicles. There are different approaches in reducing emissions from existing vehicles, which include the application of after-treatment devices.

In Hong Kong there are about 500,000 motor vehicles of which about 155,000 are diesel vehicles. Commencing from 1992, all petrol vehicles imported into Hong Kong are installed with three-way catalytic converter. Since then, emissions from petrol vehicles are considered to be under control and the government has been concentrating in reducing emissions from diesel vehicles. Diesel vehicles are widely used as commercial vehicles in Hong Kong because of the higher thermal efficiency of a diesel engine and the much lower fuel price in comparison with petrol. These include the taxis, buses, the lorries, the trucks, the container tractors, the mini-buses and the vans. The

diesel vehicles are the major emitter of particulate matters and nitrogen oxides, both of which are major air pollutants in Hong Kong.

There is an urgent need to control the emission of pollutants, especially those from diesel vehicles. On the one hand, they are running very close to people in the urban area. On the other hand, they are representing 30% of the motor vehicle population and accounting for 70% of all vehicle kilometers travelled each year; and have been identified to be more polluting. Among the various pollutants, particulate matters have more direct impact on human health. They are causing 400 premature deaths every year as estimated by the Hong Kong Government in 1995 [1]. In order to reduce the level of particulate emissions from the diesel vehicles, different strategies have been applied. For example, there is an encouragement of the diesel taxis to be replaced with the LPG taxis. There is also intension to retrofit all pre-Euro diesel vehicles with some form of exhaust gas after-treatment devices, such as oxidation catalyst and pa
Moreover, ultra-low sulphur diesel with a sulphur content of less than 50 ppm by weight of sulphur is available in the market since 2000.

Particulate matters emitted from diesel vehicles are generated during the combustion process inside the diesel engines. Diesel particulate matters are composed of three constituents, namely: soot, the Soluble Organic Fraction (SOF), and oxides. The soot is carbonaceous material, which results from incomplete combustion of mainly fuel and, to a lesser extent, lubricating oil. It is essentially carbon and gives the black smoke in the exhaust gas. The SOF is basically unburned hydrocarbons from the lube oil and fuel, with the lube oil being the dominant portion. The oxide portion is mainly the sulphate with associated water primarily derived from the sulphur in the fuel.

Based on the composition of diesel particulates as stated above, different strategies can be applied in reducing diesel particulates. Alternative fuels such as LPG can eliminate diesel particulates totally but its application at the present moment is limited to the taxis and mini-buses. Ultra low sulphur diesel fuel can be applied to all diesel vehicles but it can reduce mainly the sulphate portion of the particulates. Oxidation catalysts are known to be able to reduce diesel particulate through the oxidation of the SOF portion of the particulate. The capability is limited by the percentage of SOF in the particulate and the duty cycle of the vehicle because the level of oxidation is temperature dependent. There is controversy on the effectiveness of oxidation catalyst in reducing the number density of particulate emission since the carbon core of the particulate is not affected during the oxidation process. High quality particulate traps, including the Continuous Regeneration Traps (CRT), are available nowadays. The traps can reduce over 90% of the diesel particulate emitted. However, there are limitations on their applications. Vehicles retrofitted with high quality particulate traps are required to operate on duty cycles involving sufficiently high exhaust gas temperature for certain period of time for the particulate trapped to be oxidized. There is also reservation of retrofitting such traps to vehicles which are burning motor oil fearing contamination and hence damage to the traps. For CRT, there is strict limitation on fuel sulphur content. Hence there is a need to fill in some of these limitations, in particularly for aged vehicles.

1.2 The metallic fibrous filters

Metallic fibre was one of the earliest materials studied for filtering diesel particulate [2,3]. Due to the development of the wall flow ceramic particulate trap, little attention was given to the fibrous filters for application to diesel vehicles subsequently. The

fibrous filter, in comparison with the oxidation catalyst, is able to reduce the number of diesel particles emitted by the motor vehicle. In comparison with the high performance particulate trap, its performance is not affected by the duty cycle and working conditions of the motor vehicle, nor the fuel sulphur content. Hence, there is justification for application to the aged vehicles burning diesel fuel with high sulphur content.

A serviceable metallic fibrous particulate filter using stainless steel fibre as filtering materials has been developed by The Hong Kong Polytechnic University [4-6]. It has been identified by the government as a favourable choice for reducing particulate emissions from the light duty diesel vehicles. One of the major attractions of the fibrous filter is its low cost while one of the major drawbacks is its requirement of regular service. Figure 1.1 shows the metallic fibrous filter installed on a taxi. Details of the metallic fibrous particulate filter will be presented in Chapter 3.

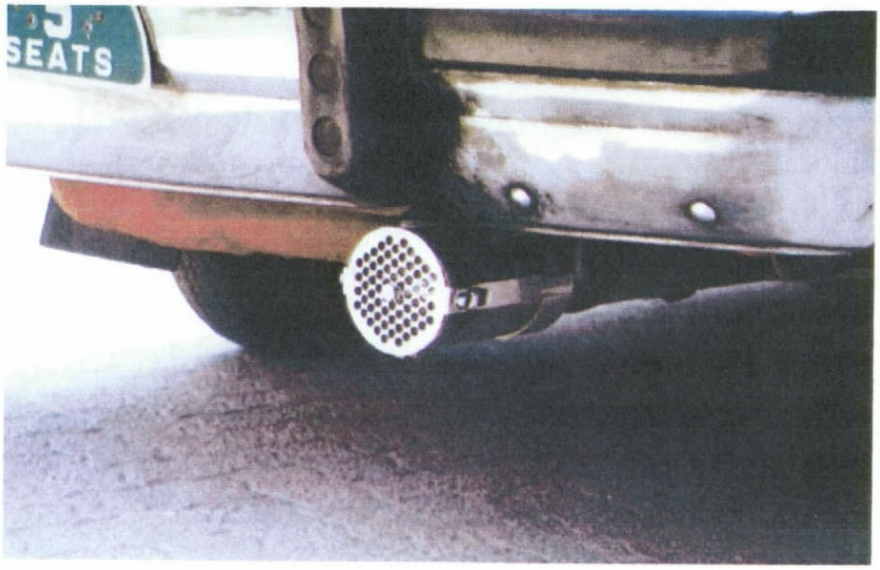

Figure 1.1 A taxi retrofitted with a metallic fibrous particulate filter

1.3 Servicing the metallic fibrous filters

Particulate filters are installed at the tailpipe of a diesel vehicle. When the filter is accumulated with diesel particulates, the engine will encounter an increase in backpressure and hence additional fuel consumption. In worst cases, the particulate will burn spontaneously causing damage to the filter. The filter should therefore be cleaned or regenerated regularly in order to retain its filtering efficiency and reduce fuel penalty. In-situ cleaning of the particulate filter is a challenging problem. The particulates are loosely attached to the stainless steel fibre and may be detached by mechanical means such as blowing with pressurized air, flushing with water or shaking manually. When blown with pressurized air, there is difficulty in handling the particulate laden air thus generated. When flushed with water, the wastewater produced will generate another pollution problem. The shaking method will also create an unhealthy atmosphere laden with loose particulate [1]. As an alternative, thermal regeneration process, which has been applied to ceramic particulate traps, may be a better way to tackle the problem.

1.4 Thermal regeneration of a particulate filter

Thermal regeneration is a process that requires external heat and sufficient oxygen supplies, to initiate combustion of the accumulated diesel particulates. The normal regeneration temperature for diesel particulates is about 500°C. Regeneration processes can be classified into three categories: catalytic regeneration, aerodynamic regeneration and thermal regeneration. The former is a passive process whereas the other two are active processes. Passive regeneration normally requires the involvement of catalyst or additive, which is either added in the diesel fuel or directly on the surface of the substrate of the particulate filter so that it finally reaches the particulates. The addition of catalyst or additive will lower the ignition temperature of the particulates by 200°C to

300°C. As a result, the particulates can be burnt under normal driving conditions. Active systems require continuous monitoring on the building up of particulates inside the filter. The control system will periodically activate some special processes to supply additional heat by means of a diesel burner or an electric heater. Active system is relatively more complex and expensive so that fewer studies have been made [7]. Many studies have been conducted on the regeneration of ceramic particulate trap while little conducted on fibrous filters. The present study is therefore conducted to fill this gap.

1.5 Objectives of study

The importance of studying thermal regeneration of a fibrous filter has been discussed. The present work concentrates on understanding the oxidation of particulates inside a fibrous media and how it is affected by several important parameters. The oxidation of particulate is reflected by a change in temperatures inside the filter and the effects of the parameters are reflected by the change of these temperatures.

There are several parameters affecting the oxidation of particulates, and consequently contributing to the performance of the regeneration of a fibrous particulate filter. Oxidation of particulates in a fibrous filter occurs when the temperature and hence the energy level inside the filter is high enough, as well as the mass transfer rate of particulates and supply of oxygen are also high. These conditions can usually be achieved when external fuel and air supplies for regeneration are sufficiently high. However, these favourable conditions may results in an uncontrolled rate of spontaneous combustion, leading damage of the fibrous filter, when they become excessive. It is important to maintain a steady regeneration so as to reduce the risk of

possible global or local overheating and subsequently damage to the stainless steel fibres. With a better understanding of the ignition and subsequent burning of the particulates, it is possible to control the rate of such spontaneous combustion. Hence, an experimental investigation will be carried out to study how thermal regeneration is affected by the factors mentioned above.

In addition to the experimental investigation, a numerical model for simulation of the thermal regeneration was also developed. Numerical modeling of thermal regeneration of a fibrous filter is very complicated since the fibrous filter is a porous media. In order to numerically simulate the temperatures inside the filter and the particulate burning rate, a model will be established to calculate the thermal regeneration of a fibrous filter and the predictions will be compared with experimental results.

In the fibrous filter being investigated, the stainless steel fibres are loosely packed with diesel particulates sticking unevenly on the surface of the fibres. There is a need to model the burning rate of the particulate and the subsequent transfer of energy to the gas and the stainless steel fibres. The former governs the rate of energy released during the regeneration process while the latter governs how fast such energy is dispersed. The mathematical descriptions of the above processes result in a system of differential equations, which need to be solved numerically.

The objectives of the present study can therefore be summarized as follow:

1. To build a test rig for thermal regeneration of diesel particulate in a metallic fibrous filter. The test rig allows thermal regeneration to be carried out and the important parameters affecting the process to be controlled and measured.

2. To investigate experimentally the effects on thermal regeneration of flow rate and oxygen concentration of the hot air supply, particulate loading, fibre packing density and thickness of filtering element of the filter.

3. To establish a numerical model, with the aid of the equations of energy conservation and particulate oxidation, to simulate the regeneration temperature profile of the filter.

1.6 Layout of the thesis

Some backgrounds to achieve a basic understanding of the problem are provided in Chapter 1, together with the objectives of the present study. In Chapter 2, review of the relevant literatures will be presented which provides a better picture of the thermal regeneration process in the fibrous filters, as well as related studies being conducted so far. Design, construction and operation principle of the fibrous particulate filter for the present study will be given in Chapter 3. Experimental investigations conducted to fulfill the first and second objectives of the present study will be presented in Chapter 4, together with an error analysis of the experimental results. Development and application of the numerical model to simulate the oxidation of particulate in a fibrous filter and the temperature profile of thermal regeneration are provided in Chapter 5. The basic assumptions and major difficulties in developing the numerical model will also be discussed. In Chapter 6, a detail comparison between the present experimental and

numerical studies will be provided. Finally, Chapter 7 concludes what have been achieved in the present study.

CHAPTER 2 LITERATURE SURVEY

2.1 Introduction

A particulate filter consists of a filter positioned in the exhaust stream of a diesel vehicle for collecting a portion of the particulate emitted by the engine while allowing the exhaust gas to pass through. The filter material used includes ceramic monoliths, woven fibers, woven silica fiber coils, ceramic foam, wire mesh, sintered metal, etc.. with ceramic monoliths being the most commonly used. The particulate matter generated by a diesel engine will fill up and plug a filter gradually, and hence need to be disposed periodically or even continuously. The process is known as regeneration. A number of techniques have been developed to facilitate regeneration of particulate filters. Regeneration can either be active or passive [7]. For active regeneration, external means are required. In case of passive regeneration, external means are not required.

The current study is concerned with the thermal regeneration of metallic fibrous filter. The temperature profiles with respect to time and space, the regeneration phenomenon and effects of some important parameters affecting the regeneration process will be studied experimentally. In addition, a numerical model will be developed to predict the thermal regeneration of particulate in the filter. So the literature review will concentrate on related experimental studies and modelling of the thermal regeneration of particulate filters.

2.2 Single particle combustion

Diesel particulates are agglomeration of particles. Several studies had been made on the investigation of single particle combustion mechanisms. Ranajit et al. [8] investigated single particle combustion with char particles of size in the range of 50-100μm, which were derived from lignite and bituminous coals. The transient temperature profile was obtained experimentally. Apparent combustion rate of char particles had been derived from a model of single particle combustion. Using that model, a good agreement had been obtained between calculated and experimental temperature-time traces. Fedotov and Tre'Yakov [9] carried out similar work on the stochastic ignition of single particle. Fu and Yan [10] deduced the ignition temperature and ignition delay for a carbon/char particle theoretically and compared with the experimental results. These studies provide a good foundation from basic to advanced single combustion mechanisms of the normal carbon or char particle. The oxidation of diesel particulate inside a particulate filter should be rather different and complicated because the particles form agglomerates and the particles are not purely carbon.

2.3 Regeneration of particulate filters

Regeneration of particulate filters can be classified into three categories: catalytic regeneration, aerodynamic regeneration and thermal regeneration.

2.3.1 Catalytic regeneration

Many studies had been performed on the catalytic regeneration of diesel particulate filters. Catalytic regeneration means that the oxidation of soot is catalyzed by the presence of catalysts such as cerium or lead sulphate.

Noirot et al.[11] studied the post-combustion of carbon black, and the diesel soots were collected on catalyzed monolith particulate filters at a laboratory scale. The important parameters, including entering gas temperature, catalytic and additive formulations, had been investigated. The oxidation of soot particulate could be started at a very low entering gas temperature of 150°C by injecting hydrocarbon inside the catalyzed filters. The regeneration peak temperature was controlled by interrupting the hydrocarbon injection at certain temperature.

Zhang et al.[12] conducted a kinetic analysis on the catalytic oxidation process of diesel particulates by using the thermo-gravimetric analysis (TGA) technique. Different combinations of four different catalysts, namely, Cu, Mn, Pd and Pt, had been tested on the effect of activation energy and ignition temperature. The oxidation of soot with the catalyst consisting of all these metals required relatively low activation energy and ignition temperature.

Mayer et al.[13] carried out tests with knitted fiber diesel particulate filters which were catalyst coated. In these tests, the deposition of soot was uniform in order to avoid local heating during regeneration. The results showed that the catalytic coating was capable to lower the regeneration temperature by 200°C and the burn-off temperature by 350°C. It was concluded that catalytic coating was effective for substantially reducing the regeneration energy requirement.

Hawker et al.[14] reported an alternative approach, in which a continuous low-temperature chemical reaction mechanism was employed. The system consisted of a special oxidation catalyst upstream of a particulate filter. Some NO emitted from the

engine was oxidized to NO_2, which was active for the continuous oxidation of soot collected in the filter above 250°C. As the result of the continuous regeneration, soot loading and the backpressure of the filter could be kept at an acceptable condition.

However, such catalytic oxidation usually shows a limitation that the fuel used in the diesel engine should contain no more than 10ppm of sulphur, which is still very expensive in the market.

Many studies of catalytic oxidation had been carried out with fuel additives, especially the cerium-based fuel additives. Peterson [15] reported a study on the oxidation of soot emitted from an internal combustion engine operating with leaded fuel. The lead particles was found to present at discrete locations in the particulates, and the size range of the quasi-spherical carbon particles in the particulates was not affected by the presence of lead during combustion. In addition, the catalytic oxidation could be kinetically controlled. Two types of oxidation processes, slow and fast, were reported. The oxidation was found to occur at a temperature around 500°C in both oxidation processes. Lepperhoff et al.[16] investigated the performance of a catalyst added with a cerium-based fuel additive in relation to regeneration quality, filtration efficiency, particle size distribution and fate of additive of a particulate filter under steady-state engine operation condition. They compared the effectiveness of cerium-based fuel additive with those of copper-based fuel additive and ferrocene-based fuel additive respectively. The cerium-based fuel additive was suggested to be the best choice as it could lower the ignition temperature to 200°C, thus quasi-continuous and smooth regenerations could occur in that temperature range. Pattas et al.[17] performed tests on the performance of a cellular ceramic diesel particulate filter on a light-duty truck with

the use of cerium-based fuel additive in various concentrations. They reported that regeneration could be initiated at exhaust gas temperature of as low as 300°C with a cerium-based fuel additive of concentration of 50 to 100ppm by weight.

Tan et al.[18] carried out tests to study the regeneration process in ceramic (Cordierite) monolith filter using a copper-based fuel additive. The various conditions leading to regeneration failure were identified. They found that copper-based fuel additive was able to lower the filter regeneration temperature from 500°C to 375°C approximately and shorten the regeneration time. A model showing the pressure drop across the filter due to the ceramic wall and particulate layer was developed using the one-dimensional Darcy's law, and correlated well with the experimental results. Koltsakis and Stamatelos [19] established a zero-dimensional mathematical model to simulate the effect of fuel additive on the regeneration of a ceramic wall-flow monolithic diesel particulate filter. The proposed mechanism was based on a dynamic oxygen storage/release model of the metal oxides accumulated in the filter, and was applicable to most types of fuel additive. Results obtained from full scale experiments were employed in the process of model development and evaluation. They modified the zero-dimensional model [20] to a one-dimensional model, and the new model was extended to predict the spatial propagation of the regeneration front and its dependence on reactor design, process conditions and catalyst dosimetry. Zelenka et al.[21] reported a study of the application of a sintered metal filter whose regeneration was supported by the use of a cerium-based fuel-borne catalyst on a delivery van, which was equipped with a conventional IDI diesel engine. The test showed that the catalyst was able to lower the ignition temperature of soot from 600°C to 400°C approximately or even 300°C, which was very close to the exhaust gas temperature. Stanmore et al.[22] carried out tests to

study the ignition and combustion mechanism of cerium-doped diesel soot. The presence of cerium gave a large increase in the kinetic rate constants but the activation energy was unchanged. They also noticed that the effectiveness of the catalyst was declining at temperature above 600°C. A simple combustion and heat transfer model had been built to predict ignition temperatures.

The literatures available for catalytic regeneration are usually concerned with the ceramic monolith filters, whereas there are no related investigations for the fibrous particulate filter.

2.3.2 Aerodynamic regeneration

One kind of active approach is the aerodynamic regeneration which requires a periodic injection of high pressure pulses of air in a direction opposite to the exhaust flow. Ichikawa et al.[23] studied the regeneration efficiency improvement of a reverse pulse air regenerating system under low exhaust gas temperature condition. They found that the modification of the system could be made by maximizing the pressure increase in the filter channel. In their study, better regeneration efficiency was obtained at high aspect ratio between diameter and length of the filter channel. Romero-Lopez et al.[24] reported a new hardware, which was a catalyzed wall-flow ceramic filter equipped with diesel exhaust flow and inverse regenerating flow. The new hardware had an advantage of simpler and economical control. The employment of catalyst greatly reduced the regeneration temperature from 700°C to 450°C, therefore ceramic could be used as the filter material. Mathematical models describing the filtering process, the pressure across the filter and regeneration process were also presented.

Larsen and Levendis [25] tested the filtration efficiency, the post filtration particulate size distribution and the aerodynamic regeneration efficiency of two SiC monolith, one with catalyst coating and one coated with cordierite monolith. The uncoated SiC monolith was suggested to perform better in all tests. Konstandopoulos and Kostoglou [26] established a mathematical model on the reverse flow regenerator and validated the predictions against experimental results for the regeneration of a monolith filter. The numerical results confirmed the success on capability of the new technique. However, the available literatures for aerodynamic regeneration are also concentrated on the monolith filter and there are none on the fibrous filter.

2.3.3 Thermal regeneration

Thermal regeneration is the process that requires external heat and sufficient oxygen supplies to initiate the combustion of particulates accumulated inside the filtering element. The external heat energy can be supplied by a fuel burner or an electric heater [7].

2.3.3.1 Experimental studies of thermal regeneration

Shadman [27] analyzed the effects of operating conditions on the regeneration kinetics of a wall-flow surface filter both experimentally and theoretically. The total regeneration time was found to increase with the initial soot loading at high temperature but insensitive to this loading at low temperature due to the two different burning mechanisms, namely, uniform burning and surface burning. Obuchi et al.[28] performed the control of thermal regeneration of a cylindrical , wall-flow type, ceramic honeycomb monolith particulate filter with a monitoring device. The main function of the device was to monitor the internal thermal radiation of an optically transparent rod probe at its

end. In their study, a stable regeneration process was achieved by controlling the flow rate of air needed for combustion. Effects of other parameters on the thermal regeneration had not been reported.

Hoj et al.[29] investigated experimentally the thermal loading of a regeneration process of an uncoated SiC filter and a cordierite filters. The high thermal inertia of the SiC filter reduced the effect of thermal loading during severe regeneration thus restricting the peak temperature to only fraction of the peak temperature of the cordierite filter. It was useful in reducing the risk of unrestricted regeneration, but on the other hand, lowering the probability of complete regeneration. A model used for interpretation of the observed temperature-time distribution at different locations in the filter had also been established. It also indicated a very board progressing reaction zone, which was extending to almost the whole filter length.

Okazoe et al.[30] performed a field test for the development of a SiC filter and a full-flow type burner. The filter was found to crack when the peak temperature during regeneration exceeded 900°C. The peak temperature could be suppressed to below 900°C by setting the maximum tolerable amount of collected particulate mass before regeneration to 50g, and controlling the burner in order to raise the temperature slowly up to the required value. Kim et al.[31-32] investigated the effects of the regeneration parameters such as inlet gas temperature, space velocity, oxygen concentrations in the exhaust gas and initial particulate loading on the oxidation of a ceramic cordierite filter experimentally. They found that the inlet gas temperature should be maintained at least at 700°C in low oxygen concentration condition to facilitate regeneration. They developed a two-stage regeneration scheme which was applicable to a wide range of

engine operating conditions. They had also described a method to control the combustion rate of the ceramic cordierite particulate filters during thermal regeneration. Lower temperature gas entrained into the filter during thermal regeneration led to a lower peak temperature, and it could be achieved by controlling the flow rate of engine exhaust gas. Theoretical study of the thermal regeneration mechanism was also performed.

However, there are no related studies on the fibrous filter.

2.3.3.2 Modelling of thermal regeneration

Garner and Dent [33] developed a generalized model describing oxidation in a porous substance and applied to the thermal regeneration of both monolith and fibrous diesel particulate filters. The regeneration processes with typical engine operating conditions in both types of filters were analysed with this model. A parametric study had been conducted to demonstrate the effects of exhaust gas oxygen concentration and flow rate, initial filter particulate loading on the regeneration time and peak temperature. The model on monolith filter was shown to be in good agreement with published experimental results while experimental data were not available for validation of the model for the fibrous filter.

Wang et al.[34] proposed a mathematical model of the thermal regeneration process for diesel particulate filter with ceramic foam element. The model could be used to estimate the regeneration parameters including oxidation rate of deposited soot particulates, regeneration peak temperature, inlet gas flow rate and temperature, and initial soot

loading. Experimental work had been carried out to verify the accuracy of the model, and the predicted results showed good agreement with the experimental results.

Opris and Johnson [35] developed a 2-dimensional CFD model to describe the heat transfer characteristics in a honeycomb structured ceramic diesel particulate filter. The model was capable to describe the steady-state and transient flow and heat transfer characteristics during the regeneration process. The effect of filter material properties on the filter regeneration behaviour was studied with and without a copper-based fuel additive, for both controlled and uncontrolled regeneration tests. The model indicated that the regeneration time for a SiC filter was twice of that of the cordierite filter. In addition, the regeneration rate was highly dependent on the local exhaust gas temperature. Gadde and Johnson [36] developed a model for calculating the filter pressure, various particulate properties, filtration characteristics and filter temperature using the theory originated by Opris and Johnson [35]. The model was validated with the results obtained from the steady-state cycles operating with an SiC diesel particulate filter. A sub-model describing the oxidation of collected particulates was established with the addition of catalyst.

Konstandopoulos et al.[37] extended a previously developed 1-dimensional perimeter-average model for prediction of the flow behaviour of diesel particulate filter to include the non-Darcian flow effect and permeable wall plugs. The extended model was used on the design and selection of the wall flow diesel particulate filter, regarding the sizing for the application in the CRT^{TM} system. Predictions from the extended model were validated against a 3-dimensional CFD simulations and experimental results.

Despite of the various models available, the thermal regeneration model on fibrous filter developed by Garner and Dent [33] is the only one available in literature for application to fibrous filters.

2.3.3.3 Electric regeneration

Thermal regeneration of diesel particulate filter, with the aid of an electric heater, has also been widely studied. Kojetin and Kittelson [38] developed a mathematical model to simulate systematically the operation of an electric regeneration diesel particulate filter. The model was used to predict the regeneration performance of a ceramic wall flow filter on an urban bus in terms of regeneration interval, average backpressure, fuel economy penalty and backpressure variation. Comparison between the predicted values with experimental results had also been made. Shirk et al.[39] studied the performance and durability of the electrically regenerable diesel particulate filter in an engine test with hydraulic loading under both steady-state and transient operating conditions. The filter cartridge consisted of a unique tubular heater wrapped with ceramic fiber. They found that the regenerating process required only very low attention, and was effective and stable with low electric power consumption and short regeneration time. Kazushige et al.[40] developed a heater type automatic regeneration system for a SiC diesel particulate filter, which could be mounted on an automobile. In order to apply the system to wider applications, they had performed studies on electric power consumption of the regeneration, pressure drop of the filter and improvement of axial insulation.

Electrical regeneration depends a lot on the physical contact between the heating element and the filter material for proper heating transfer. It does not seem to be applicable to fibrous filters.

2.4 Summary on literature review

Many researchers have made good efforts to study experimentally or to develop models of the thermal regeneration of various kinds of particulate filter, which are fabricated from different materials, with and without the use of catalyst. However, very little attention has been paid on the investigation of the thermal regeneration of metallic fibrous diesel particulate filter, which is much simple in structure and low in cost. So far as thermal regeneration of metallic fibrous filter is concerned, there is lack of systematic experimental study, while there is only one published model which has not been validated. Hence, this study will fill in the gap by performing a systematic experimental study on the effect of different operational parameters on the regeneration process and to validate a model to be established.

CHAPTER 3 THE METALLIC FIBROUS PARTICULATE FILTERS

3.1 Introduction

In order to study the mechanism of the thermal regeneration of the fibrous particulate filter, its construction and operation principle should be understood. In addition, the factors affecting the performance of the regeneration process should also be identified. In this chapter, construction details of the filter, as well as the operation principle of the filtering mechanisms will be presented.

3.2 Construction of the metallic fibrous filter

The fibrous filter developed by the Hong Kong Polytechnic University is for light duty diesel vehicles [1,4-6], the thermal regeneration of such fibrous filter will be studied. Figure 3.1 shows the structure of the fibrous filter. It consists of a cylindrical casing containing a filter cartridge of stainless steel fibres. The connector can be mounted to the end of the tail pipe of a diesel vehicle directly. The body of the filter, i.e. the casing and the filter cartridge, is attached to another end of the connector to capture the diesel particulates from the exhaust. The body of the filter could be removed for service and replaced by a clean one when excess particulates have accumulated.

A typical filter has the following dimensions:

Internal diameter of filter : 125 mm

Length of filter : 150 mm

Volume of filter : 1.8 litre

Since the exhaust gas has a temperature varying from 100°C to 400°C and is corrosive in nature, stainless steel fiber with rectangular cross-section of 0.4 mm x 0.04 mm is used as the filtering material. Moreover, the connector and the case of the fibrous filter are also made of stainless steel due to its durability and very good resistance to corrosion.

The backpressure created is dependent on the porosity of the filter, which is defined as the portion of the space occupied by the filtering material to the total volume of the filter [41]. In general, fibrous filters have a porosity ranging from 60% to 99%. In the present study, the porosity of the filters varied from 98.8% to 99.2%.

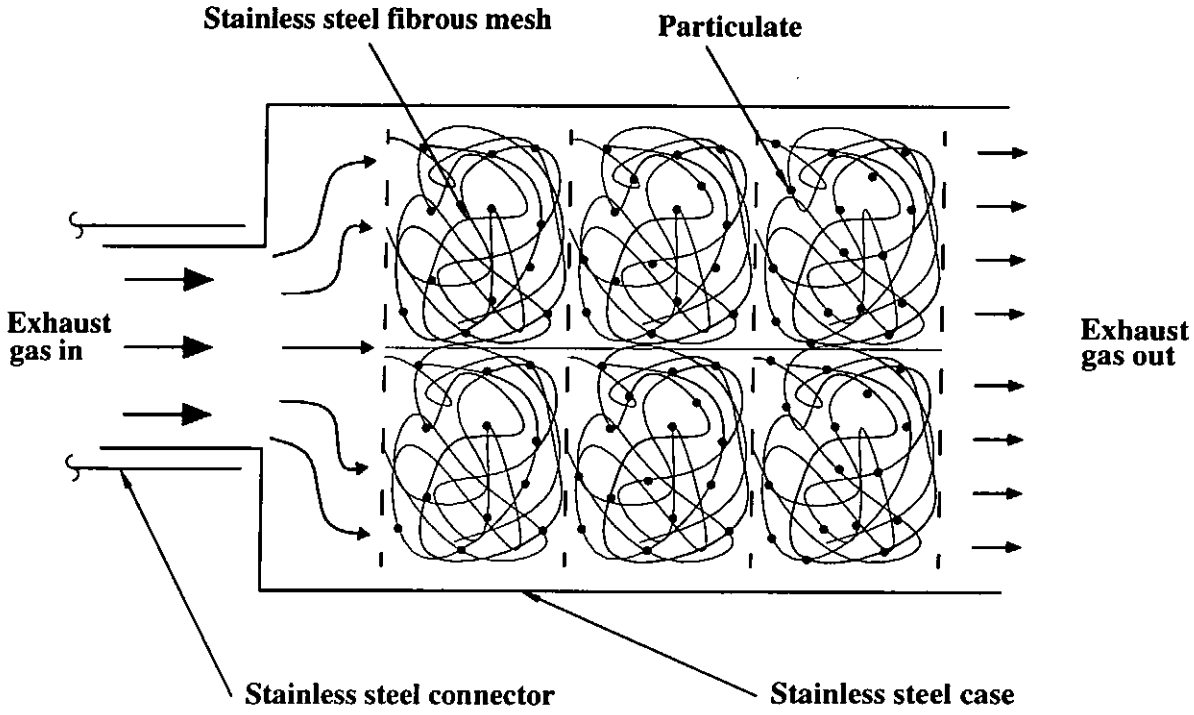

Figure 3. 1 The metallic fibrous filter

3.3 Operation principle of the metallic fibrous filter

Fibrous particulate filters are used to remove diesel particulates from the exhaust gas stream emitting from diesel vehicles. In general, the particulates flowing through a fibrous filter can be captured via three collection mechanisms, namely, Brownian diffusion, interception and inertial impaction[42], as shown in Figure 3.2(a), (b) and (c) respectively. Figure 3.3 shows effect of diameter of the particulates on the single fibre collection efficiency. The overall filtration efficiency is heavily dependent on the single fibre collection efficiency, which represents the effectiveness of an isolated fibre in collection particles.

The single fibre efficiency can be better expressed as the sum of the single fibre efficiency of diffusion, impaction and interception, i.e. $\eta_{sf} = \eta_{diff} + \eta_{inter} + \eta_{imp}$. Lee and Liu [41] gave the single-fibre efficiency due to diffusion as below:

$$\eta_{diff} = 2.58\left(\frac{1-\alpha}{K_h}\right)^{1/3} Pe^{-2/3} \quad \ldots \quad (3.1)$$

Use the Kuwabara flow, the single-fibre efficiency due to interception is shown below:

$$\eta_{inter} = \frac{1-\alpha}{K_h}\frac{R_{inter}^2}{1+R_{inter}} \quad \ldots \quad (3.2)$$

Stechkina et al. [41] expressed the single-fibre efficiency due to impaction as below:

$$\eta_{imp} = \frac{1}{(2K_h)^2}[(29.6-28\alpha^{0.62})R_{inter}^2 - 27.5R_{inter}^{2.8}]Stk \quad \ldots \quad (3.3)$$

Fine particulates with diameter less than 0.3μm undergo significant Brownian diffusion. A particulate will deviate from the gas streamline to reach the surface of the fibre, as shown in Figure 3.2(a). A lower gas velocity will increase the particulate residence time close to the surface and increase the collection efficiency.

Figure 3.2(b) shows the interception of a particulate with the fibre when it is travelling along the streamline because of its size. It is an efficient mechanism to collect the particulate when its diameter is between 0.3μm and 1μm.

For a particulate with a diameter larger than 1μm, it will keep on with its trajectory, rather than following the streamline, and strike on the surface of the fibre due to its inertia. This inertial impaction, as shown in Figure 3.2(c) is effective for large particulates, which are travelling with high inertia.

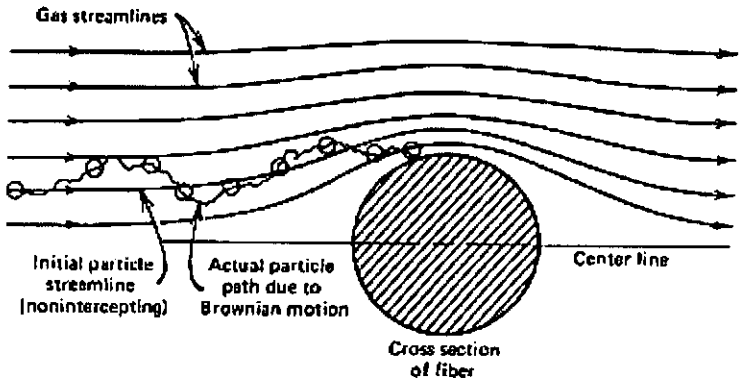

Figure 3.2(a) Brownian diffusion [42]

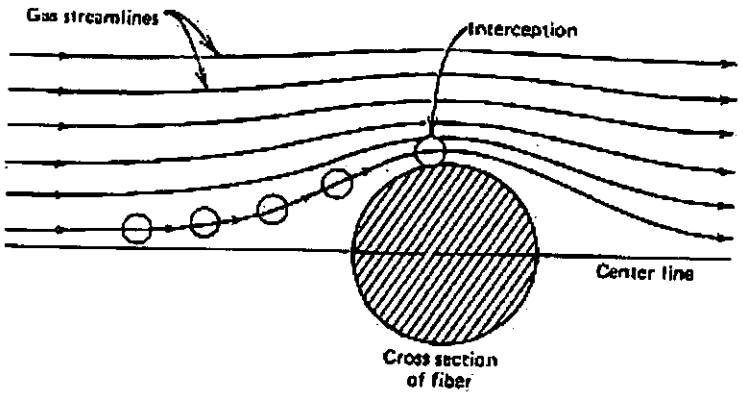

Figure 3.2(b) Interception [42]

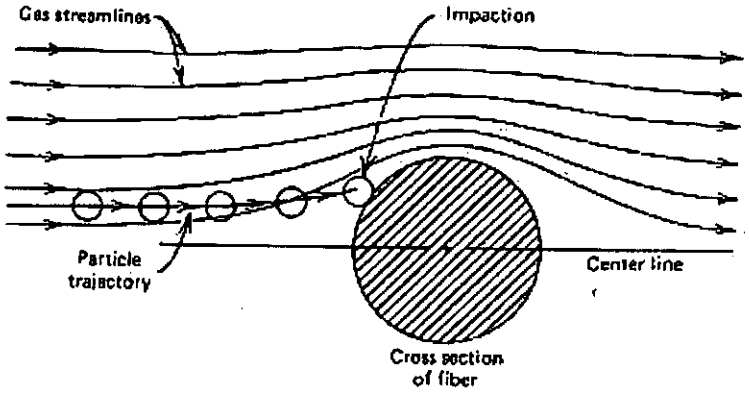

Figure 3.2(c) Inertial impaction [42]

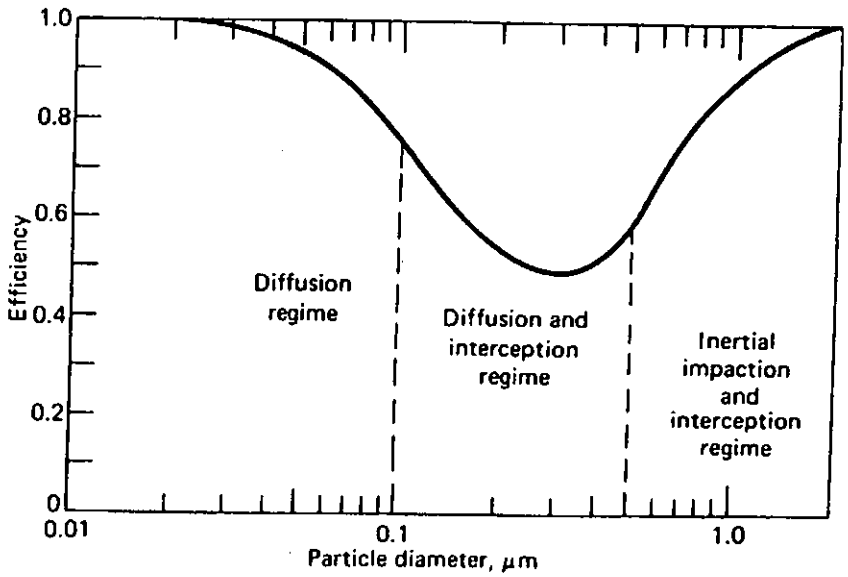

Figure 3.3 Effect of particulate diameter on single fibre collection efficiency [41]

Due to the three filtering mechanisms mentioned above, diesel particulates are captured on the surface of the fibre. A layer of particulate is formed on the surface of the fibre and it grows thicker and thicker due to further capturing. This thick layer of particulate occupied the space between the fibres. When the filter is over-accumulated with diesel particulates, it must be cleaned by regeneration process otherwise the vehicle will result from a serious fuel penalty. Thermal regeneration is a very good choice for the cleaning of the fibrous filter. The diesel particulates will be oxidized after regeneration so that the filter becomes clean again. However, it is important to note that the diesel particulate can only be oxidized when their temperature reaches the ignition temperature and an oxidizer is available. The performance of the thermal regeneration also depends directly on the external heat supply and the amount of oxygen supply, as well as the amount of particulates captured.

There are five important parameters affecting the thermal regeneration of a fibrous particulate filter as suggested from a previous study [1,4-6].

- The flow rate and the temperature of the inlet heated air determines the heat input to the particulates and fibre
- The oxygen concentration of inlet heated air and the level of dilution controls the amount of oxygen gas available.
- The packing density of the filter affects the heat transfer especially conduction directly.
- The initial particulate loading in the filter provides limit of the fuel supply for the oxidation.

- The stainless steel fibre serves as a reservoir for the heat accumulation so that the particulates can be heated up to a high temperature before combustion is initiated, and thickness of the filtering element affects the heat accumulation.

Based on the five parameters mentioned above, a test rig had been designed and built for studying the thermal regeneration of a metallic fibrous particulate filter. Details of the experimental setup and the measurement system will be presented in Chapter 4.

CHAPTER 4 EXPERIMENTAL STUDY

4.1 Experimental setup

4.1.1 Introduction

This chapter describes the experimental system used to study the thermal regeneration of the metallic fibrous filter. Experiments can be conducted either on an engine test rig or on a combustor. In the former case, the filter is connected to the exhaust pipe of the engine and collects particulate. Regeneration is initiated by increasing the exhaust gas temperature or through injection of oil fuel. In the latter case, particulate is collected and then the filter is transferred to a separate combustor for thermal regeneration. A combustor is used for regeneration in this study due to the following two reasons. Firstly, the filter used in this study is designed for periodic removal for regeneration rather than for in-situ regeneration. Secondly, it is easier to control the regeneration parameters on a combustor than on an engine. Hence a test rig was designed and built in a laboratory scale as shown in Figure 4.1. Since the oxygen concentration of exhaust gas from diesel engines is always lower than that of air, therefore compressed air was diluted so that its range matches with the exhaust gas. This can benefit further study for in-situ regeneration. In the test rig, diluted air was heated up in a combustor, through a heat exchanger, to provide the energy for regeneration. Tests were conducted to measure the variation of temperature with time at different positions of the filter, under different operation conditions.

4.1.2 Experimental system

An experimental system, consisting of an experimental rig and a measuring system, was designed and built for this investigation. The main components of the experimental rig were a combustor, a heat exchanger, the metallic fibrous filter and the air and nitrogen supply unit. Figure 4.1 and Figure 4.2 are the schematic diagram of the experimental setup and photograph of the combustion chamber respectively.

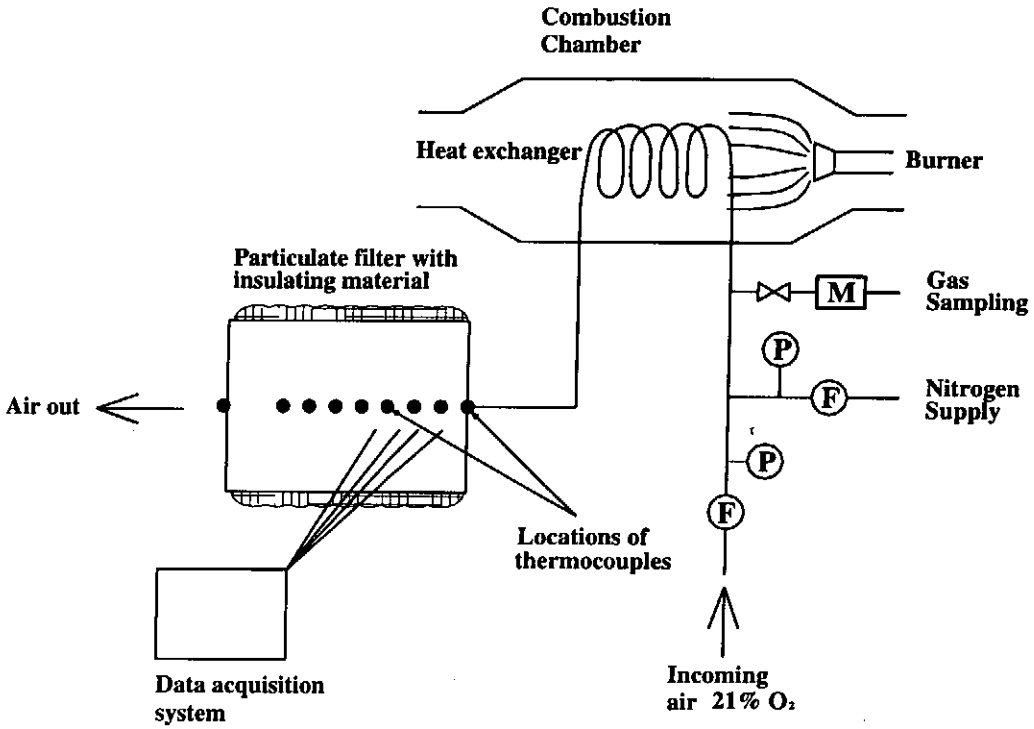

Figure 4.1 Schematic diagram of the experimental setup

In order to produce hot air of controllable quality, an existing combustion chamber was used to heat up the air for regeneration, rather than using the combustion product for direct regeneration. The combustion chamber included a fuel and air supply unit, which was used to supply fuel and air to the burner head to produce a premixed flame after ignition. The fuel used was LPG containing 92% butane and 8% propane. The fuel flow was controlled with a pressure regulator and a valve, and measured with a calibrated rotameter. A blower was used to provide the air for combustion. The air supply was

split into two branches, one providing the premixed air and the other providing the secondary air. The primary air and the fuel mixed uniformly in the premixing chamber before entering into the combustion chamber. The secondary air flowed around the premixed air-fuel mixture to provide extra air required for combustion and helped to stabilise the flame. The volume flow rate of the premixed air and the secondary air were each controlled by a valve and measured by a flow meter.

Figure 4.2 Combustion chamber

Air for regeneration was obtained from a compressed air line. It was heated up and supplied to the particulate filter via the combustion chamber. Oxygen concentration in the air was adjusted to the desired value by controlling the amount of nitrogen injected into the air, and monitored by a Digital 5-Gas (3700 Series) gas analyzer (M). Volumetric flow rate of regenerating air was controlled by the pressure regulators (P) and measured by the flow meters (F). Air was passed through a heat exchanger in the

combustion chamber and heated up to approximately 500°C by the LPG burner. The hot air provided the necessary heat energy to start the oxidation of the diesel particulate collected in the fibrous filter. The hot air temperature and the filter temperatures at different locations were monitored by K-type thermocouples of 0.8mm diameter. The temperatures were captured and stored with a data acquisition system at a time interval of 5 seconds during the periods of heating up, thermal regeneration and cooling down of the metallic filter. To facilitate the regeneration process in the laboratory, the filter casing was insulated with a blanket of fibreglass in order to reduce heat loss from the filter to its surroundings.

4.1.3 The measurement system

The system included the measurement of temperatures at different positions within the filter, and the measurement of the values of different experimental parameters.

4.1.3.1 Measurement of temperature

The thermocouples were embedded in the filter, as shown in Figure 4.3, with their junctions exposed to the gas flow. Due to the high porosity of the filter, which is usually in the range of 99%, there should be little contact between the thermocouple junctions with the solid phase of the filter. There were 12 thermocouples inserted along the length of the filter with a separation of 12mm between consecutive points. The first thermocouple measured the temperature of the hot air used for initiating the regeneration process. The second to the eleventh thermocouples measured the temperatures of the different zones of the filter, while the last thermocouple measured the temperature of the gas exiting from the filter.

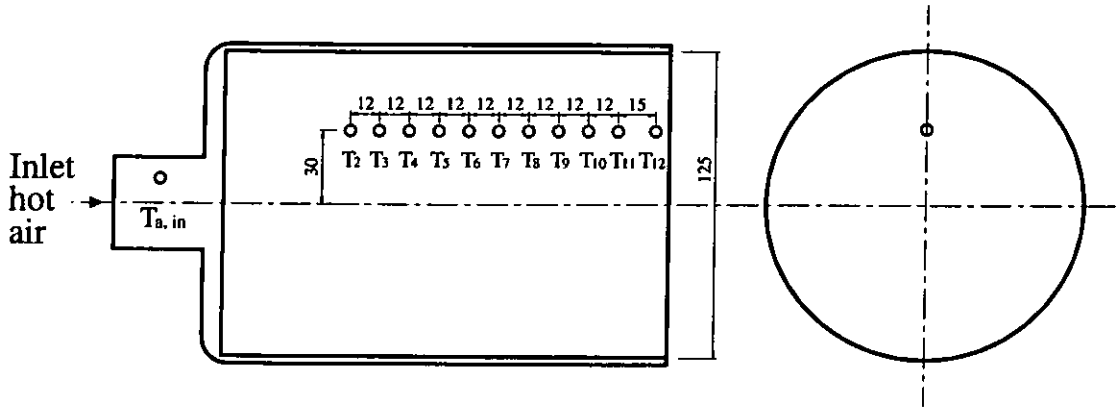

Figure 4.3 Locations of thermocouples in particulate filter (all dimensions in mm)

The thermocouples used in the present study were type K with magnesium oxide (MgO) as the insulation material and 600 inconel as the sheath material since inconel is capable to withstand a temperature over 1370°C without damaging. Thermocouple signals were connected to a scanning thermometer which gave the values of the temperature. The recorded temperatures were stored in a desktop personal computer with a time interval of 5s, due to limitation of the signal transfer rate.

4.1.3.2 Measurement of flow rate of inlet air

Inlet air for regeneration was diluted with nitrogen to the desired oxygen concentration. The volumetric flow rate of the inlet air was the sum of that of the compressed air and the nitrogen, the flow rate of each was controlled with a pressure regulator (P) and a valve, and measured with a calibrated rotameter (F).

4.1.3.3 Measurement of concentration of oxygen of inlet air

A gas sampling point was provided to obtain an air sample before it reached the combustor as shown in Figure 4.1, where measurement of oxygen content could be

made. The oxygen content was measure with a Digital 5-Gas (3700 Series) gas analyzer.

4.1.3.4 Measurement of initial particulate loading

The filter was initially installed along the tailpipe of a diesel taxi of pre-Euro emissions standard to collect the particulate. The weight of particulate in the filter was determined by comparing the weight of the filter before and after the collection process. During the collection period, the taxi was allowed to operate as usual. After the desired amount of particulate had been collected, the filter was removed from the taxi and connected to the test rig for regeneration test.

4.1.3.5 Measurement of packing density

Packing density is defined as the ratio of the volume of stainless steel fibre to the volume of the filter cartridge. It is very difficult to measure the volume of fibre since it is of irregular shape. However, volume of the fibre can be calculated from the mass divided by density of the fibre, and mass of the fibre was measured with an electronic balance.

4.1.3.6 Measurement of thickness of filtering element

The thickness of the filtering element was measured with a vernier caliper. Since the fibre was loosely packed, the presented thickness was the average value of several measurements.

4.1.4 Experimental conditions

Thermal regeneration of the metallic fibrous filter can be affected by several parameters, including the oxygen concentration and flow rate of inlet hot air, the initial particulate loading, the packing density and the thickness of the filter cartridge. In order to carry out the experimental study, the parameters mentioned above should be capable to be varied. The ranges of the parameters are tabulated in Table 4.1.

Parameters	Lowest value	Highest value
Oxygen Concentration of inlet hot air, %	3	21
Inlet air flow rate, l/min at 1 atm and 25°C	67	112
Initial particulate loading of filter, g	1	20
Packing density of filter, %	0.8	1.2
Thickness of the filtering element, mm	50	150

Table 4.1 Ranges of the experimental parameters

4.2 Experimental results

4.2.1 Introduction

In order to achieve good thermal regeneration of a fibrous particulate filter, its mechanism has to be intensively studied. Good thermal regeneration should be of high regeneration efficiency, short regeneration time and low peak filter temperature during regeneration. Experiments were carried out to investigate the regeneration process and to investigate the effects of the influencing parameters. The data to be obtained include temperature, volume flow rate and oxygen concentration of the inlet hot air, and temperature of the filter matrix. According to a preliminary study, regeneration could not be initiated in the particulate filter when the initial particulate loading was less than 2 grams, and thickness of the filtering material was less than 50mm. On the other hand,

regeneration was still observed when the oxygen concentration was down to 6% and the flow rate of the hot air was 67 l/min respectively. In this Chapter, calculation of energy released from the oxidation of diesel particulate during the thermal regeneration process was demonstrated. The relationship of temperature with time and the axial location within the filter was analysed and presented. The regeneration efficiency of the fibrous filter was found to have relationship with the temperature profile, and was discussed and presented. Further investigation from the point of view of conservation of energy of the entire filter and in specific regions of the filter was also performed.

4.2.2 Definition of some important terms

- Regeneration efficiency

Regeneration efficiency is defined to be the ratio of the mass of the particulate oxidized to that captured and is mathematically given in equation (4.1)[32]. The higher the regeneration efficiency, the better is the thermal regeneration.

$$\eta_{reg} = \frac{m_{filter,c} - m_{filter,o}}{m_{filter,c} - m_{filter,i}} \times 100\% \quad \ldots \quad (4.1)$$

- Regeneration peak temperature

Regeneration peak temperature is the maximum temperature which exists in a zone of the filter during the regeneration process. Hence, each zone of a filter has its own regeneration peak temperature.

- Peak filter temperature

Peak filter temperature is the maximum value among the regeneration peak temperatures. It always exists in the region near the exit end of the filter.

- Regeneration time

Regeneration time is the time required for the entire process of oxidation of particulate to occur. It can be measured from the temperature-time relationship. It starts when the first sudden rise in temperature is observed and ends immediately after the occurrence of the peak filter temperature.

4.2.3 Temperature-time relationship

A number of experiments with different values of regeneration parameters including oxygen concentration and volume flow rate of the inlet hot air, the initial particulate loading, packing density and thickness of the filtering matrix, were carried out. The operating conditions of the experiments were listed in Table 4.2 below while the corresponding temperature profiles are given in Appendix A. It can be seen from the appendix that all the experimental results showed similar temperature-time profiles. Since temperature traces close to each other have similar properties, it is found more useful to look at typical temperature traces for three regions of a filter, as shown in Figure 4.4.

Experiment number	Oxygen Concentration	Inlet gas flow rate	Initial particulate loading	Packing density	Matrix thickness
	(%)	(l/min)	(g)	(%)	(mm)
1	21	90	10	1.2	150
2	17	90	10	1.2	150
3	13	90	10	1.2	150
4	13	67	10	1.2	150
5	13	90	10	1.2	150
6	13	112	10	1.2	150
7	13	90	6	1.2	150
8	13	90	8	1.2	150
9	13	90	10	1.2	150
10	21	90	10	0.8	150
11	21	90	10	1.0	150
12	21	90	10	1.2	150
13	13	90	3.3	1.2	50
14	13	90	6.6	1.2	100
15	13	90	10	1.2	150
16	6	90	20	1.2	150
17	13	90	2	1.0	150

Table 4.2 Operating conditions of the experiments

Operation conditions:

Inlet air flowrate : 90 l/min, Oxygen concentration: 17%,
Initial particulate loading : 10g, Packing density : 1.2%,
Filter thickness : 150mm

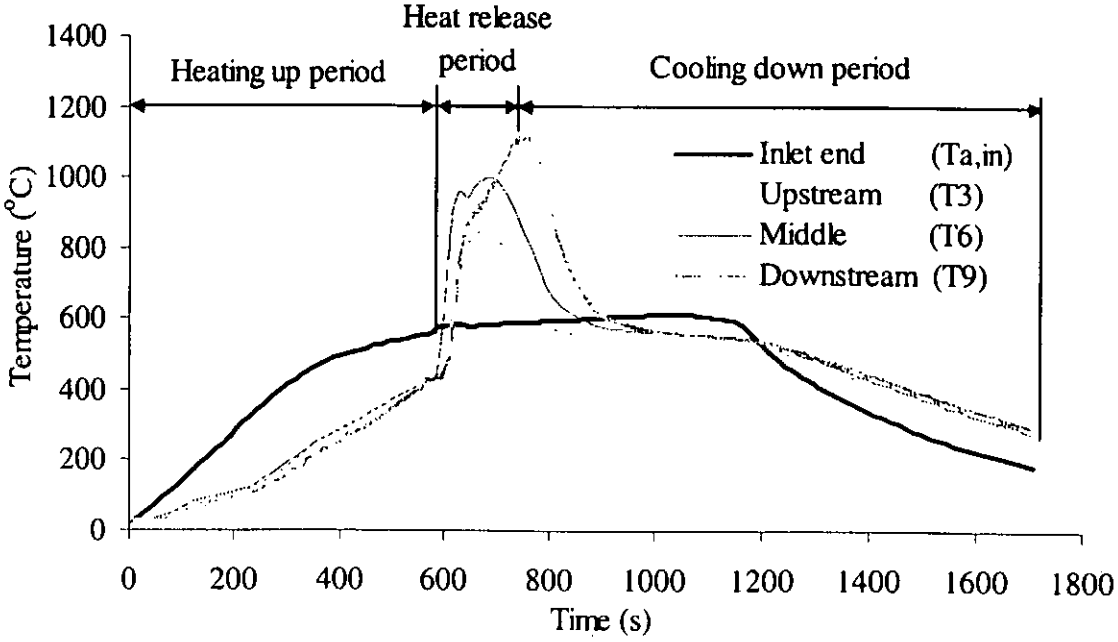

Figure 4.4 Temperature profiles at different locations against time

In Figure 4.4, temperatures at inlet end ($T_{a,in}$), upstream (T_3), middle (T_6) and downstream (T_9) regions of the filter are shown. The corresponding experiment was performed with the following operating conditions: hot air flow rate of 90 l/min, oxygen concentration of 17%, initial particulate loading of 10 gram, packing density of 1.2% and thickness of filtering material of 150mm. The regeneration process can be clearly divided into three periods, namely, the heating up period, the heat release period and the cooling down period. The temperature profiles within different zones of the filter cartridge, namely, T_3, T_6 and T_9, were similar to each other. Each temperature profile, like the regeneration process, can be divided into three periods, namely, the heating up period, the heat release period and the cooling down period.

The inlet air temperature had a sharp initial increase from room temperature to 500°C in the first 400 seconds, as it was heated up in the combustor. The temperature tended to stabilize at 550°C thereafter, since it was limited by the energy supply of the LPG flame. The final drop in temperature as shown in the figure was due to the shut down of energy supply to the inlet air upon completion of the test.

The hot air expanded into a larger volume as it entered into the filter cartridge. Due to the dispersion of energy to the particulate and the stainless steel fibres and the metal casing, there was a drop in temperature of the air as it flowed along the different zones of the filter until regeneration occurred. Due to the positional effect, there was a time lag in different zones for the temperature rise to occur. The zones at the inlet end were heated up first while those towards the exit end later.

The heating up period corresponded to the initial heating up of the filter from room temperature to around 400°C in 600 seconds. It was suggested that some regeneration was already occurring in this heating up period [31,32], but the magnitude of regeneration was small. The heat release period started with the oxidation of particulate in the fibrous filter, usually beginning at the first zone, and ending immediately after the occurrence of the last maximum temperature. Duration of the heat release period was taken to be the regeneration time. In this heat release period, there was a subsequent sharp increase in temperature to give the maximum temperature. Commencement of the sharp temperature increase corresponded to the commencement of intensive regeneration of the diesel particulate. The time and temperature at which intensive regeneration occurred were found to vary in each zone of the filter. It commenced earlier and at a higher temperature at the inlet end, but occurred later and at lower temperatures towards the exit end of the filter.

Figure 4.4 shows that T_9 has a regeneration peak temperature higher than those at T_6 and T_3, i.e. the peak filter temperature is obtained at T_9. This is generally true as the heat released at earlier zones tends to accumulate at later zones. However, there were some cases in which the regeneration peak temperatures of all the zones were about the same. The normal regeneration peak temperature was around 800°C to 1000°C, but could be as high as 1300°C. The maximum temperature was maintained for a very short period of time, and dropped faster at the inlet end than those towards the exit end.

The cooling down period commenced once the last regeneration peak temperature of the filter started to decrease. The inlet air was supplied throughout the regeneration process, from the heating up period to the cooling down period. However, energy supply to the

inlet air when it was inside the filter was stopped when the heat release period was over. The solid matrix of the filter was then cooled down by the inlet air by convection. Moreover, the heat loss to the surrounding from casing of the filter and the radiative heat loss at the exit end assisted the cooling process.

In the case as shown in Figure 4.4, the filter peak temperature was 1110°C, the regeneration time was 215 seconds.

4.2.4 Comparison of temperature profiles

Although the temperature-time profiles of the thermal regeneration were quite similar macroscopically, they can be classified into four major categories. Each of them has its own characteristics. The typical temperature profiles of each category were presented in this section.

Figure 4.5 to Figure 4.8 showed these typical temperature profiles. In all the temperature profiles, temperatures at the inlet end ($T_{a,in}$), upstream (T_3), middle (T_6) and downstream (T_9) regions of the filter are shown. The temperature profiles in the heating up period were very similar while significant differences were observed in the heat release period so that discussion will be concentrated on that period. The differences between the shape of the profiles, the sequence of temperature rise, the duration of heat release, the moment and the position for the regeneration peak temperature to occur are significant enough to affect the regeneration efficiency and regeneration time.

Figure 4.5 shows a typical case of slow and poor regeneration. It shows the temperature profile of the thermal regeneration process of a fibrous diesel particulate filter consisting

of a filtering material of 150mm thick, an initial particulate loading of 10 gram and with a volumetric packing density of 1.2%. Heat was provided to the particulate filter via the hot air supply, with an oxygen concentration of 13% and at a volumetric flow rate of 90 liters per minute. The hot air flowing into the particulate filter was heated up from room temperature to approximately 520°C. Temperature at the position nearest to the filter inlet, T_3, rose gradually from room temperature first, which was followed by those in the other zones in the sequence of the geometrical arrangement. When T_3 reached about 440°C, there was an obvious change in the rate of change of temperature, indicating the commencement of thermal regeneration. Thermal regeneration proceeded gradually with a gradual increase in temperature until the maximum temperature was reached. Subsequently, the temperature dropped. T_6 and T_9 showed similar changes in temperature but with time lag between each other.

In the thermal regeneration process of the particulate filter, the peak filter temperature was 886.6°C, the regeneration time was 290 seconds and the regeneration efficiency was 39%. Temperatures of the filtering matrix were relatively low, indicating that the oxidation rate of particulate was not high. It is mainly due to the low oxygen concentration of the inlet nitrogen-enriched air and the amount of particulate was also low. The difference between the regeneration peak temperatures at each position of the filtering matrix was small, which showed that the distribution of the particulate was quite even in the filter and thus no local over-heating was observed.

During the regeneration process, the heat released during the exothermic reaction between particulate and oxygen at the inlet end was transferred downstream to the rear part of the filter. Hence, the temperature at the inlet end began to rise and the

temperature wave-front moved downstream towards the filter exit. Thus the filter was regenerated with a sweeping action starting mainly at inlet end of the filter. In normal case, the heat carried downstream, coupled with regeneration occurring downstream would result in much higher regeneration peak temperature downstream.

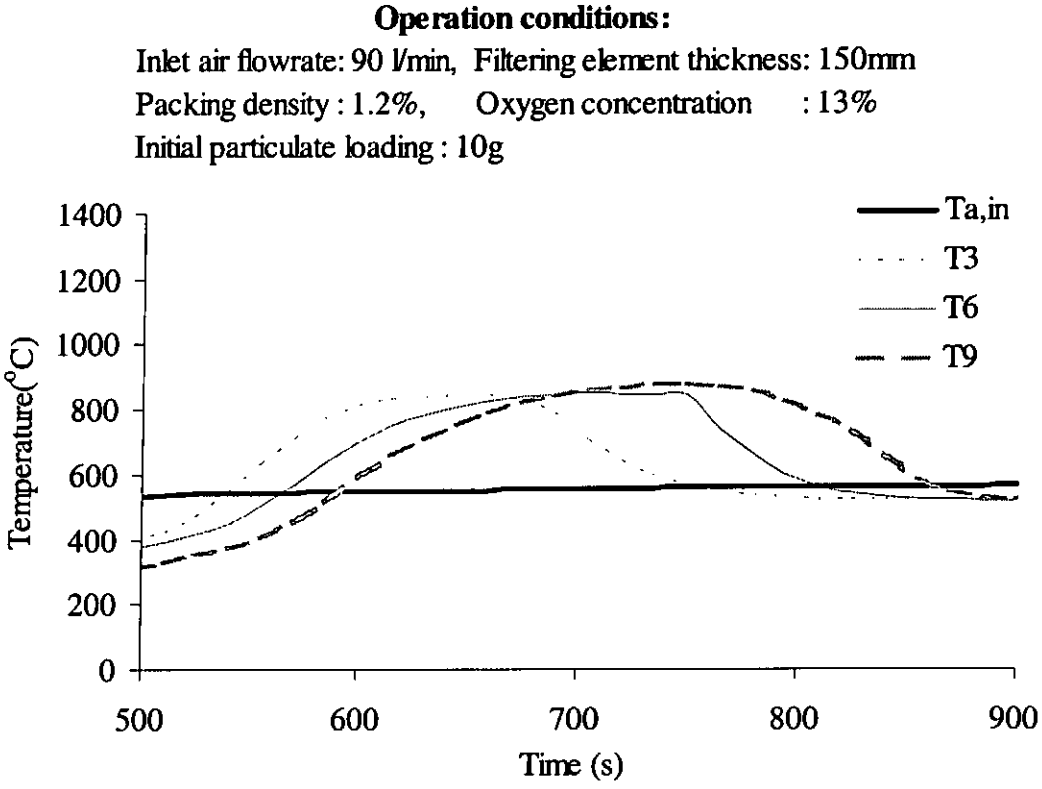

Figure 4.5 Temperature time relationship, with regeneration efficiency of 39%

In this case, the similar temperature profiles at different regions of the filter indicated that heat released in the inlet region did not accumulate in the downstream regions, or the regeneration in the inlet region did not enhance regeneration in the downstream region. It could also be seen from the temperature profile that temperature at the inlet end started decreasing while temperatures at other parts of the filter were still increasing. In this case, regeneration was slow but the inlet air flow rate was high. The low regeneration heat released was transferred downstream rapidly which was

unfavourable for sustaining regeneration. Moreover, the heat released at the rear of the filter was lost to the surroundings hence oxidation of particulate at that region could not be sustained. As a result, oxidation of particulate was incomplete throughout the filter and hence the regeneration efficiency was low.

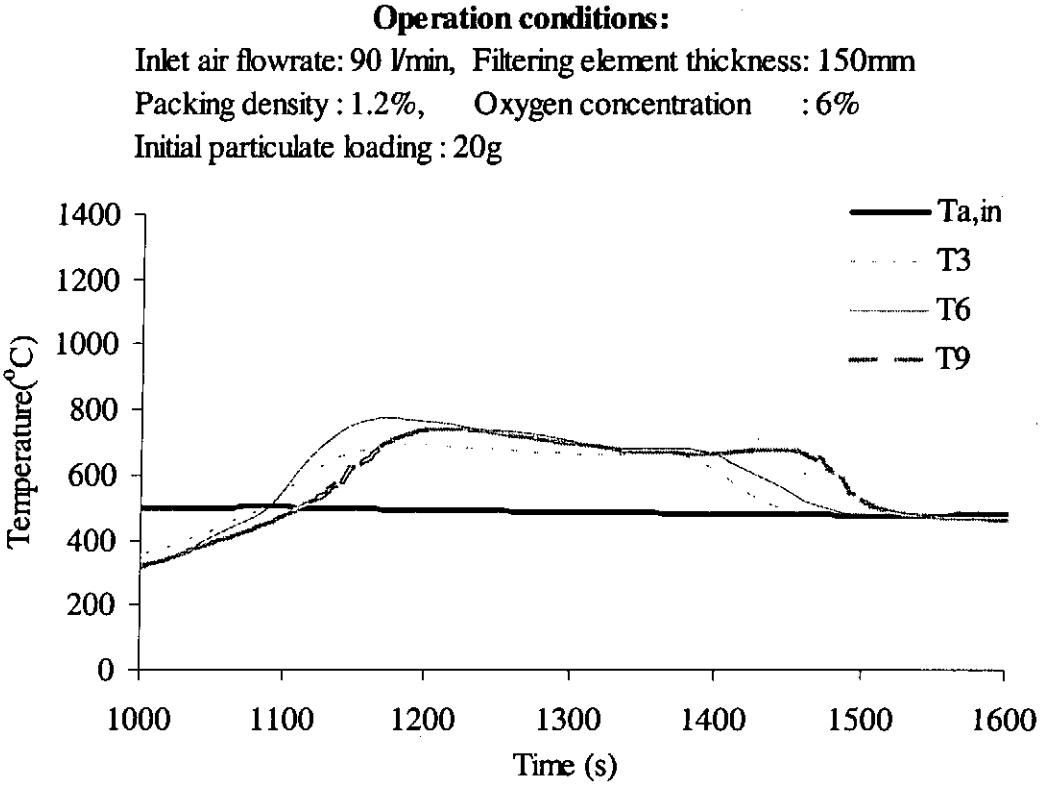

Figure 4.6 Temperature time relationship, with regeneration efficiency of 75%

Figure 4.6 shows the case of heavy initial particulate loading but low oxygen concentration in the heating air. All experimental parameters were the same as those presented in the case of Figure 4.5, except that the initial particulate loading was increased to 20g but the oxygen concentration was only 6%. Temperature at position nearest to the filter inlet, T_3, rose gradually from the room temperature almost at the same time as the others. Upon reaching the point of regeneration, there was an initial fast increase in temperature, followed by a prolonged cooling down period with signs of

secondary regeneration. The regeneration peak temperatures were lower but occurred much earlier compared with the case shown in Figure 4.5.

In the thermal regeneration process of this particular particulate filter, the peak filter temperature, regeneration time and regeneration efficiency were 771.5°C, 430 seconds and 74.5% respectively. The regeneration peak temperatures of the filtering matrix were lower mainly due to the very low oxygen concentration supply of only 6% in the inlet air. Besides, the difference between the regeneration peak temperatures at each position of the filtering matrix was rather small, which showed a rather even distribution of particulate in the filter and thus no local over-heating was observed. After reaching the regeneration peak temperature, there was a gentle decrease in temperature observed during the regeneration process. Because a very high initial particulate loading of 20 gram had been used in this experiment, the layer of accumulated particulate was rather thick and some of them could not be oxidized immediately. The outermost layer of accumulated particulate was first oxidized to form a layer of ash on its surface, which lower down the reaction between the particulate and the hot air stream. However, when this ash layer was removed by the hot air stream, rapid oxidation re-occurred to produce a temperature rise. It increased the regeneration time and improved the regeneration efficiency.

Figure 4.7 shows the case of a low inlet air supply. All the experimental parameters were same as those presented on Figure 4.5, except that the inlet hot air flow rate was reduced to 67l/min. Because of the lower flow rate of hot air, the filter was heated up more slowly and hence regeneration was delayed. Regeneration occurred first at the upstream region, then the middle, and finally the upstream regions of the filter, which

was the same sequence as that presented in Figure 4.5 and Figure 4.6. However, the peak temperature, which occurred around the filter exit, was much higher than that at the filter inlet (i.e. 1088°C against 800°C). This might be a result of the lower convection due to the lower flow rate of heating air. Temperatures at latter part of the filter were still increasing when temperatures at former part of the filter started to decrease.

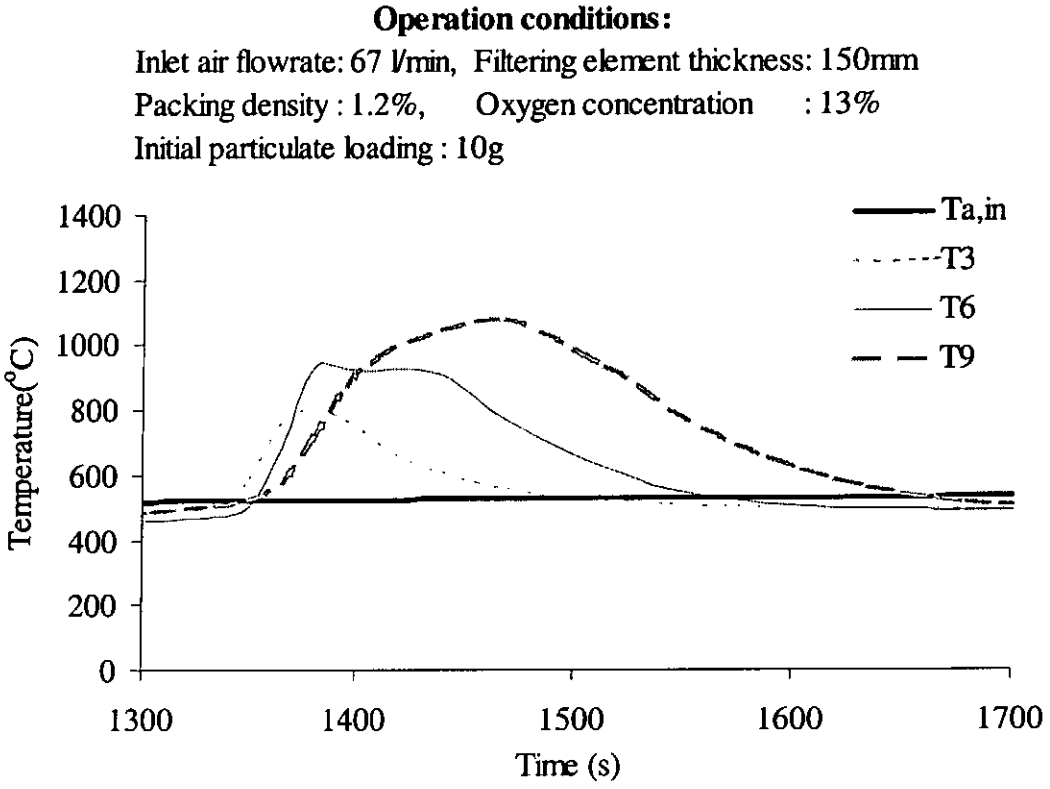

Figure 4.7 Temperature time relationship, filter melted after regeneration

In the thermal regeneration process of the particulate filter, the peak filter temperature was 1088°C and the filtering matrix was partially melted, thus the regeneration time and efficiency cannot be determined. The rate of change of all the temperatures of the filtering matrix was high, indicating a very high rate of the oxidation of particulate. It was mainly due to the small flow rate of the heating air. The exothermic reaction

between oxygen and the particulate liberated a large amount of heat energy. This heat energy was partly stored in the filtering matrix so that its internal energy was much increased, and the rest was carried away via convection by the heating air. Since the flow rate of the air was low, the amount of heat energy carried away was small and most of the energy was stored inside the fibre matrix. The heat energy continued to accumulate until the end of the oxidation reaction, leading to a very high regeneration peak temperature of the fibre matrix. As a result, overheating occurred and the filter matrix was melted.

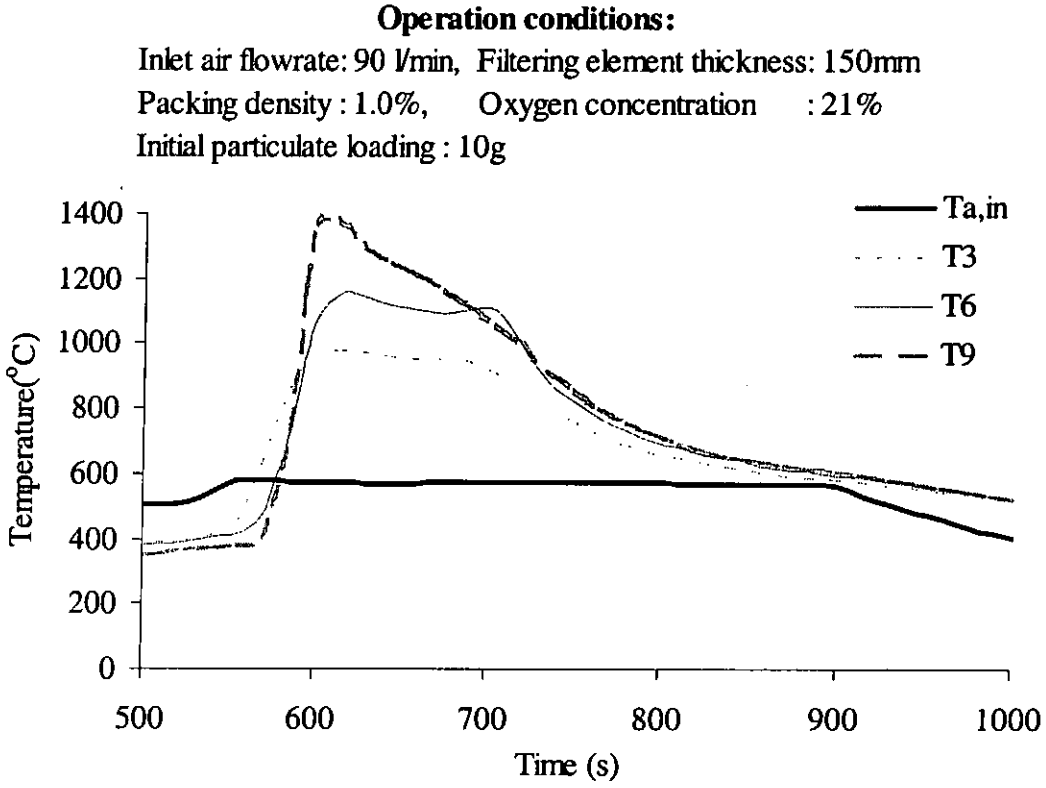

Figure 4.8 Temperature time relationship, with regeneration efficiency of 70%

Figure 4.8 shows a typical case of good thermal regeneration. Experimental parameters were the same as those presented in Figure 4.5, except that the oxygen concentration was increased to 21% and the packing density was decreased to 1.0%. Upon

regeneration, the temperature rose suddenly and rapidly throughout the filter with a peak filter temperature of 1362°C, due mainly to the very high oxygen concentration available for oxidation of accumulated particulate. Regeneration at the upstream, middle and downstream regions of the filter occurred almost simultaneously, but there was a great difference of 438.7°C between the regeneration peak temperatures of the upstream and downstream regions of the filter.

Although the peak filter temperature was comparatively high, it was only maintained for a very short period of time, thus no melting was found inside the filter. The high oxygen concentration in the inlet air led to a very high temperature in the filtering matrix, especially at the region near to the exit end. The regeneration peak temperature at T_9 occurred almost immediately upon regeneration at that region and then cooled down gradually. Hence, over accumulation of energy in this region, and hence, melting, was avoided. The regeneration efficiency of 70% was rather high. The short regeneration time of 65 seconds was good in this case to avoid the melting of filter matrix. Hence, a high inlet air flow rate is beneficial in reducing the chance of filter damage.

4.2.5 Heat release during regeneration

A review of published literature shows that all analysis of thermal regeneration was based on the comparison of temperature and rate of temperature change. However, the analysis of energy release during regeneration can be an alternative approach to study the phenomenon of thermal regeneration of the metallic fibrous filter, and is applied in this study.

The global heat released during regeneration was the sum of the heat released in each zone of the filter while the local heat release was the heat release at that particulate zone. The global energy release can be applied as an indicator for comparing different operation conditions, while the local heat release can be used for comparing the regeneration in different zones of a filter.

4.2.5.1 Global heat release during regeneration

When hot air passes through the filter, it brings heat energy into the stainless steel fibres and the particulate to increase their internal energy. The particulate will be oxidized after absorbing sufficient heat energy, and release their enthalpy of combustion. Part of the energy released will heat up the neighbouring materials, while the rest will be carried downstream by the incoming air. Since the filter was thermally insulated from its surroundings by a glass fibre blanket, temperature of its outer surface was maintained below 50°C throughout the regeneration process. Hence, heat loss to the surroundings was considered negligible during the regeneration process. Under these assumptions, the energy equation for the thermal regeneration can be shown as below:

$$\dot{m}_{a,in}h_{a,in} + \dot{H}_{comb} = m_f c_{p,f}\frac{\partial \overline{T_f}}{\partial t} + m_p c_{p,p}\frac{\partial \overline{T_p}}{\partial t} + m_a c_{p,a}\frac{\partial \overline{T_a}}{\partial t} + \dot{m}_{a,ex}h_{a,ex} \quad \ldots \quad (4.2)$$

In equation (4.2), the first term on the LHS represents the rate of energy input via the incoming hot air, while the second term represents the rate of energy released due to combustion of the particulate in the filter. The last term on the RHS represents the rate of energy carried away by the air leaving the filter, while the other terms represent the increase in internal energy of the fibres, the particulate and the air in the filter.

Equation (4.2) describes the heat balance inside the whole filter when thermal regeneration is taking place. $\overline{T_f}$, $\overline{T_p}$, and $\overline{T_a}$ are mean temperatures of the stainless steel fibre, the particulate and the air in the filter respectively. $\dot{m}_{a,in}$ and $\dot{m}_{a,ex}$ are the mass flow rate of air at the inlet and the outlet of the filter respectively. The difference between them is due to the mass of particulate regenerated, which can be obtained by dividing the instantaneous heat release rate, $\dot{H}_{comb}$, by the calorific value of diesel particulate, U, which is taken to be 32,800 kJ/kg after Garner and Dent [33]. The calculation is presented in equation (4.3) as below:

$$m_p = \frac{\dot{H}_{comb} \cdot \Delta t}{U} \qquad \ldots \quad (4.3)$$

The mass flow rate of air through the filter element, $\dot{m}_a$, is taken to be the mean value of those at the inlet and the outlet. The specific heat capacity of steel fibres $c_{p,f}$ and the specific heat capacity of particulate $c_{p,p}$ have been taken as 0.46 kJ/kg-K and 1.51 kJ/kg-K respectively [33]. The specific heat capacity of air, enthalpy of air at the inlet end and enthalpy of air at the exhaust, $c_{p,a}$, $h_{a,in}$ and $h_{a,ex}$ are calculated based on the temperature and gas composition, and the gas properties tables provided in [43].

Based on equation (4.2), the measured temperature can be used to evaluate the rate of heat release, $\dot{H}_{comb}$, as described below. The entire filter is divided into ten zones which are equal in volume, packing density and particulate loading. The temperature of each zone is measured with an embedded thermocouple, and the total change in internal energy is calculated by summing up the change in internal energy of each zone. In this way, equation (4.2) can be expressed in the following form:

$$\dot{m}_{a,in}\, h_{a,in} + \dot{H}_{comb} = m_f c_{p,f} \sum_{j=2}^{11} \frac{\partial T_{fj}}{\partial t} + m_p c_{p,p} \sum_{j=2}^{11} \frac{\partial T_{pj}}{\partial t} + m_a c_{p,a} \sum_{j=2}^{11} \frac{\partial T_{aj}}{\partial t} + \dot{m}_{a,ex}\, h_{a,ex} \quad \ldots \quad (4.4)$$

T_{fj}, T_{pj} and T_{aj} are the local temperatures inside each zone. The inlet position is designated to be the first position of the filter. Therefore the value of "j" starts from 2 to 11 in the calculation. Moreover, the particulate are adhered onto the surface of the very thin stainless steel fibres, so a reasonable assumption of $T_{pj} = T_{fj} = T_{aj} = T_j$ can be made and equation (4.4) becomes,

$$\dot{m}_{a,in} \cdot h_{a,in} + \dot{H}_{comb} = (m_f c_{p,f} + m_p c_{p,p} + m_a c_{p,a}) \sum_{j=2}^{11} \frac{\partial T_j}{\partial t} + \dot{m}_{a,ex} \cdot h_{a,ex} \quad \ldots \quad (4.5)$$

Using this approach, the rate of heat release, $\dot{H}_{comb}$, at any time can be calculated as shown in equation (4.6) and the instantaneous heat release in the filter, $E(t)$, is presented in equation (4.7). The values are negative in the heating up phase, during which the filter is absorbing heat energy from the hot air. They become positive once oxidation of particulate occurs. Negative values appear again when oxidation of particulate ceases. Based on these, the total heat energy released during regeneration, E_{total}, can also be evaluated as shown in equation (4.8).

$$\dot{H}_{comb} = (m_f c_{p,f} + m_p c_{p,p} + m_a c_{p,a}) \sum_{j=2}^{11} \frac{\partial T_j}{\partial t} + \dot{m}_{a,ex} \cdot h_{a,ex} - \dot{m}_{a,in} \cdot h_{a,in} \quad \ldots \quad (4.6)$$

$$E(t) = \dot{H}_{comb} \cdot \Delta t \quad \ldots \quad (4.7)$$

$$E_{total} = \sum \dot{H}_{comb} \cdot \Delta t; \quad \text{for } \dot{H}_{comb} > 0 \quad \ldots \quad (4.8)$$

The instantaneous heat release, $E(t)$, was evaluated for comparing the heat release pattern of different regeneration process, while E_{total} was computed to compare the total energy released in each regeneration process.

4.2.5.2 Local heat release during regeneration

The calculation of the local energy released in a small zone can provide further information on the mechanism of thermal regeneration of the metallic fibrous filter. The local energy can be obtained with the energy equation as shown below:

$$\dot{H}_{comb} + h_{conv} v_{filter} a_{conv} (T_a - T_s) + (1-\phi) v_{filter} k_s \frac{\partial^2 T_f}{\partial x^2} = m_f c_{p,f} \frac{\partial T_f}{\partial t} + m_p c_{p,p} \frac{\partial T_p}{\partial t} + m_a c_{p,a} \frac{\partial T_a}{\partial t} \quad \ldots \quad (4.9)$$

In equation (4.9), h_{conv} is the convective heat transfer coefficient, a_{conv} is the specific area for convection and k_s is the conductivity of stainless steel fibre.

Since the convective heat transfer coefficient is unknown in this case, the local heat release cannot be computed directly from equation (4.9). In order to overcome this difficulty, the change in local internal energy was computed instead. The change in internal energy is the sum of the three terms on the RHS of equation (4.9). In this way, comparison between the local heat release is transformed to compare with the change in internal energy between different zones. The change in internal energy in a particular zone is the difference between the internal energy of that zone at the inlet air temperature and the zonal temperature. Equation (4.9) can be rewritten as below:

$$\dot{E}(j) = m_{fj} c_{p,f} \frac{T_{fj} - T_{in,air}}{\Delta t} + m_{pj} c_{p,p} \frac{T_{pj} - T_{in,air}}{\Delta t} + m_{aj} c_{p,a} \frac{T_{aj} - T_{in,air}}{\Delta t} \quad \ldots (4.10)$$

$$E(j) = \dot{E}(j) \cdot \Delta t \quad \ldots (4.11)$$

where $\dot{E}(j)$ is the rate of change in internal energy in the jth zone and $E(j)$ is the change in internal energy in the jth zone.

The change of internal energy, $E(j)$, is the comparison between the heat energy input and the internal energy of the filtering matrix. Before oxidation of diesel particulate occurs, internal energy of the filtering matrix should be lower than energy of the incoming hot air since the former was at room temperature while the latter was being heated. Once intensive oxidation commenced, heat release during the process transferred a large amount of energy to the filtering matrix, which was greater than the energy input to produce a positive $E(j)$.

4.2.5.3 Experimental uncertainty analysis

Before the calculation of heat release, the overall experimental uncertainty should first be determined. Experiments had been performed under different experimental conditions and their values (experimental data) were obtained by measurements. However, the measured values were not exact and contained errors, which were defined as the difference between the measured value and the true value. Experimental error includes fixed error and random error. Fixed error comes from the gross blunders in apparatus or instruments construction while random error is usually caused by personal fluctuations and random electronic fluctuations in apparatus or instruments. It is impossible to know the true value of a quantity, therefore the error cannot be known.

However, if the possible value of error is known, the uncertainty can be defined as that value.

In the present experimental study, the overall experimental uncertainty came from the uncertainty in measuring each individual experimental parameter(s), including flow rate of the hot air, initial particulate loading, mass of stainless steel fibre and temperatures inside the filter. The overall experimental uncertainty was estimated with the method presented by Kline and McClintock (1953) [44]. The measurement uncertainty was obtained based on the accuracy of each measuring instrument. Uncertainty odds should be specified. The odds in the present study were assigned as 20 to 1, i. e., the confidential level was 95%.

Assuming a calculated value "M" is a function of the "b" independent variables, y_1, $y_2 \ldots\ y_b$, i.e.,

$$M = M(y_1, y_2, ..., y_b) \quad \ldots \quad (4.12)$$

Assuming $w_M, w_1, w_2, ..., w_b$ are the estimated uncertainties of M and each of the independent variables, i.e.,

$$M = M \pm w_M \quad \ldots \quad (4.13)$$

$$y_i = y_i \pm w_i \quad \ldots \quad (4.14)$$

If all the independent variables are assigned the same odds, the overall experimental uncertainty can be calculated from equation (4.15) as below:

$$w_M = [(\frac{\partial M}{\partial y_1} w_1)^2 + (\frac{\partial M}{\partial y_2} w_2)^2 + ... + (\frac{\partial M}{\partial y_b} w_b)^2]^{1/2} \quad \ldots \quad (4.15)$$

In this experimental study, the heat release was calculated by equation (4.6) and the overall uncertainty, $w_{\dot{H}_{comb}}$, was determined by the uncertainty in each term, i.e.

$$\dot{H}_{comb} = (m_f c_{p,f} + m_p c_{p,p} + m_a c_{p,a}) \frac{\partial T}{\partial t} + \dot{m}_{a,ex} \cdot h_{a,ex} - \dot{m}_{a,in} \cdot h_{a,in} \quad \ldots \quad (4.6)$$

Using equation (4.15) to estimate the uncertainty, we have:

$$w_{\dot{H}_{comb}} = [(\frac{\partial \dot{H}_{comb}}{\partial m_f}.w_{m_f})^2 + (\frac{\partial \dot{H}_{comb}}{\partial m_p}.w_{m_p})^2 + (\frac{\partial \dot{H}_{comb}}{\partial \frac{\partial T}{\partial t}}.w_{\frac{\partial T}{\partial t}})^2$$

$$+ (\frac{\partial \dot{H}_{comb}}{\partial \dot{m}_{a,ex}}.w_{\dot{m}_{a,ex}})^2 + (\frac{\partial \dot{H}_{comb}}{\partial \dot{m}_{a,in}}.w_{\dot{m}_{a,in}})^2]^{1/2}$$

$$\ldots \quad (4.16)$$

The mass flow rates of air entering and leaving the filter were calculated as below:

$$\dot{m}_{a,ex} = q_{a,ex} \cdot \rho_{a,ex} \quad \ldots \quad (4.17)$$

$$\dot{m}_{a,in} = q_{a,in} \cdot \rho_{a,in} \quad \ldots \quad (4.18)$$

The corresponding uncertainties were:

$$w_{\dot{m}_{a,ex}} = \frac{\partial \dot{m}_{a,ex}}{\partial q_{a,ex}}.w_{q_{a,ex}} \quad \ldots \quad (4.19)$$

$$w_{\dot{m}_{a,ex}} = \frac{\partial \dot{m}_{a,ex}}{\partial q_{a,ex}}.w_{q_{a,ex}} \quad \ldots \quad (4.20)$$

The physical parameters in the experimental study were not constant, but rather varied according to the experimental condition. The overall experimental uncertainty calculated here was based on the physical parameters as presented in the following section. The instrument accuracy uncertainties are given in Table 4.3.

Instrument and Parameter	Uncertainty
K-type Thermocouple, ($w_{\frac{\partial T}{\partial t}}$)	0.1%(1°C)
Electronic balance, (w_{m_f}, w_{m_p})	1%(0.0056kg, 0.0001kg)
Flow meter, ($w_{q_{a,ex}}$, $w_{q_{a,in}}$)	2%(1.5×10^{-5} m^3/s)

Table 4.3 Instrument accuracy and parameter uncertainty

Then:

$$\frac{\partial \dot{m}_{a,in}}{\partial q_{a,in}} = \rho_{a,in} = 0.3925 \text{ kg/m}^3 \quad \ldots (4.21)$$

$$\frac{\partial \dot{m}_{a,ex}}{\partial q_{a,ex}} = \rho_{a,ex} = 0.4149 \text{ kg/m}^3 \quad \ldots (4.22)$$

$$\frac{\partial \dot{H}_{comb}}{\partial m_f} = c_{p,f} \cdot \frac{\partial T}{\partial t} = 461\times0.04 \text{ J/kg-s} \quad \ldots (4.23)$$

$$\frac{\partial \dot{H}_{comb}}{\partial m_p} = c_{p,p} \frac{\partial T}{\partial t} = 1510\times0.04 \text{ J/kg-s} \quad \ldots (4.24)$$

$$\frac{\partial \dot{H}_{comb}}{\partial m_{a,ex}} = h_{a,ex} = 461645 \text{ J/kg} \quad \ldots (4.25)$$

$$\frac{\partial \dot{H}_{comb}}{\partial m_{a,in}} = h_{a,in} = 650321 \text{ J/kg} \quad \ldots (4.26)$$

$$\frac{\partial \dot{H}_{comb}}{\partial \frac{\partial T}{\partial t}} = m_f c_{pf} + m_p c_{pp} + m_a c_{pa} = 17.71 \text{J/°C} \quad \ldots (4.27)$$

From the results as shown above, $\frac{\partial \dot{H}_{comb}}{\partial m_{a,in}}$ was a dominant term such that it had the largest influence on the overall uncertainty. Therefore, the nominal values for equation (4.21-4.27) were chosen according to the value of $h_{a,in}$, as shown above. The nominal value was –310.8 J/s and $w_{\dot{H}_{comb}}$ was 18.35 J/s. The maximum uncertainty of the calculated heat release was therefore suggested to be 5.9%.

4.2.5.4 Instantaneous heat release during regeneration

Operation conditions:

Inlet air flowrate : 90 l/min, Oxygen concentration: 17%,
Initial particulate loading : 10g, Packing density : 1.2%,
Filter thickness : 150mm

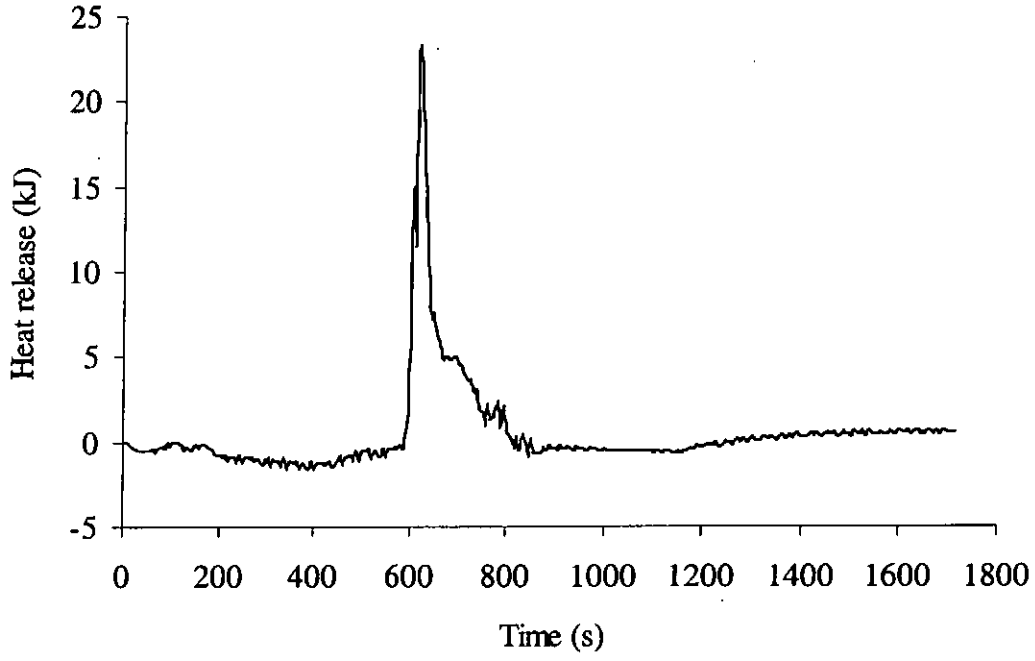

Figure 4.9 Instantaneous heat release throughout the regeneration

Figure 4.9 shows a typical instantaneous global heat release during the regeneration, as calculated from equation (4.7). In the heating up period, the heat release was negative as the filter was mainly heated up by the incoming hot air. Even though minor regeneration might have occurred during this period of time, it could not be reflected in the heat release diagram. During the heat release period, intensive regeneration occurred and there was a sharp increase in the heat release. After a peak heat release had been reached, it dropped down in two consecutive stages: an initial sharp decrease and a subsequent more gentle decrease. The sharp decrease corresponded to a slow down in

thermal regeneration while the gentle decrease corresponded to the situation where regeneration was maintained only in a few zones towards the exit end of the filter.

4.2.6 Axial Temperature Distribution

Figure 4.10 shows the temperature profiles in the axial direction of the filter, the temperature profiles of which are shown in Figure 4.4. It can be observed that the peak filter temperature occurs at the location of 150mm to 180mm away from the inlet position. This phenomenon can be explained by the conservation of energy. As the hot air flowed through the filter, the stainless steel fibres closer to the inlet end absorbed more energy and were heated up earlier than those towards the outlet end. Hence the particulate at the inlet end were ignited earlier than those towards the outlet end. The heat liberated by combustion of the particulate at the inlet end would be carried downstream and absorbed by the fibre and particulate there.

When the particulate at the downstream zones were ignited to liberate energy, it would couple with the energy flowing from the upstream zones to cause a higher increase in temperature. At the exit of the filter, the ambient air tended to cool down the exhaust gas and the cooling effect was transmitted slightly into the filter. Together with the radiative heat loss, the hottest part of the filter was formed slightly inside the filter, as shown in Figure 4.10. This was the situation usually encountered in an enclosure with open ends subjected to internal heating [45]. The stainless steel fibres had been melted in two experiments and it was observed that the molten part occurred at the hottest region.

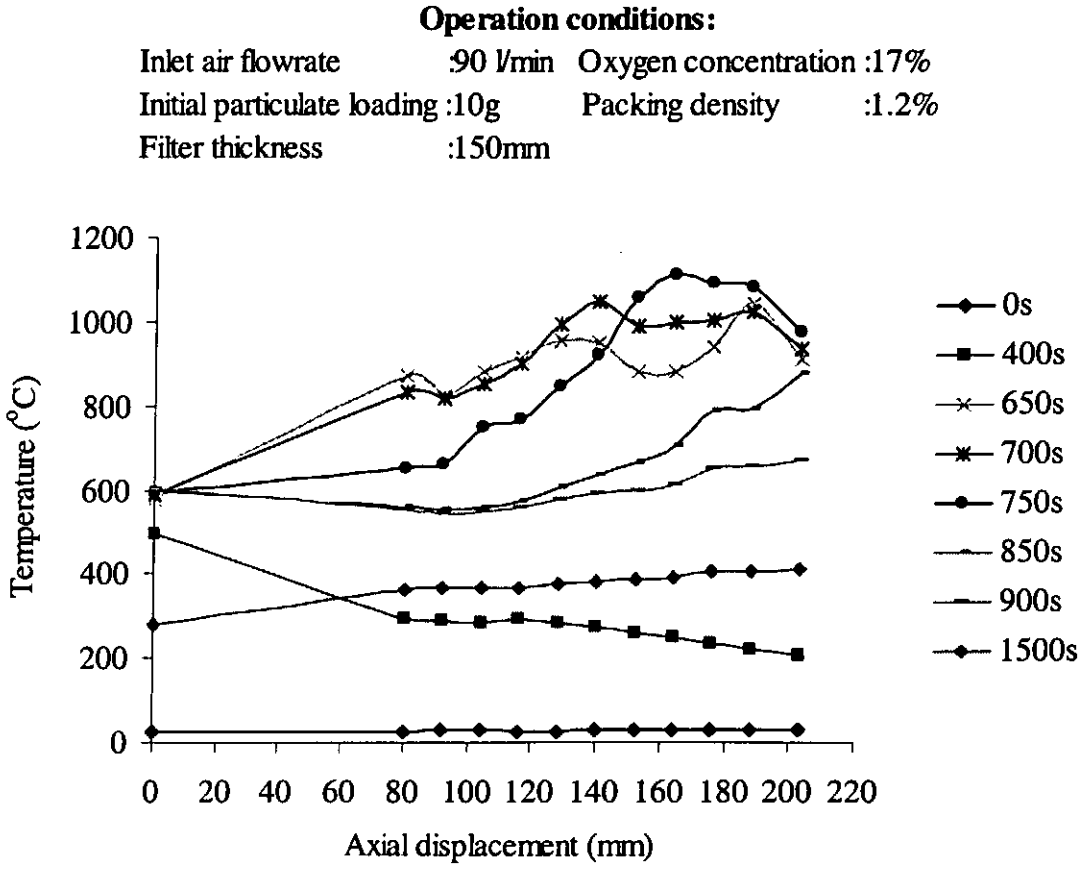

Figure 4.10 Temperature change with respect to axial displacement during regeneration

4.2.7 Axial energy distribution

Figure 4.11 shows the changes in internal energy at the upstream, middle and downstream regions of the metallic fibrous filter during thermal regeneration. The corresponding temperature profiles are shown in Figure 4.4 and Figure 4.10. Values of the change in internal energy were calculated with equations (4.10) and (4.11). Details of the operation conditions are given in the figure above. During the time period of 0s to 600s, which was corresponding to the heating up period as specified in Figure 4.4, the changes in internal energy of the three zones were negative. A negative value indicated that the filtering matrix was absorbing energy from the inlet hot air. For the time period of 600s to 755s, which was corresponding to the heat release period in Figure 4.4,

values of the change in internal energy became positive and increased sharply to the maximum values of 24kJ, 37.7kJ and 47.5kJ at the upstream, middle and downstream of the filter respectively. It was obvious that the change in internal energy at the downstream region of the filter was higher than those at the middle and the upstream regions. It was due to the energy transferred from the upstream region of the filter and the uneven distribution of diesel particulate captured by the filter. The downstream region of the filter was usually accumulated with more diesel particulate such that more intensive oxidation occurred in that region to release more heat. Values of the change in internal energy were still positive after the heat release period. It was because the temperature of the filtering matrix was still higher than that of the inlet hot air. The decrease in internal energy change indicated the filter was cooled by the inlet air. The internal energy change reached zero when temperature of the inlet heat air was same as that of the matrix temperature. The energy supplied to the inlet air was stopped at 1170s. After this time instant, temperature of the inlet air was decreasing so that the filter was cooled down, resulting in a positive internal energy change again.

This analysis indicates that regeneration is most intense at the downstream region of the filter, which hence is the location of damage.

Operation conditions:

Inlet air flowrate : 90 l/min, Oxygen concentration: 17%,
Initial particulate loading : 10g, Packing density : 1.2%,
Filter thickness : 150mm

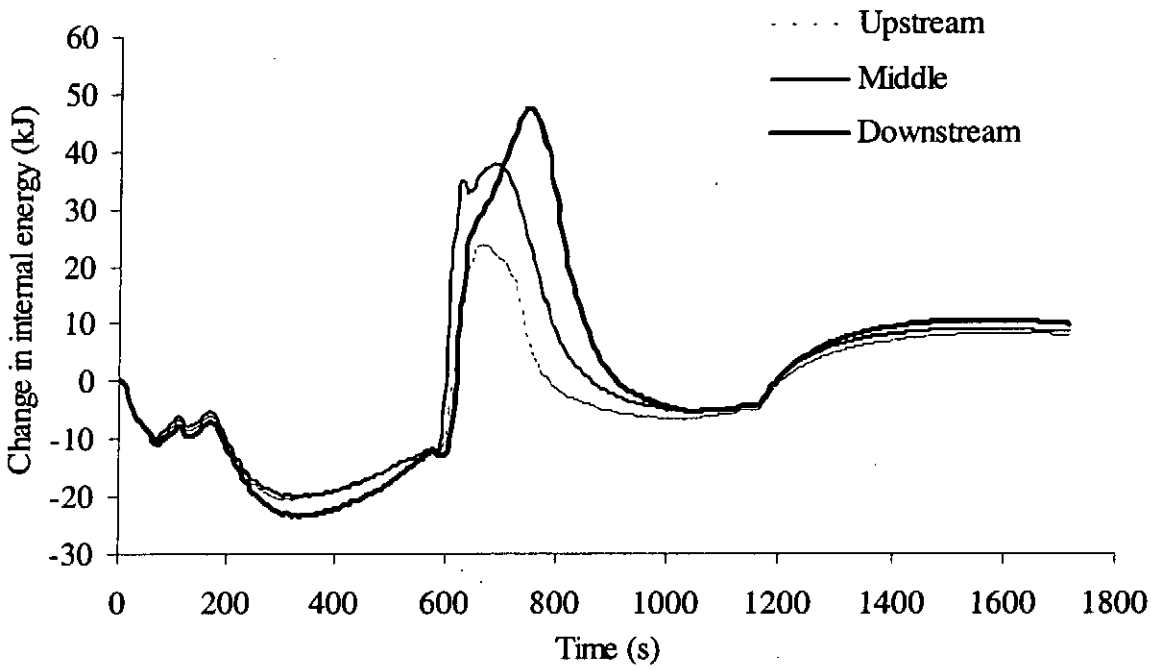

Figure 4.11 Change in internal energy in different zones of the filter

4.2.8 Effect of influencing parameters

In addition to the investigation of the regeneration phenomenon, effects of different influencing parameters including inlet air flow rate, inlet air oxygen concentration, packing density of filter, thickness of filter and initial particulate loading of the filter, on the regeneration were also investigated. The results are shown in Figure 4.12 to Figure 4.20. In these figures, t=0 corresponds to the time when the inlet air reaches 500°C. In each case, comparisons are made with respect to the temperature profiles and the instantaneous heat release. The former is a comparison on local behaviour while the latter is a comparison of the summed behaviour of the regeneration process. The results had also been compared with those of Kim et al. [31] and Park et al. [32] obtained

experimentally with ceramic filter and the simulated predictions of Garner and Dent [33].

4.2.8.1 Effect of oxygen concentration of inlet hot air

Figure 4.12 and Figure 4.13 show the effect of oxygen concentration on the regeneration. The peak filter temperature and the peak heat release increased as the oxygen concentration was increased. The effect on the peak filter temperature agrees with the work done by Kim et al. [31] and Park et al. [32]. However, Garner and Dent [33], based on their simulated results, suggested that the oxygen concentration affects the regeneration time but not the peak temperature.

The reaction rate between the particulate and the hot air should be proportional to the oxygen concentration. During the heating up period, some oxidation of the particulate could have occurred at random locations and hence an increase in oxygen concentration would enhance these local and small scale particulate burning, which could then speed up the heating up process. The reaction rate was higher as more oxidizer was supplied, which led to a more rapid combustion and consequently the heat release. When the oxygen concentration is low, part of the particulate captured inside the filter had not been oxidized due to insufficient supply of oxidizer. Therefore the total heat release was lower when the oxygen concentration was lower.

Operation conditions:

Inlet air flowrate: 90 l/min, Filtering element thickness: 150mm
Packing density : 1.2%, Initial particulate loading : 10g
Oxygen concentration: 13% and 21%

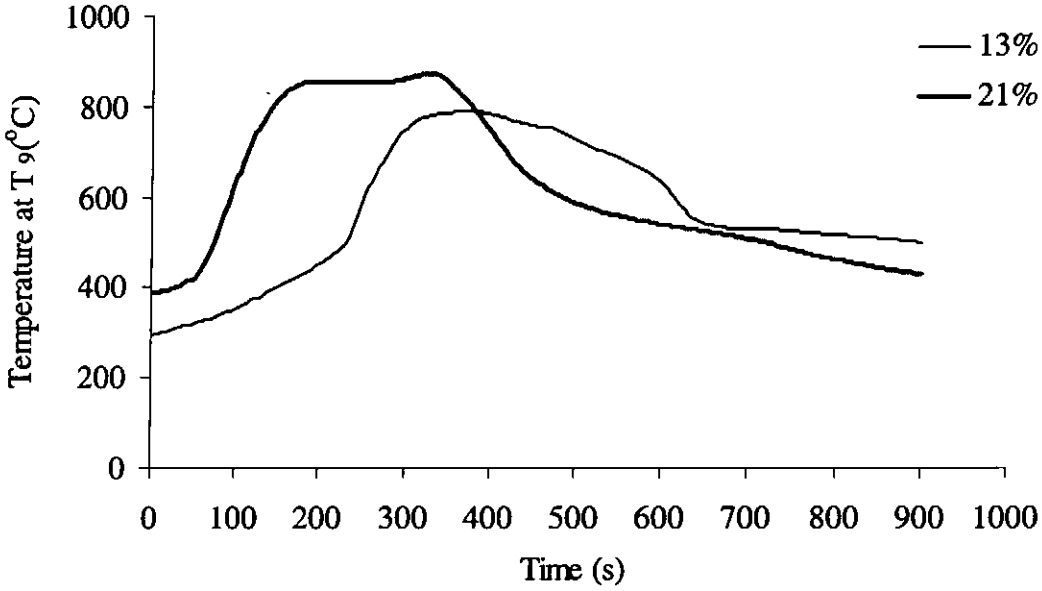

Figure 4.12 Effect of oxygen concentration on filter temperature

Operation conditions:

Inlet air flowrate: 90 l/min, Filtering element thickness: 150mm
Packing density : 1.2%, Initial particulate loading : 10g
Oxygen concentration: 13% and 21%

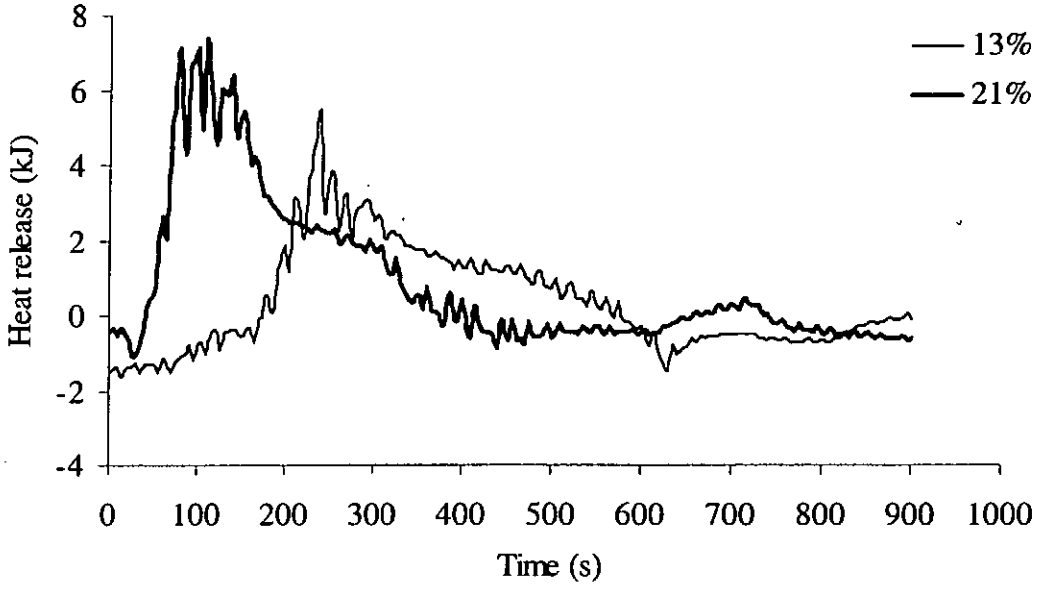

Figure 4.13 Effect of oxygen concentration on heat release

4.2.8.2 Effect of flow rate of inlet hot air

Figure 4.14 and Figure 4.15 show the effect of change in flow rate of the inlet hot air on the regeneration. At a higher flow rate, the regeneration occurred earlier but the peak filter temperature and the peak heat release were lower, which were inline with the findings of Kim et al. [31] and Park et al. [32]. Garner and Dent [33], however, suggested that the change in inlet gas flow rate only affected the regeneration time.

A higher flow rate will provide a larger energy input to the filter and hence achieve an earlier heating up and particulate oxidation. However, the higher flow rate also carries away a larger amount of heat generated during the particulate oxidation. It is therefore quite reasonable to have an earlier regeneration, lower peak temperature and lower peak heat release associated with the higher flow rate of inlet hot air.

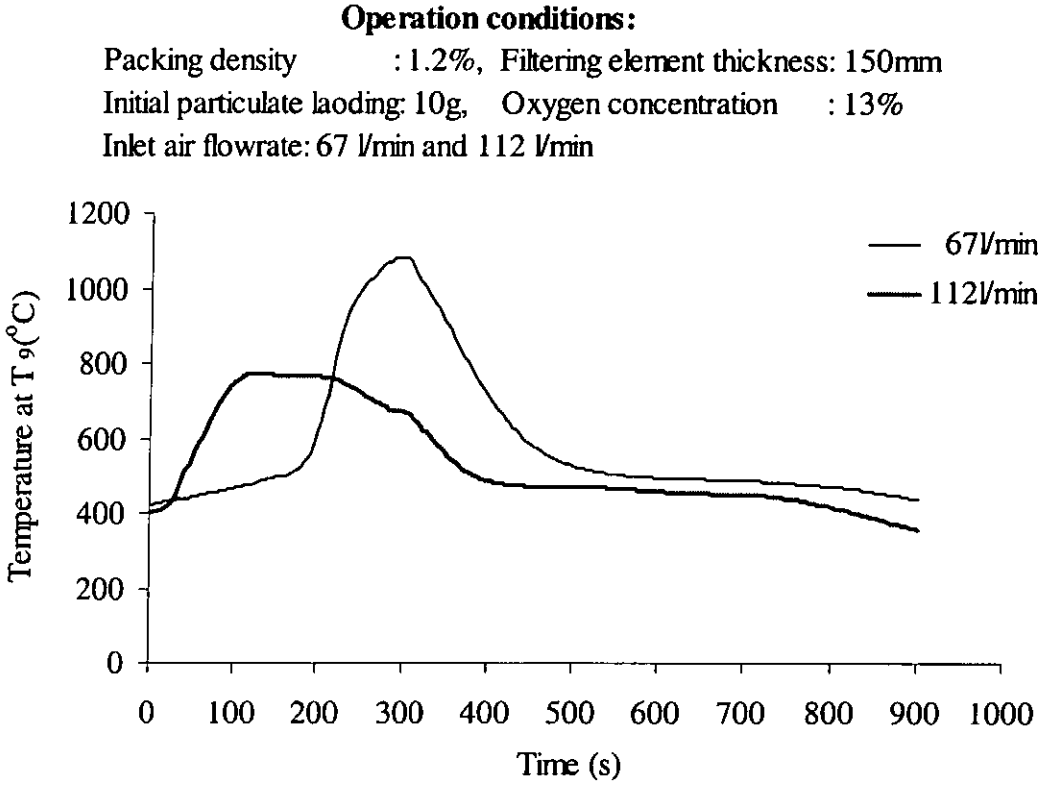

Figure 4.14 Effect of inlet air flow rate on filter temperature

Operation conditions:

Packing density : 1.2%, Filtering element thickness: 150mm
Initial particulate laoding: 10g, Oxygen concentration : 13%
Inlet air flowrate: 67 l/min and 112 l/min

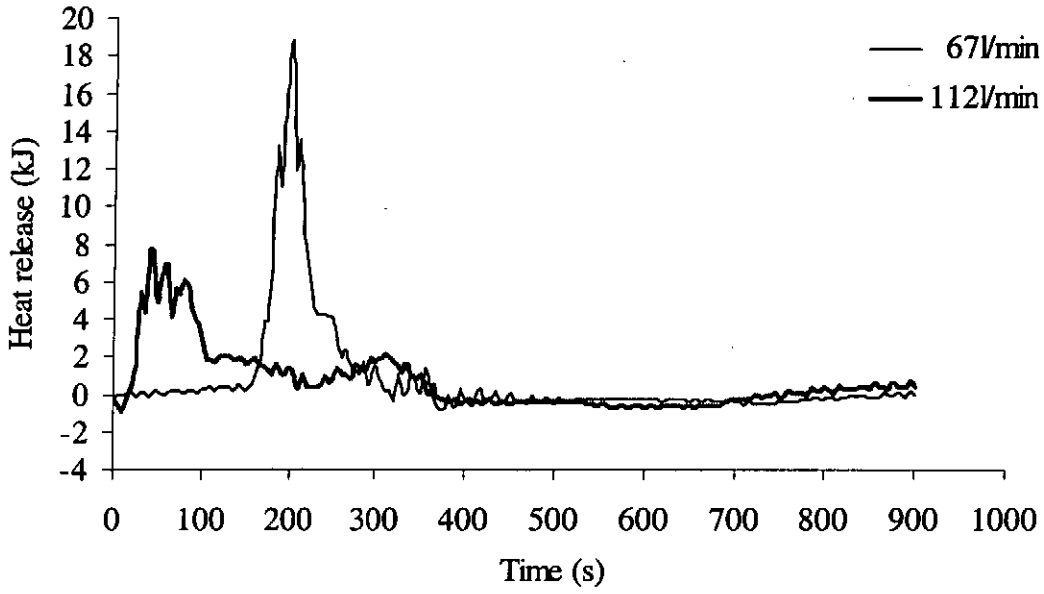

Figure 4.15 Effect of inlet air flow rate on heat release

4.2.8.3 Effect of packing density of filtering element

Effect of packing density of the filter on the regeneration is shown in Figure 4.16 and Figure 4.17. The peak filter temperature and the peak heat release were more or less the same for the two values of packing density, but the thermal regeneration was found to start earlier for a filter with a lower packing density. At a lower packing density, the heating up of less material inside the filter should be faster.

Operation conditions:

Inlet air flowrate : 90 l/min, Initial particulate loading : 10g
Oxygen concentration: 21%, Filtering element thickness: 150mm
Packing density: 0.8% and 1.2%

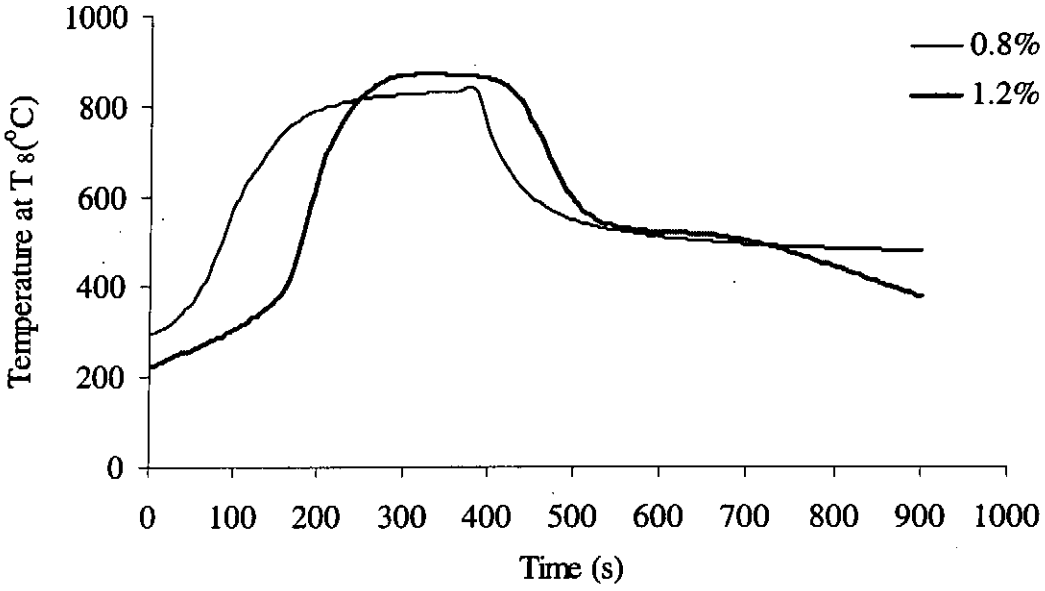

Figure 4.16 Effect of packing density on filter temperature

Operation conditions:

Inlet air flowrate : 90 l/min, Initial particulate loading : 10g
Oxygen concentration: 21%, Filtering element thickness: 150mm
Packing density: 0.8% and 1.2%

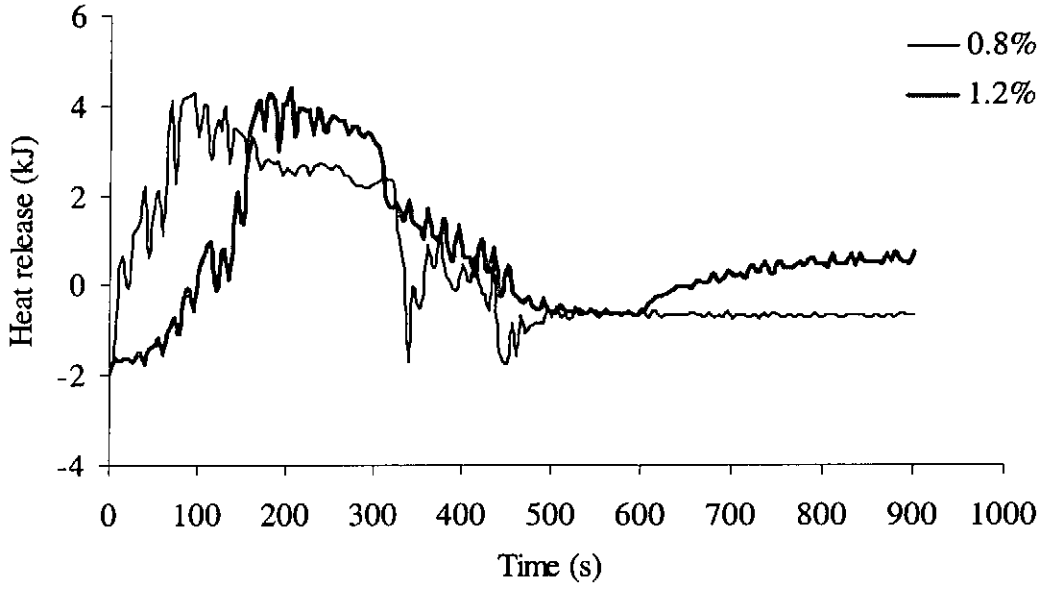

Figure 4.17 Effect of packing density on heat release

4.2.8.4 Effect of thickness of filtering element

It was found that regeneration could not take place when thickness of the filter was reduced to smaller than 50mm with an initial particulate loading of 3.3 grams as shown in Figure 4.18. The energy contained in the hot air was distributed to the filter, its casing and the exhaust. The shorter the filter, the larger will be the ratio of energy loss to the casing and the exhaust. Therefore, a short filter will have difficulty in accumulating sufficient energy for the regeneration to occur.

Operation conditions:
Inlet air flowrate: 90 l/min, Oxygen concentration : 13%
Packing density : 1.2%, Initial particulate loading: 3.3g and 10g
Filtering element thickness: 50mm and 150mm

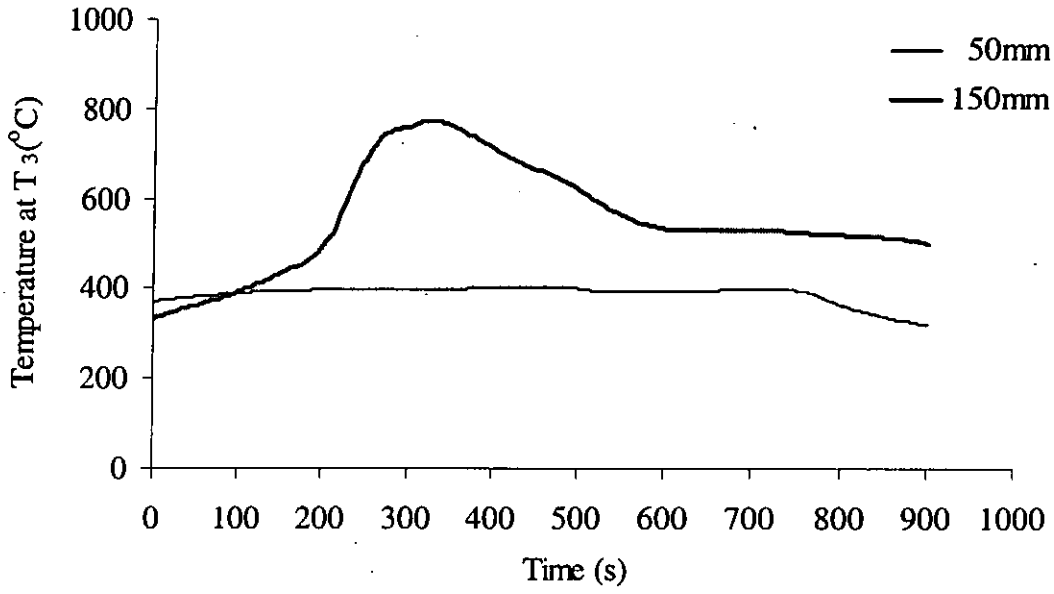

Figure 4.18 Effect of filter thickness on filter temperature

4.2.8.5 Effect of initial of particulate loading of filtering element

Particulate acts as the fuel in the regeneration process. Effects of initial particulate loading of the filter are shown in Figure 4.19 and Figure 4.20. The peak filter temperature and the peak heat release increased as the initial particulate loading

increased because more fuel was available for regeneration. In Figure 4.20, the instantaneous peak heat release were the same but the total heat release for the 10g case was correspondingly higher than that of the 8g case. For the same reason, regeneration started earlier at a higher initial particulate loading. When the initial particulate loading was reduced to 2 grams, no regeneration was recorded. Garner and Dent [33], Kim et al. [31] and Park et al. [32] also suggested that an increase in initial particulate loading would increase the peak temperature of the filter.

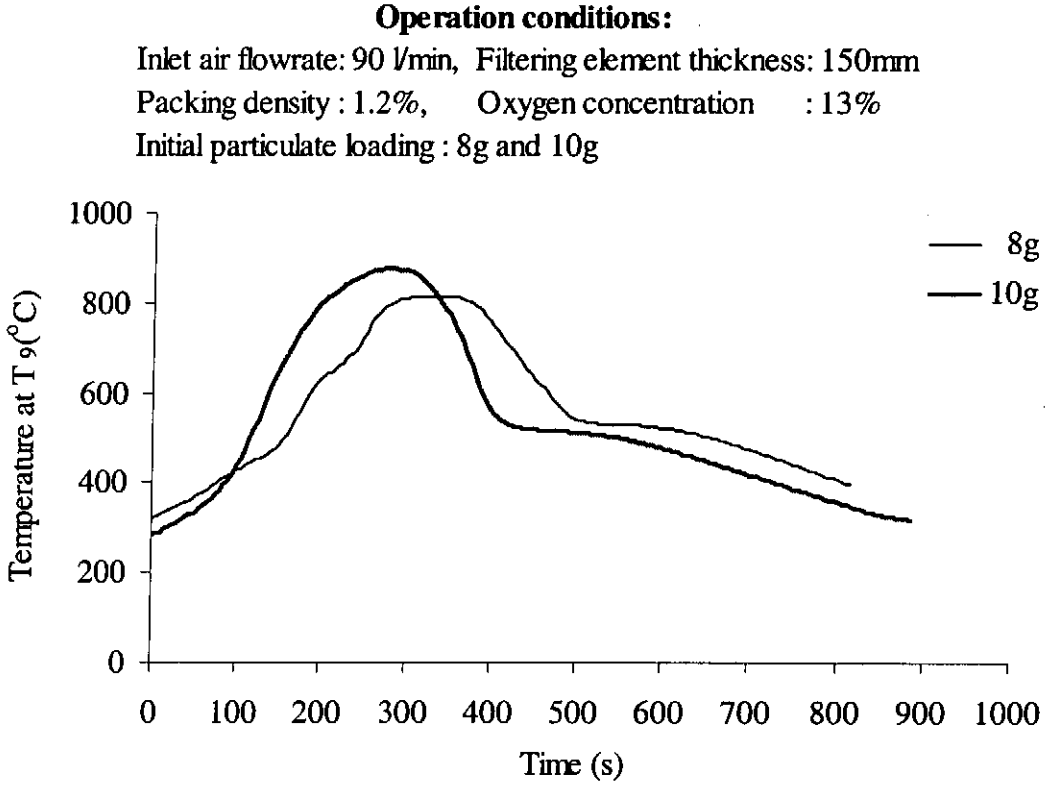

Figure 4.19 Effect of initial particulate loading on filter temperature

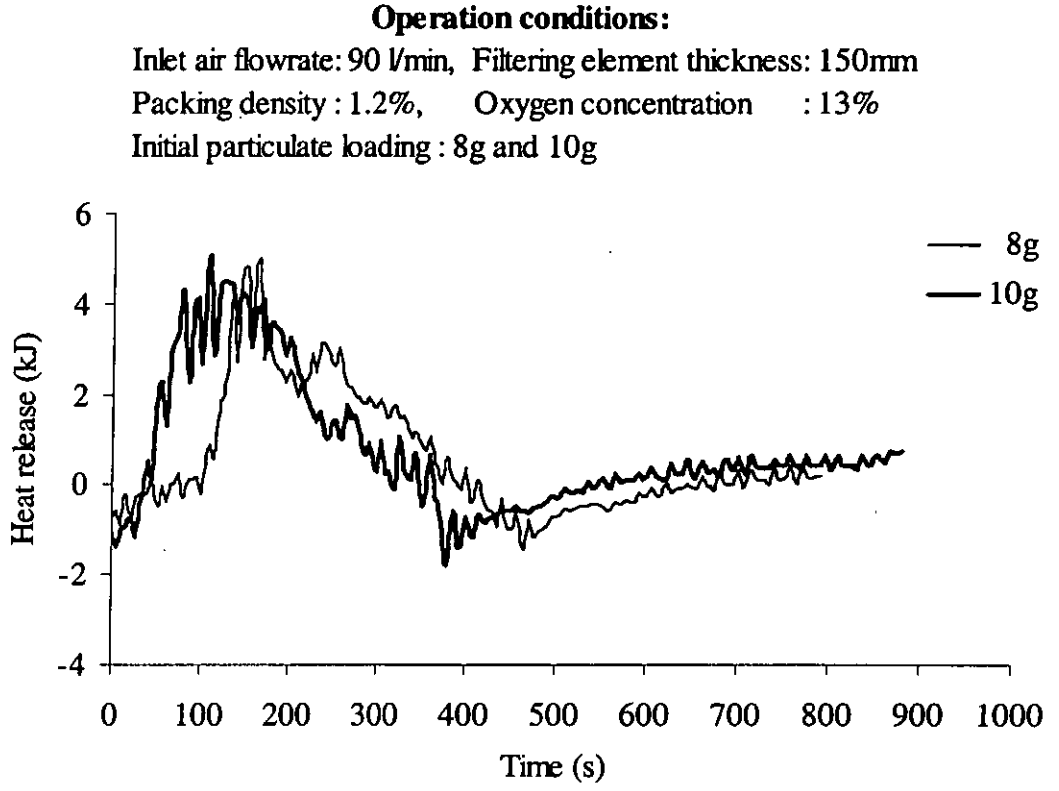

Figure 4.20 Effect of initial particulate loading on heat release

4.2.9 Summary of experimental study

A test rig had been constructed for studying the thermal regeneration of a metallic fibrous filter. The test rig enabled thermal regeneration to be initiated and the various parameters affecting the regeneration to be studied. This is the first systematic experimental study on the thermal regeneration of a metallic fibrous filter loading with diesel particulate.

Based on the measured temperature profiles, the regeneration process can be divided into three periods, namely, the heating up period, the heat release period and the cooling down period. These are in line with the results of previous investigators who performed experimental studies on ceramic filters.

Based on the temperature profiles, the heat release rate of the regeneration process was also derived and which provide further information for understanding the regeneration process.

Effect of the experimental parameters had been discussed in detail in the previous section individually. The significance of the parameters and the interaction between them will be discussed below. The thickness of the filtering element is a causal parameter since regeneration could not be performed when the thickness is 50mm or smaller from the experimental observation within the present range of parameter. Oxygen concentration and the flow rate of incoming air have great effect on the peak filter temperature. In order to avoid melting of the filtering matrix, the incoming air should have a low oxygen concentration of 13% and but a high flow rate of 112 l/min. The initial particulate loading has small effect on the peak filter temperature. Packing density in the range of this study has no obvious effect on the regeneration behaviour of the filter. It may have influence on the filtering efficiency instead.

The experimental results obtained will provide data for analytical and numerical study of the thermal regeneration of the metallic fibrous filter.

CHAPTER 5 NUMERICAL MODELLING

5.1 Introduction

In addition to the experimental investigation on the thermal regeneration of the metallic fibrous filter, a numerical model was developed to simulate the oxidation of diesel particulate and the heat transfer processes inside the filter. Numerical model is a very useful tool to assess and investigate a complicated problem involving many physical phenomena, especially in the situations where experimental studies are not cost effective and become difficult. Besides, the information extracted during derivation of the model can provide solid understanding of the problem. In this study, with the aid of the developed numerical model, further investigation of the effects of the influencing parameters can be conducted.

This chapter describes the development of the numerical model, including the assumptions made. The model consists of two parts: one part is concerned with diesel particulate oxidation while the other part is on the heat transfer process. Both parts of the model were developed essentially with fundamental equations, including the oxidation rate equation of diesel particulate and the energy equation. However, empirical expressions for some physical parameters had been employed such as the heat transfer coefficient in the energy equation and the rate coefficient in the oxidation rate equation. Numerical results will be presented in this chapter and compared with the experimental findings in Chapter 6.

5.2 Oxidation of diesel particulate inside the filter

5.2.1 Background of the problem

When the metallic fibrous particulate filter has been over-accumulated with diesel particulate, thermal regeneration will be carried out to retain its efficiency and reduce fuel penalty. The main process of thermal regeneration is oxidation of diesel particulate collected. The particulate can only be oxidized when its temperature is high enough and an oxidizer is available. Both of them are supplied from the inlet hot air. The particulate oxidation model is focusing on the rate of chemical reaction.

5.2.2 Heterogeneous reaction

Burning of solid is different from burning of gas since the former is a heterogeneous reaction while the later is a homogeneous one. A heterogeneous reaction involves species existing in different physical states, i.e., gas-liquid and gas-solid. The oxidation of diesel particulate is certainly the gas-solid reaction. The gas-solid reaction was subdivided into the following constituent processes by Gardiner [43]:

1. Transport of the reactant molecule to the surface by convection and/or diffusion.
2. Adsorption of the reactant molecule on the surface.
3. Elementary reaction steps involving various combinations of adsorbed molecules, the surface itself, and gas-phase molecules.
4. Desorption of product molecules from the surface.
5. Transport of the product molecules away from the surface by convection and/or diffusion.

Diesel particulate was assumed to be carbonaceous substance and development of the oxidation model was based on the burning mechanism of carbon. The principal product at the carbon surface is CO, which diffuses away from the surface through the boundary layer where it combines with the inward-diffusing O_2 according to the following global homogeneous reactions:

Gas-phase reaction:

$$CO + \frac{1}{2}O_2 \rightarrow CO_2 \quad \ldots \quad (5.1)$$

Carbon surface heterogeneous reactions:

$$C + O_2 \rightarrow CO_2 \quad \ldots \quad (5.2)$$

$$2C + O_2 \rightarrow 2CO \quad \ldots \quad (5.3)$$

$$C + CO_2 \rightarrow 2CO \quad \ldots \quad (5.4)$$

$$C + H_2O \rightarrow CO + H_2 \quad \ldots \quad (5.5)$$

As a result, the overall reaction of the carbon oxidation is represented by:

$$C + O_2 \rightarrow CO_2 \quad \ldots \quad (5.6)$$

In general, burning of solid can be diffusionally, intermediately or kinetically controlled. In the present study, oxygen was continuously supplied by the inlet hot air and the porosity of the filter was very high. Oxygen gas could easily diffuse to the surface of the diesel particulate thus the oxygen concentration at its surface was high. Hence, oxidation of the diesel particulate was assumed to be kinetically controlled and the reaction rate, R, is of the following form:

$$R = K \cdot [O_2]' \qquad \ldots \quad (5.7)$$

where K is the rate coefficient and $[O_2]'$ is the molar concentration of oxygen.

5.2.3 Oxidation model

Since the filter was installed onto the tailpipe of a motor vehicle for the collection of diesel particulate, the distribution of particulate captured could not be controlled and local variation might exist. It is difficult to obtain the distribution of particulate within the filter and it is beyond our scope of study. An assumption, as stated above, had been made that the particulate was evenly distributed inside the entire filter. In fact, the same assumption was used by other investigators [24, 33, 36].

The oxidation model was thus established with the following assumptions:

1. Diesel particulate was evenly distributed inside the filtering matrix.
2. The accumulated diesel particulate was considered to have the same local temperature as the fibrous matrix.
3. The reaction rate was assumed to be kinetically controlled.
4. Particulate was carbonaceous, such that the heterogeneous chemical reaction between the carbon and oxygen, i.e., $[C + O_2 \rightarrow CO_2]$, was applied.
5. The particulate started to oxidize when their temperature was reaching 500°C [7].

Several models for the oxidation of carbon particles and diesel particulate were found from the literatures. Peterson [15] gave the expression for the carbon oxidation rate as below:

$$R = -\frac{1}{A_c}\frac{dm_c}{dt} = KP_{Ox}^{q} \quad \ldots \quad (5.8)$$

Wang et al. [34] gave the following expression for the mass burning rate of diesel particulate:

$$\dot{m}_p = m_p A[O_2]\rho_{O_2} \exp(-\frac{E}{R_u T}) \quad \ldots \quad (5.9)$$

The mass of particulate left at time, t, can be calculated with the following expression:

$$m_p = m_{po} \exp(-\dot{m}_p t) \quad \ldots \quad (5.10)$$

Equations (5.7) and (5.9) are of the same form, because in equation (5.7), the rate coefficient, K, is usually assumed to be in the Arrhenius form as follows:

$$K = A \cdot \exp(\frac{-E}{R_u T}) \quad \ldots \quad (5.11)$$

where A is the frequency factor, E is the activation energy and R_u the universal gas constant.

Equation (5.9) and (5.10) had been adopted in the present model to calculate the oxidation rate of particulate and the mass of particulate left after each time-step respectively. However, a proper rate coefficient has to be determined.

Various researchers had derived expressions for the rate coefficient for carbon-oxygen reaction. Garner and Dent [33] surveyed a number of expressions and found great variation between them. They finally adopted an expression, K_1, as shown below, in their regeneration model for monolith and fibrous traps, which gave a reaction rate

within the range of those obtained by the different investigators they had surveyed. Wang et al. [34] used an expression, K_2, to simulate the thermal regeneration of diesel particulate trap with cerium foam element. Marcuccilli et al. [46] performed experiments for measuring soot reactivity and based on their experimental results, they suggested another empirical expression, K_3, for the rate coefficient. The unit of the frequency factors of these expressions are slightly different. These expressions are shown below:

$$K_1 = 1\times10^5 \exp(\frac{-54500}{8.314\times T}) \quad \ldots (5.12)$$

$$K_2 = 3\times10^5 \exp(\frac{-111000}{8.314\times T}) \quad \ldots (5.13)$$

$$K_3 = 6.9\times10^{12} \exp(\frac{-207000}{8.314\times T}) \quad \ldots (5.14)$$

It has to be determined if any of these rate coefficients could be applied in this study.

In Chapter 4, equation (4.6) was applied to calculate the energy released during regeneration, using the measured temperature data. A reverse method was adopted here for determining if any of the rate coefficients specified above was suitable for this study. In this reverse method, it was assumed that diesel particulate was regenerated according to equation (5.9) while a temperature T could be solved to represent the temperature of the filter. The total energy release could then be calculated and should match with the energy released as calculated by equation (4.6) and the temperature T thus simulated should match with a typical temperature profile in the filter. Based on the above, the energy equation governing this reverse method can be represented by:

$$(m_a c_{p,a} + m_f c_{p,f}) \frac{\partial T}{\partial t} = \dot{m}_p U + \dot{m}_{a,in} \cdot h_{a,in} - \dot{m}_{a,ex} \cdot h_{a,ex} \quad \ldots \quad (5.15)$$

where U is the calorific value of carbon particle and $\dot{m}_p$ is calculated from equation (5.9). In equation (5.15), the two terms on the left hand side are the change of internal energy of fibre and air inside the filter with respect to time, the first term on the right hand side is the rate of heat release during combustion of particulate, the last two terms are the energies carried in and out by air.

The above model was solved numerically using the finite difference method. Thus equation (5.15) can be rewritten as below:

$$(m_a c_{p,a} + m_f c_{p,f}) \frac{T_{(i+1)} - T_{(i)}}{\Delta t} = m_p A[O_2] \rho_{O_2} \exp[\frac{-E}{R_u T_{(i)}}] \cdot U + \dot{m}_{a,in} \cdot h_{a,in} - \dot{m}_{a,ex} \cdot h_{a,ex}$$

$$\ldots \quad (5.16)$$

$$T_{(i+1)} = \frac{m_p A[O_2] \rho_{O_2} \exp[\frac{-E}{R_u T_{(i)}}] \cdot U + \dot{m}_{a,in} \cdot h_{a,in} - \dot{m}_{a,ex} \cdot h_{a,ex}}{(m_a c_{p,a} + m_f c_{p,f})} \cdot \Delta t + T_{(i)} \quad \ldots \quad (5.17)$$

The temperature of the filter is written explicitly in equation (5.17). The filter is heated up from room temperature so that $T_{(0)}$ is equal to 25°C, i.e. the initial condition. The temperature of air at the inlet of the filter is input from the experimental data such that they are known at every time-step. The temperature of air at the outlet of the filter is considered to be the same as that of the filter. With such information, simulation was carried out for each of the Arrhenius expressions, K_1, K_2 and K_3.

Figure 5.1 compares the simulated temperature profiles obtained with different Arrhenius expressions to the experimental results. T_5 was chosen to represent the temperature of the filter, because it could better reflect the nominal temperature of the filter. It can be observed that the simulated temperature obtained from the Arrhenius expression, K_2, showed a very good agreement with the experimental results. The magnitude and the timing of appearance of the regeneration peak temperature were the closest to the experimental results. Besides, the total heat releases calculated from the simulations using, K_1, K_2 and K_3, were 7 kJ, 168 kJ and 82 kJ respectively, while the total heat release as calculated from the experimental data was 168 kJ. Hence, K_2 was chosen to be the rate coefficient in this study.

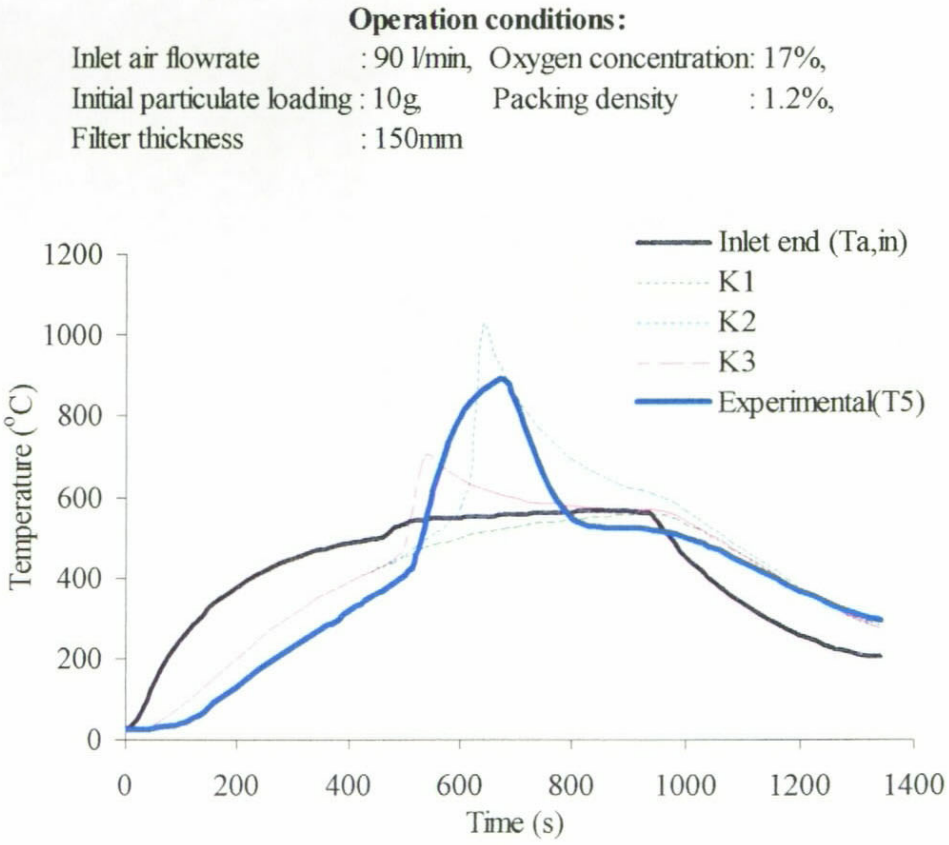

Figure 5.1 Comparison of simulated temperature profiles to experimental result

5.3 Heat transfer inside the filter

5.3.1 Introduction

In the presence of oxidizer, the diesel particulate can only be oxidized when their temperature is high enough. In the present study, diesel particulate was heated up to their ignition temperature by the inlet hot air. A heat transfer model is required to simulate the transfer of the regeneration energy to the stainless steel fibres and the gas surrounding the fibres.

5.3.2 Convective heat transfer inside the filter

Convection was normally a major form of heat transfer in a flow process. The energy equations including convection for solid-phase and gas-phase could be written as follows:

For solid-phase:

$$(1-\phi)\rho_s v_{filter} c_{p,s} \frac{\partial T_s}{\partial t} = \dot{m}_p U + h_{conv} a_{conv} v_{filter} (T_a - T_s) + (1-\phi) v_{filter} k_s \frac{\partial^2 T_s}{\partial x^2} \quad \ldots \quad (5.18)$$

For gas-phase:

$$\phi \rho_a u_a c_{p,a} \frac{\partial T_a}{\partial x} = h_{conv} \cdot a_{onv} \cdot (T_s - T_a) \quad \ldots \quad (5.19)$$

In equation (5.18), the left hand side represented the change in internal energy of the solid phase with respect to time. The first term in the right hand side represented the energy release from the oxidation process of diesel particulate. The second term

represented the convective heat transfer between the gas-phase and the solid-phase. The third term represented the conductive heat transfer in the solid-phase. In equation (5.19), the left hand side represented the change in internal energy of gas in the axial direction while the right hand side was the convective heat transfer between solid and gas.

Empirical expression for the prediction of convective heat transfer coefficient, h_{conv}, which can be exactly applicable to the present situation has not been found in literatures. However, it might significantly affect the overall heat transfer rate throughout the entire thermal regeneration process of the filter. Expression used to calculate the average convective heat transfer coefficient for flow across cylinders as suggested by Hilpert [47] and Katz [47] may be suitable for the present study:

$$\frac{hd}{k_f} = C_1 \left(\frac{u_\infty d}{\nu_f} \right)^p \mathrm{Pr}_f^{1/3} \quad \ldots \quad (5.20)$$

The constant "C_1" and power index "p" depend on value of the Reynolds number. This expression is valid for the range of Reynolds number from 0.4 to 4×10^5. Fand [47] showed that the heat transfer coefficient from liquid to cylinder in cross flow might be better represented by:

$$Nu_f = (0.35 + 0.56\,\mathrm{Re}_f^{\,0.52})\,\mathrm{Pr}_f^{\,0.3} \quad \ldots \quad (5.21)$$

This relationship is valid for $10^{-1} < \mathrm{Re_f} < 10^5$, when excessive free-stream turbulence is not encountered.

Empirical expressions to determine the heat transfer coefficients in porous media, which may be useful, are available in literatures. Lee et al. [48] used the following equation to calculate the convective heat transfer in a channel filled with porous media:

$$Nu = \frac{4h_w H}{k_{f,eff}} \quad \ldots (5.22)$$

The above equations had been applied in turn, but were found not suitable to the present study for the following reasons. The flow velocity inside the multi-channels of the filter is much slower than that over a cylinder. Flow over a cylinder will be less restricted than that in a small channel and lead to a much higher heat transfer coefficient. Therefore the expressions for flow across a cylinder are not appropriate. Moreover, the ratio of surface area to volume of the fibrous filter is much higher than that of the porous media. Ratio between conduction, convection and radiation would be significantly affected, and therefore expressions for heat transfer in porous media are not suitable. The convective heat transfer in the present case will be overestimated by many times if they are calculated from those expressions.

It was found that reasonable simulated results were obtained only when the value of the convective heat transfer was suppressed to a small value. In order to solve this problem, the change in enthalpy of gas was included in the numerical model instead of considering the convective heat transfer directly.

5.3.3 Overall heat transfer model

The stainless steel fibres were randomly and loosely packed inside the filter casing. The micro-channels inside the fibre matrix were very small. With the large interfacial area between the fibre matrix and gas, it was reasonable to assume that the gas temperature was equal to that of the fibre matrix. Moreover, the present model does not consider the heat transfer between solid and gas but rather between zones inside the filter. The

viewing factor from one zone to another is very small because most of the paths are blocked by the irregular arrangement of stainless steel fibres. Therefore radiation emited from one zone can hardly reach another zone. Furthermore, the working fluid in the present situation is air, which is considered as clear gas so that it absorbs little radiation emitted from particulate and fibres. Therefore it is reasonable to neglect the radiation effect in the present model. Garner and Dent neglected the radiation effect in their simulation on the thermal regeneration of fibrous filter [33]. Besides, Romero-Lopez et al. [24] and Stanmore et al. [22] also neglect radiation in their soot burning model. The overall heat transfer model was then setup based on these major assumptions. In addition, the following assumptions had also been made:

1. A single zone inside the filter had a uniform temperature.
2. Heat transfer was one-dimensional.
3. Inlet hot air flow rate was steady.
4. The heat released in the combustion was totally absorbed by the fibrous matrix.
5. The particulate accumulated on the fibre surface had the same local temperature as the fibrous matrix.
6. Negligible heat loss to surroundings was assumed since the filter was thermally insulated by a thick glass-fibre blanket.

The fibrous filter was heated up by the inlet hot air. Upstream region of the filter was heated up earlier to set up a temperature gradient so that conduction carried out within the solid-phase. The hot air leaving the upstream region also carried heat energy to heat up the downstream region. When the fibre matrix reached the ignition temperature of

diesel particulate at 500°C, it was oxidized to release heat energy. This would cause an increase in internal energy of the filter. The energy equation can be represented by:

$$(m_a c_{p,a} + m_f c_{p,f}) \frac{\partial T}{\partial t} = \dot{m}_p U + (1-\phi) k_s \frac{\partial^2 T}{\partial x^2} + \dot{m}_a \cdot \Delta h_a \quad \ldots \quad (5.23)$$

In equation (5.23), the term in left hand side was the rate of change in internal energy of gas and fibre matrix of the filter. The first term in the right hand side was the heat release rate from the oxidation of diesel particulate. The second term in the right hand side was the conduction of heat inside the fibre matrix. The last term in the right hand side was the rate of change in enthalpy of gas inside the filter. The equation can be applied to the filter as a whole or to discrete zones of a filter. It can be solved numerically to obtain the temperature of filter or temperature of discrete zones.

5.3.4 Calculation of the numerical model

In order to compare the experimental results with the numerical predictions, the entire fibrous filter is divided into "n" zones of same volume and geometry. The discrete zone volume, v_{filter}, is given by dividing the total volume of the filter, V_{filter}, by the number of zones, n, as below:

$$v_{filter} = \frac{V_{filter}}{n} \quad \ldots \quad (5.24)$$

Similarly, the mass of fibre, m_f, and diesel particulate, m_p, in a discrete zone are given below:

$$m_f = (1-\phi) \rho_f \cdot v_{filter} \quad \ldots \quad (5.25)$$

$$m_p = \frac{M_p}{n} \qquad \ldots \quad (5.26)$$

With the above information, the mathematical model could be solved numerically. Opris and Johnson [35] solved a 2-D computational model describing the heat transfer, reaction kinetics and regeneration characteristics of a ceramic diesel particulate trap by discretizing the governing equations using forward time, backward space for the convective terms and central space for the conductive term. This discretization method would be employed to solve the overall heat transfer model in the present study.

Figure 5.2 shows the notation of temperature at the i^{th} time step for the overall heat transfer model consisting of "n" zones.

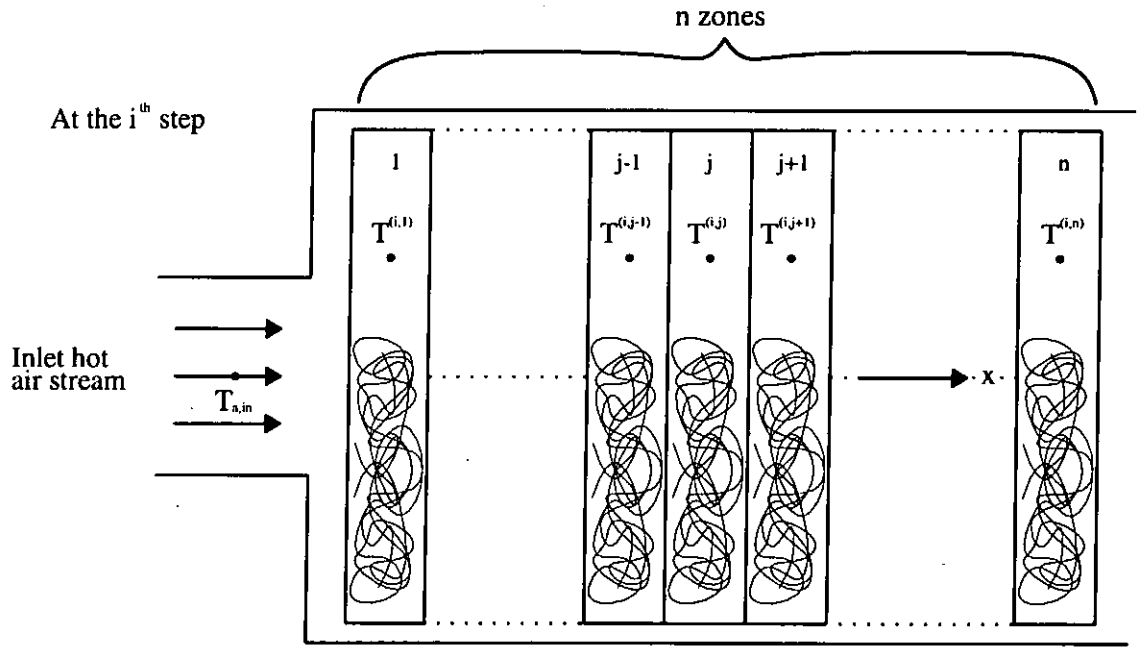

Figure 5.2 Notation of temperature at the i^{th} time step for the overall heat transfer model

Using finite difference method, equation (5.23) can be rewritten as:

$$(m_a c_{p,a} + m_f c_{p,f}) \frac{T_{(i+1,j)} - T_{(i,j)}}{\Delta t} = \dot{m}_p U + (1-\phi) k_s \frac{T_{(i,j+1)} + T_{(i,j-1)} - 2T_{(i,j)}}{(\Delta x)^2} + \dot{m}_a \cdot (h_{a(i,j-1)} - h_{a(i,j)})$$

... (5.27)

Equation (5.27) can be rearranged to give:

$$T_{(i+1,j)} = T_{(i,j)} + \frac{\left[\dot{m}_p U + (1-\phi) k_s \frac{T_{(i,j+1)} + T_{(i,j-1)} - 2T_{(i,j)}}{(\Delta x)^2} + \dot{m}_a \cdot (h_{a(i,j-1)} - h_{a(i,j)}) \right] \cdot \Delta t}{m_a c_{p,a} + m_f c_{p,f}}$$

... (5.28)

Let:

$$\Delta T = \frac{\left[\dot{m}_p U + (1-\phi) k_s \frac{T_{(i,j+1)} + T_{(i,j-1)} - 2T_{(i,j)}}{(\Delta x)^2} + \dot{m}_a \cdot (h_{a(i,j-1)} - h_{a(i,j)}) \right] \cdot \Delta t}{m_a c_{p,a} + m_f c_{p,f}}$$

Then:

$$T_{(i+1,j)} = T_{(i,j)} + \Delta T \quad \text{... (5.29)}$$

5.3.5 Input data for numerical model

The data used for the numerical model are shown in the following table:

Fibre Size	0.4 (H) x 0.04 (W)	(mm^2)
Specific heat capacity of steel fibres, c_{pf}	0.46	(kJ/kgK)
Density of stainless steel fibres, ρ_f	7100	(kg/m^3)
Thermal conductivity of steel fibres, k_f	0.05	(kW/mK)
Calorific value of particulate, U	28000	(kJ/kg)

Table 5.1 Input data for numerical model

In addition to the input data tabulated above, referring to equation (5.23), the gas properties such as specific heat capacity and conductivity, were calculated based on the prevalent temperature and air composition.

5.3.6 Initial conditions and boundary conditions

The initial temperature of the filter at every zone was equal to room temperature. The initial mass of diesel particulate was input by the user. Enthalpy of inlet gas was found according to its inlet temperature obtained experimentally. The concentration of oxygen supply at the first zone at every time step was equal to the input value for each simulation. The above initial conditions and boundary conditions are summarized as below:

Initial conditions:

$$T_{(0,j)} = \text{room temperature} \quad \ldots (5.30)$$

$$m_{p(0,j)} = m_p \quad \ldots (5.31)$$

Boundary conditions:

$$h_{a,in} = h(T_{a,in})_{experimental} \quad \ldots(5.32)$$

$$[O_2]_{(i,1)} = [O_2]_{input\ value} \quad \ldots(5.33)$$

The oxygen concentration is the same in every zone of the filter during the heating up period. Once oxidation occurs, it will decrease as it pass along the length of filter. The initial mass of oxygen gas is calculated by equation (5.34).

$$m_{O_2,0} = \frac{MW_{O_2}}{MW_{air}} \cdot [O_2]_{input\ value} \cdot \dot{m}_{a,in} \cdot \Delta t \quad \ldots \quad (5.34)$$

During regeneration, the mass of oxygen consumed to oxidize the particulate is calculated by equation (5.35).

$$m_{O_2,cons} = m_{p,oxid} \cdot \frac{MW_{O_2}}{MW_p} \quad \ldots \quad (5.35)$$

The mass of oxygen remain is calculated by subtracting the mass of oxygen consumed from the initial value as shown in equation (5.36).

$$m_{O_2,remain} = m_{O_2,0} - m_{O_2,cons} \quad \ldots \quad (5.36)$$

The concentration of oxygen in the latter zone can be calculated back with equation (5.37).

$$[O_2]_{remain} = \frac{m_{O_2,remain} \cdot MW_{air}}{MW_{O_2} \cdot \dot{m}_{a,in} \cdot \Delta t} \quad \ldots \quad (5.37)$$

5.3.7 Flowchart of the program

Flowchart of the program is presented in Figure 5.3:

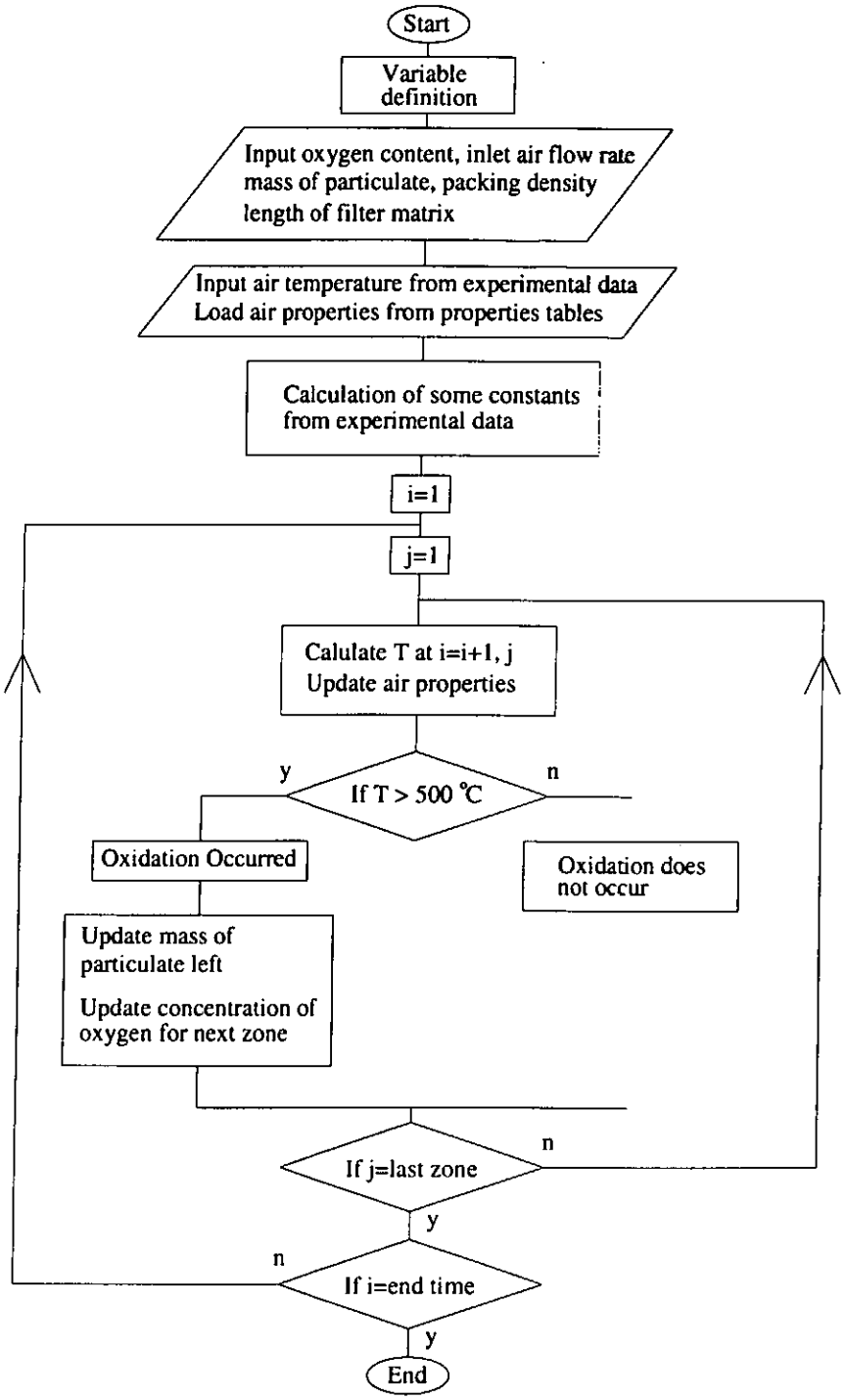

Figure 5.3 Flowchart of the program for the overall heat transfer model

5.3.8 Programming Language and programs developed

The looping calculation of the governing differential equations can be done efficiently and effectively using computer programming. Matlab is a high-performance language for technical computing, which integrates computation, visualization, and programming in a user-friendly manner. Matlab is a system whose basic data element is an array that does not require dimensioning. This feature is suitable for technical computing problems, especially those with matrix and vector formulations, just like the governing equations of the present models. Matlab is therefore selected to run in Microsoft Windows as the operating system. Details of the developed programs to solve the present models are presented in Appendix B.

5.4 Simulated results

5.4.1 The present model

In the present model, the filter was divided into two zones, however, the developed model could be extended to a larger number of smaller zones if better accuracy was required. It should be emphasized that temperature profiles inside the fibrous filter were dependent on both position as well as time, and their predictions required solving the oxidation model and the overall heat transfer model simultaneously. Consequently, a large amount of computation was already needed for a two-zones model.

As a general remark, rather good predictions were obtained with the developed model, which were in good agreement with the experimental results. The accuracy could

certainly be improved by the adoption of a larger number of smaller zones, but the computer's capacity needs to be considered carefully.

5.4.2 Temperature-time relationship

Operation conditions:

Inlet air flowrate : 90 l/min, Oxygen concentration: 17%,
Initial particulate loading : 10g, Packing density : 1.2%,
Filter thickness : 150mm

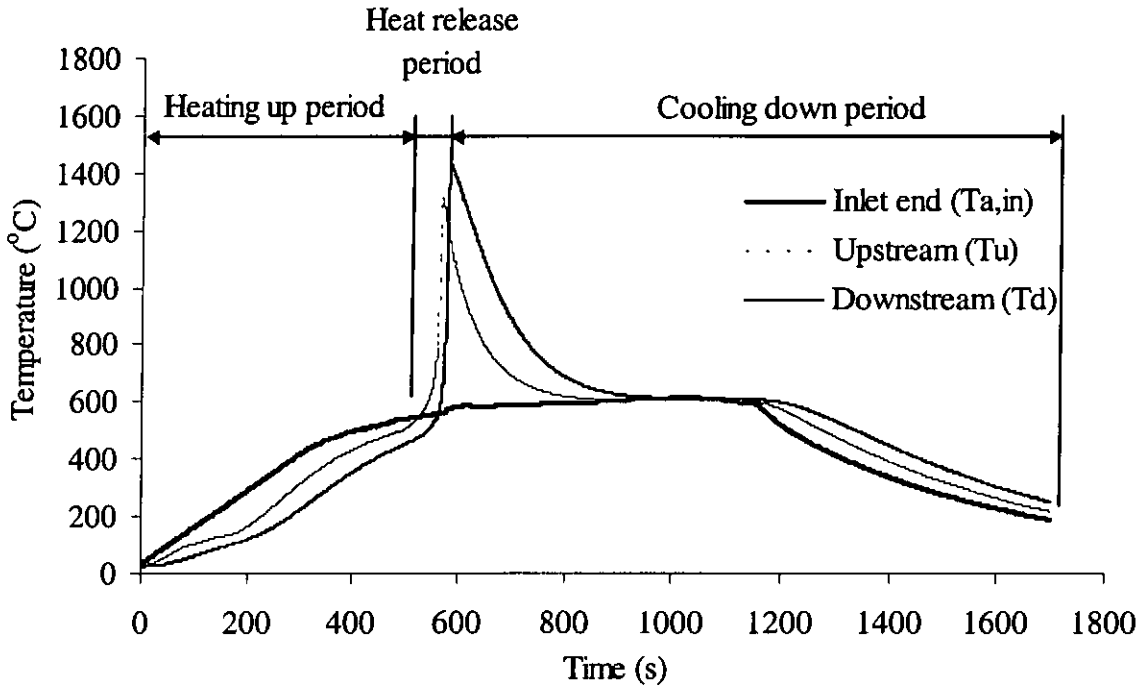

Figure 5.4 Simulated temperature profiles again time

Figure 5.4 shows the typical predicted temperature-time profiles inside the filter. Temperatures at the inlet end ($T_{a,in}$), upstream zone (T_u) and downstream zone (T_d) of the filter are shown. $T_{a,in}$ was input from the experimental data for the simulation of T_u and T_d. The simulation was performed with the same operation conditions as the experiment, i.e.: hot air flow rate of 90 l/min, oxygen concentration of 17%, initial

particulate loading of 10 gram, packing density of 1.2%, thickness of filtering material of 150mm.The simulated results compared well with the experimental results shown in Figure 4.4, qualitatively. In Figure 5.4, it was pointed out that the regeneration of the filter and each temperature profile could be divided into three periods, namely, the heating up period, the heat release period and the cooling period. The simulated results showed similar profiles and the three periods.

Temperature profiles of the two zones of the filter cartridge, namely, T_u and T_d, were similar to each other in shape. Each temperature profile could be divided into three periods: heating up period, heat release period and cooling down period.

Similar to the experimental results, as the hot air entered the filter cartridge, its energy was dispersed to the particulate, the stainless steel fibers and the metal casing, causing a drop in temperature of the air as it flowed along the different zones of the filter until thermal regeneration occurred. Because of the positional effect, the zone at the upstream region was heated up earlier than that at the downstream region. The heating up effect was properly reflected in the simulated results.

The heat release period started from oxidation of the particulate in the fibrous filter. In this heat release period, there was a subsequent sharp increase in temperature to the maximum value. Commencement of the sharp temperature increase corresponded to the commencement of intensive regeneration of the diesel particulate. The time for such intensive regeneration to occur in each zone of the filter, and the associated peak temperature, varied. In this two-zone model, it commenced earlier at the upstream zone, but the peak temperature was higher in the downstream zone. Hence, the simulated

results shown in Figure 5.4 reflected all the basic features of the heat release period as shown in Figure 4.4. A closer comparison showed that the simulated temperatures were higher and the rate of temperature increase was sharper in the simulated results than the experimental results. The simulated heat release period was much shorter.

The simulated results in the cooling down period also compared well with the experimental results.

In the simulation work of Garner and Dent [33], which was the only one available in literature on simulation of thermal regeneration of a fibrous filter, the temperature profiles showed similar results. The temperature profiles downstream zones lagged behind those in the upstream zones, and the peak temperature was progressively higher in downstream zones.

Based on this comparison, it can be concluded that the numerical model is applicable for studying the basic features of the regeneration process in the fibrous particulate filter.

5.4.3 Oxidation of diesel particulate

The major process of thermal regeneration of a particulate filter is the oxidation of particulate. It is oxidized when its temperature reaches the ignition temperature of 500°C -600°C [7] in the presence of oxygen. The regeneration efficiency, which is an indication on the regeneration behaviour, purely depends on the amount of diesel particulate oxidized. The more the particulate is oxidized, the higher is the regeneration

efficiency. The rate of particulate oxidation partly depends on the oxygen availability and more significantly depends on the particulate temperature in rate coefficient which is in form of the Arrhenius expression. The oxygen concentration and flow rate of the inlet hot air and the amount of initial particulate loading affect the rate of oxidation and the total time for oxidation. The mass of particulate remaining inside the filter can be calculated from equations (5.9) and (5.10) and the simulated results are shown in Figure 5.5 to Figure 5.7. In each profile, the initial particulate mass consumption is very low, despite the oxygen availability is high, mainly due to the comparatively low temperature in the filter. The consumption rate increased exponentially due to the increase in the temperature inside the filter as energy is released during regeneration. Since the filter is divided into two zones, each profile can also be observed to be divided into two regions; as marked by a sudden reduction in particulate consumption rate in the middle of the regeneration process. The particulate in the upstream zone oxidized firstly and rapidly. Intensive oxidation in the downstream zone occurs when the oxidation of particulate in the upstream is almost finished. These changes are due to the time lag in the particulate oxidation in the two zones. However, the particulate captured inside the filter will oxidize continuously throughout the filter so a rather smooth curve is expected. This sudden change in particulate oxidation rate does not reflect the real fact but rather considered as a model deficiency.

Figure 5.5 shows the oxidation of diesel particulate in a filter under different oxygen concentration supplied by the inlet hot air. It is observed that the oxidation rate is higher and the time for complete oxidation is shorter when the oxygen concentration is higher. The particulate oxidation rate depends on the oxygen concentration in equation (5.9)

thus leading to this phenomenon. Garner and Dent [33] also got the same result in their simulation.

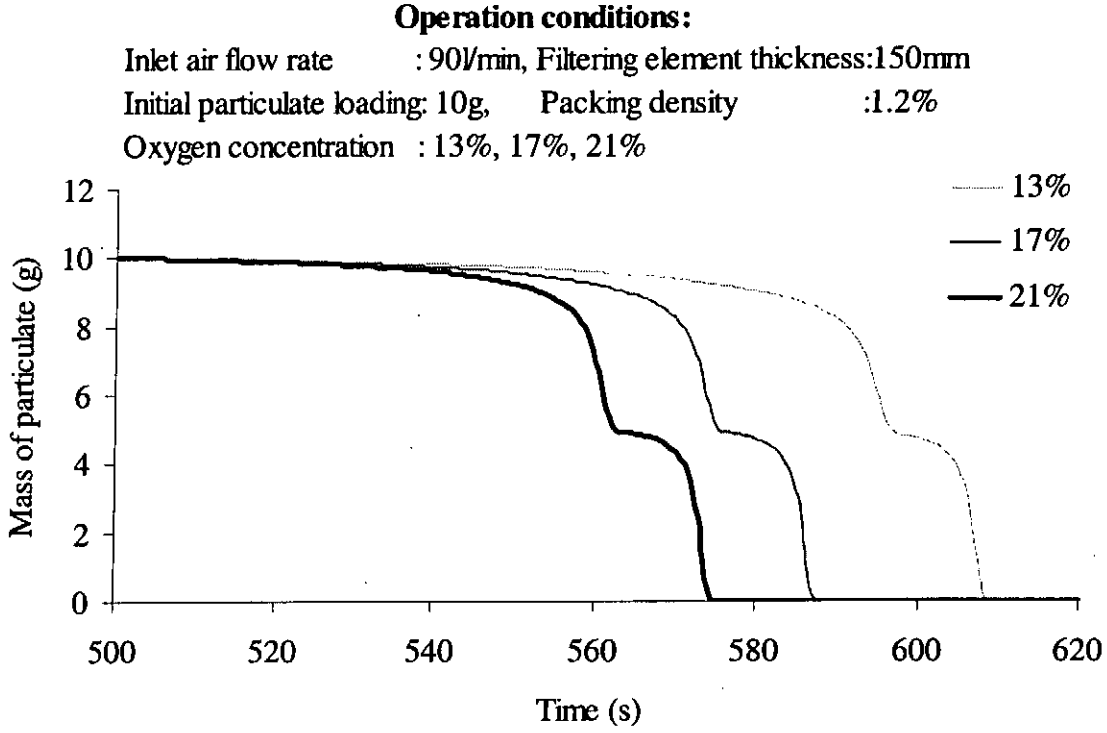

Figure 5.5 Oxidation of particulate in a filter under different oxygen concentration

Figure 5.6 shows the oxidation of diesel particulate in a filter under different inlet hot air flow rate. The oxidation rate is higher and the time for complete oxidation is shorter when the inlet hot air flow rate is higher. A higher inlet hot air flow rate enhances the heat and mass transfer from the air to the particulate so that particulate is heated up faster and more oxygen is available leading to a higher oxidation rate. Garner and Dent [33] also got the same result in their simulation.

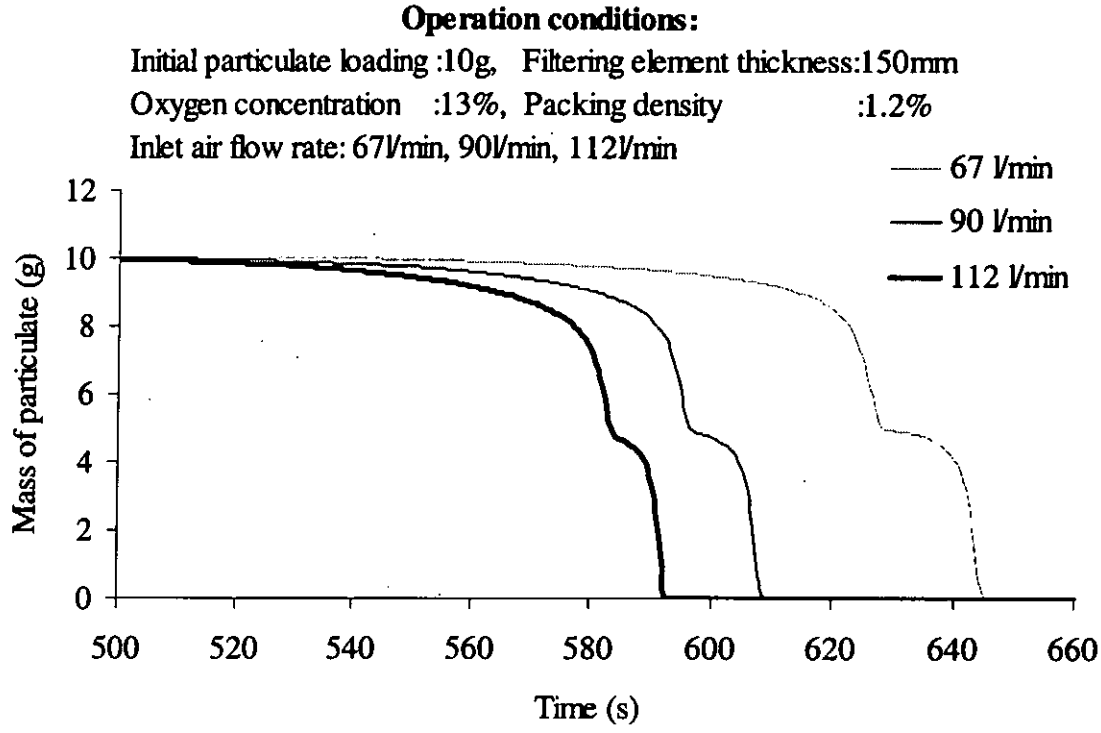

Figure 5.6 Oxidation of particulate in a filter under different inlet air flow rate

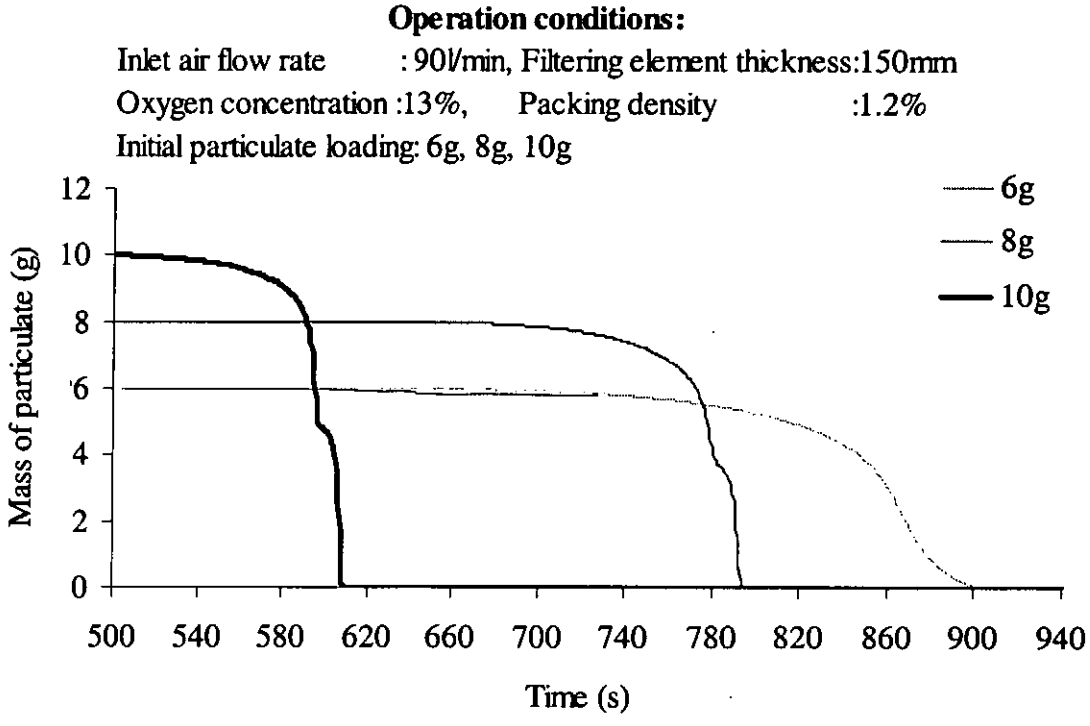

Figure 5.7 Oxidation of particulate in a filter under different initial particulate loading

Figure 5.7 shows the oxidation of particulate in a filter under different initial particulate loading. The oxidation starts earlier and with a higher rate when the initial particulate loading is higher. A larger amount of particulate is oxidized at the same oxidation rate when the initial amount of particulate is larger. The heat release from the oxidation increases the particulate temperature so that the reaction rate, which depends on the particulate temperature, is enhanced. Therefore, the time for oxidation is shorter despite the larger amount of particulate has to be oxidized. The results are different from those of Garner and Dent [33] in which the higher the particulate loading the longer the time for regeneration.

5.4.4 Heat release during regeneration

Calculation of the heat release during thermal regeneration from the numerical model was based on the calorific value of carbon particles and oxidation rate of the particulate. In the experimental study, the heat release was determined from difference between the energy input and output to the filter, as shown in equations (4.6) and (4.7). However, deviation should not be large if the calorific value of carbon and the rate coefficient for the oxidation of diesel particulate were adopted accurately.

Oxidation of diesel particulate commenced once their temperature exceeded 500°C, which was kinetically controlled since oxygen supply was rich. The reaction rate highly depended on the particulate temperature. The local heat release during regeneration at the j^{th} zone of the fibrous filter was calculated by the following equation:

$$H_{comb,(j)} = \dot{m}_{p,(j)} U \cdot \Delta t \qquad \ldots \quad (5.38)$$

The instantaneous global heat release of the filter is the sum of the local heat release in discrete zones as shown below:

$$H_{comb} = \sum \dot{m}_{p,(j)} U \cdot \Delta t \qquad \ldots \quad (5.39)$$

Operation conditions:

Inlet air flowrate : 90 l/min, Oxygen concentration: 17%,
Initial particulate loading : 10g, Packing density : 1.2%,
Filter thickness : 150mm

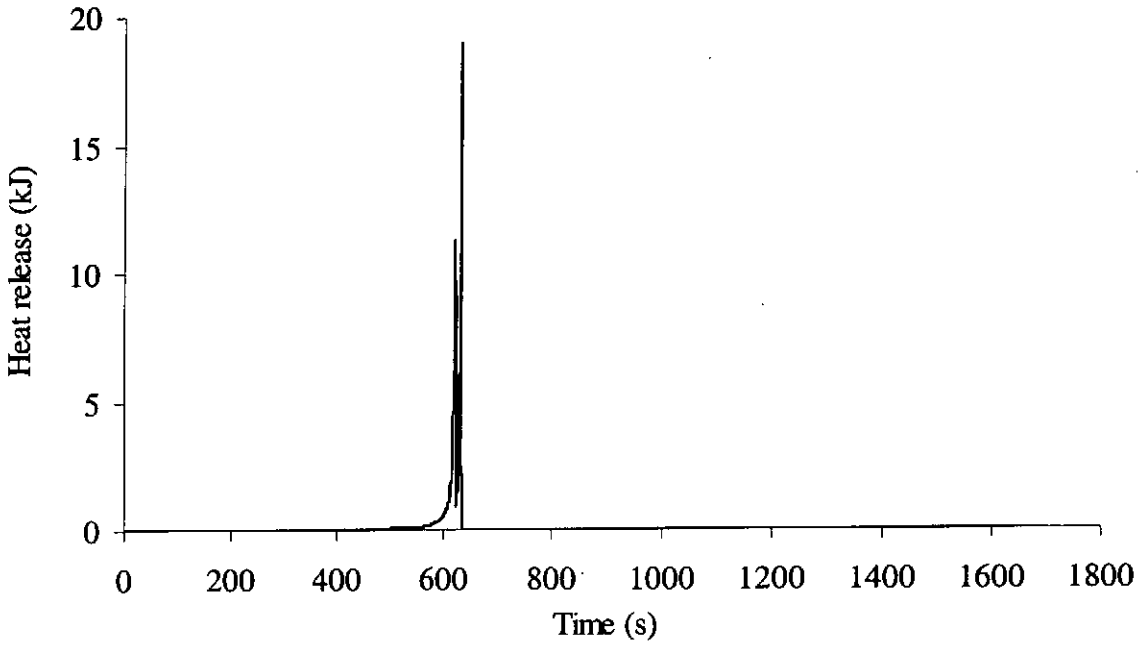

Figure 5.8 Instantaneous global heat release during thermal regeneration of the filter

Figure 5.8 shows a typical instantaneous global heat release during the regeneration, as calculated from equation (5.39). In the heating up and cooling down periods, the heat release was assumed to be zero since no oxidation actually occurred. In the heat release period, intensive regeneration occurred and two peaks were observed from the heat release diagram. The two peaks corresponded to the two rapid regenerations occurring in the upstream and downstream regions. The peak at the downstream zone was higher

than the peak at the upstream zone, while the heat release period was longer in the upstream zone. Upon regeneration, the heat release from oxidation of particulate in the upstream region was transferred to the downstream region, leading to a higher regeneration temperature at the downstream region increased. Although certain amount of oxygen had been consumed in the upstream region, leading to lower oxygen availability in the downstream region, the regeneration rate was related to the temperature exponentially but only related to the oxygen concentration linearly. Hence, regeneration was more intense in the downstream zone, leading to a higher peak heat release rate and thus a shorter heat release period.

5.4.5 Effects of influencing parameters

The effects of different influencing parameters, including inlet air flow rate, inlet air oxygen concentration, packing density of filter, thickness of filter and initial particulate loading of filter, on the thermal regeneration had been investigated experimentally and the results presented in Chapter 4. Effects of these influencing parameters could also be predicted individually with the developed model, and the predictions are shown in Figure 5.9 to Figure 5.18. In these figures, t=0 corresponds to the time when the inlet air reaches 500°C. In each case, comparisons had been made with respect to the temperature-time profile and the instantaneous global heat release. The former was a comparison on local behaviour while the latter was the summed behaviour of the regeneration process. The predicted results will be compared with those of Garner and Dent [33] whenever possible. The predicted results will be compared with the experimental results in Chapter 6.

5.4.5.1 Effect of oxygen concentration of inlet hot air

Figure 5.9 and Figure 5.10 show the effect of oxygen concentration of the inlet hot air. Garner and Dent predicted at a lower oxygen concentration, regeneration occurred later but at a slightly higher peak temperature, and the regeneration period was longer. In this study, similar results were obtained. With a richer oxygen supply, intensive regeneration occurred earlier and the peak filter temperature was slightly lower, as shown in Figure 5.9. Moreover, the peak heat release was higher at higher oxygen concentration due to the higher oxidation rate.

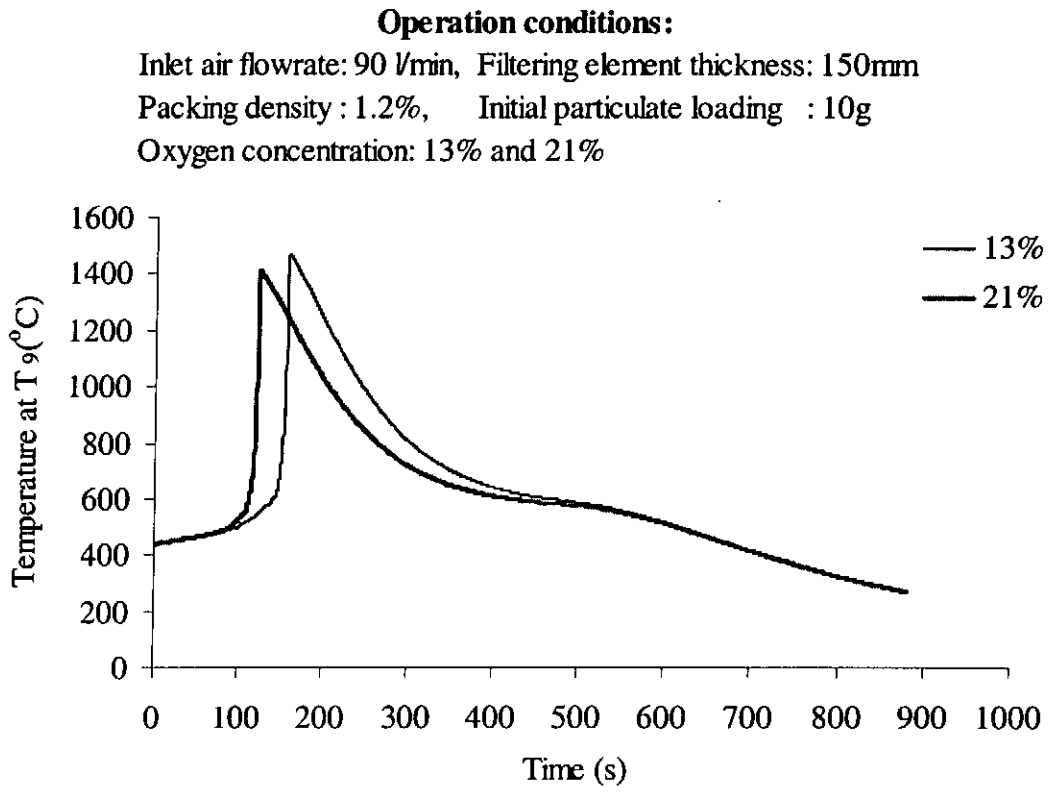

Figure 5.9 Effect of oxygen concentration on filter temperature

When the oxygen concentration was higher, rapid oxidation occurred at a lower temperature. Conversely, when the oxygen concentration was lower, rapid oxidation

occurred mainly at a higher temperature. The rapid heat release helped to build up the temperature and hence the peak temperature was higher in the case of lower oxygen concentration.

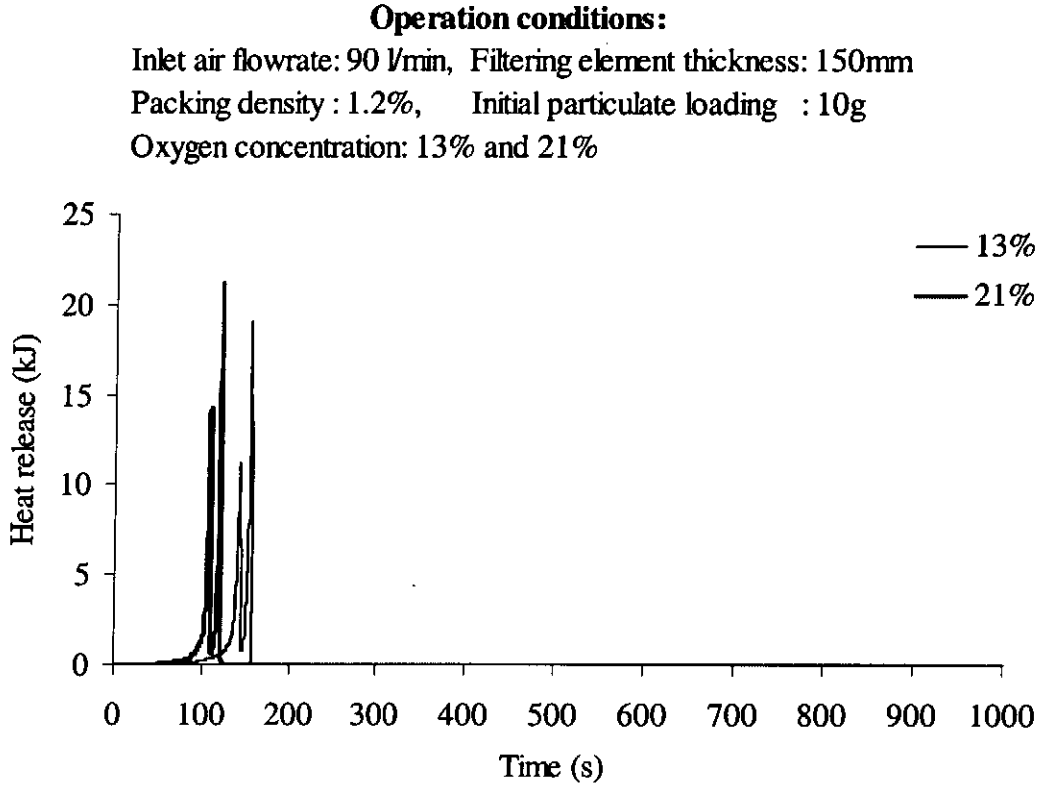

Figure 5.10 Effect of oxygen concentration on heat release

5.4.5.2 Effect of flow rate of inlet hot air

Figure 5.11 and Figure 5.12 show the effect of change in flow rate of the inlet hot air on the regeneration. Garner and Dent [33] predicted that at a higher flow rate, there would be a more rapid rise but a slight increase in the peak temperature, and the regeneration period was shorter. In this study, at higher flow rate, similar results were obtained.

At a higher flow rate, the regeneration occurred earlier and the peak filter temperature was higher. However, the instantaneous heat release was lower at the higher flow rate.

A higher flow rate will provide a more rapid energy input to the filter and hence achieves an earlier heating up of the filter and particulate oxidation. The higher flow rate carries away a larger amount of heat generated in the upstream region to the downstream. As a result, oxidation of particulate in the downstream region is started at a higher temperature leading to a higher peak filter temperature. But the instantaneous heat release is not higher since less oxygen is available when the flow rate is lower.

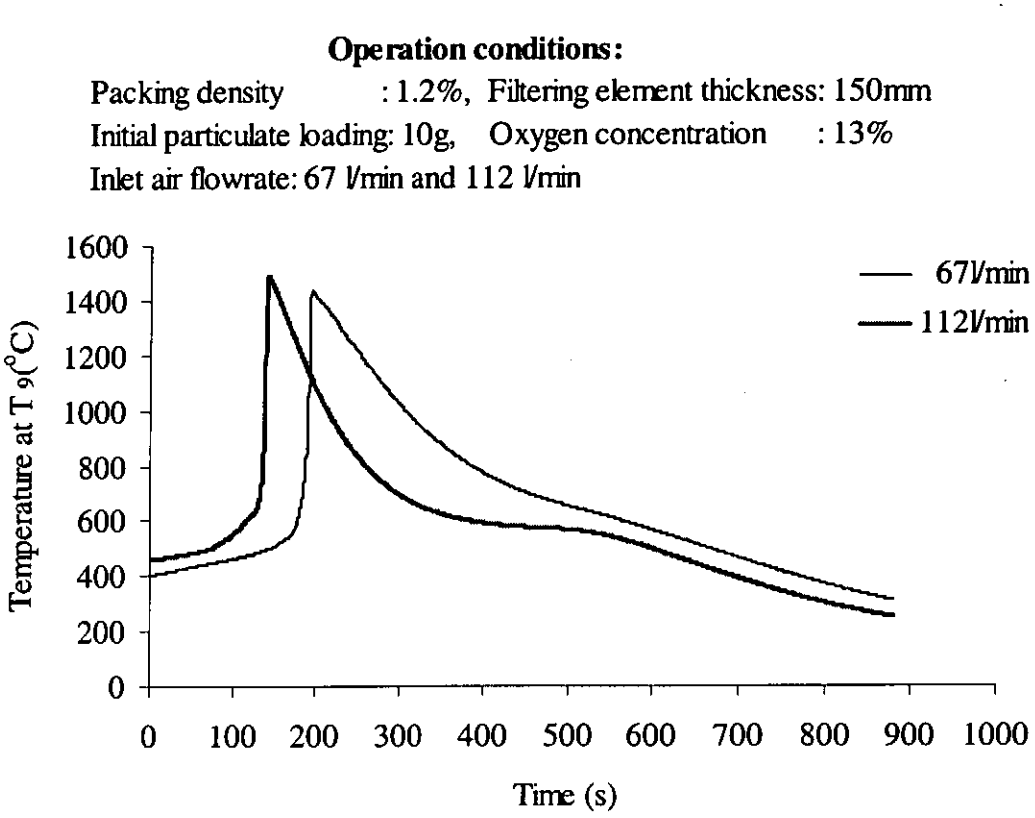

Figure 5.11 Effect of inlet gas flowrate on filter temperature

Operation conditions:

Packing density : 1.2%, Filtering element thickness: 150mm
Initial particulate loading: 10g, Oxygen concentration : 13%
Inlet air flowrate: 67 l/min and 112 l/min

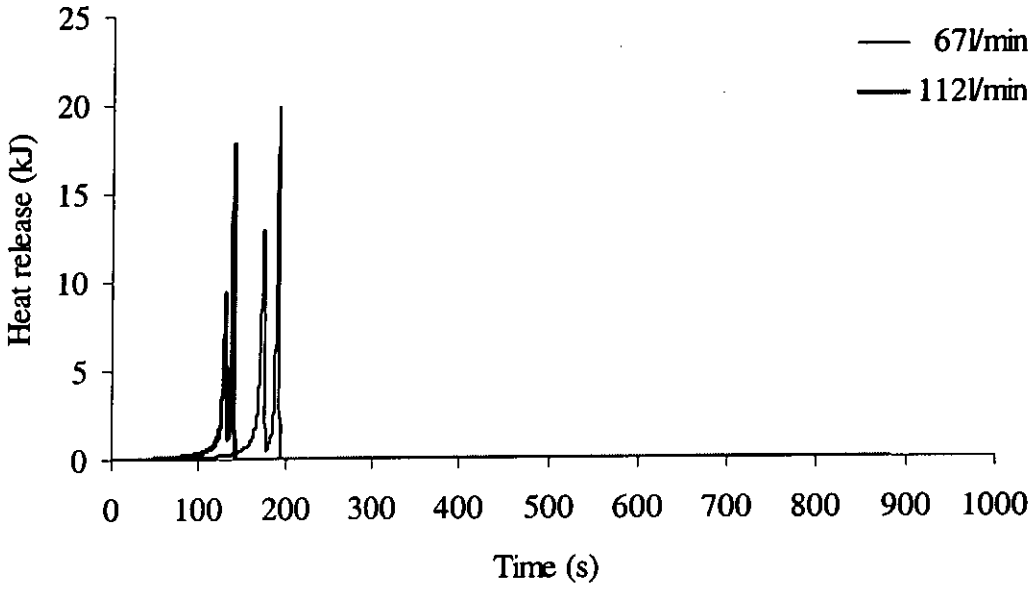

Figure 5.12 Effect of inlet air flowrate on heat release

5.4.5.3 Effect of packing density of filtering element

Effect of packing density of the filter on the thermal regeneration of the filter is presented in Figure 5.13 and Figure 5.14. The peak filter temperature and the peak heat release were rather similar for the two values of packing density, but the thermal regeneration was found to start just earlier for a filter with a lower packing density. At a lower packing density, heating up of less amount of material inside the filter to the same temperature will require less heat input, and should therefore be faster.

Operation conditions:

Inlet air flowrate :90 l/min, Initital particulate loading : 10g
Oxygen concentration: 21%, Filtering element thickness:150mm
Packing density: 0.8% & 1.2%

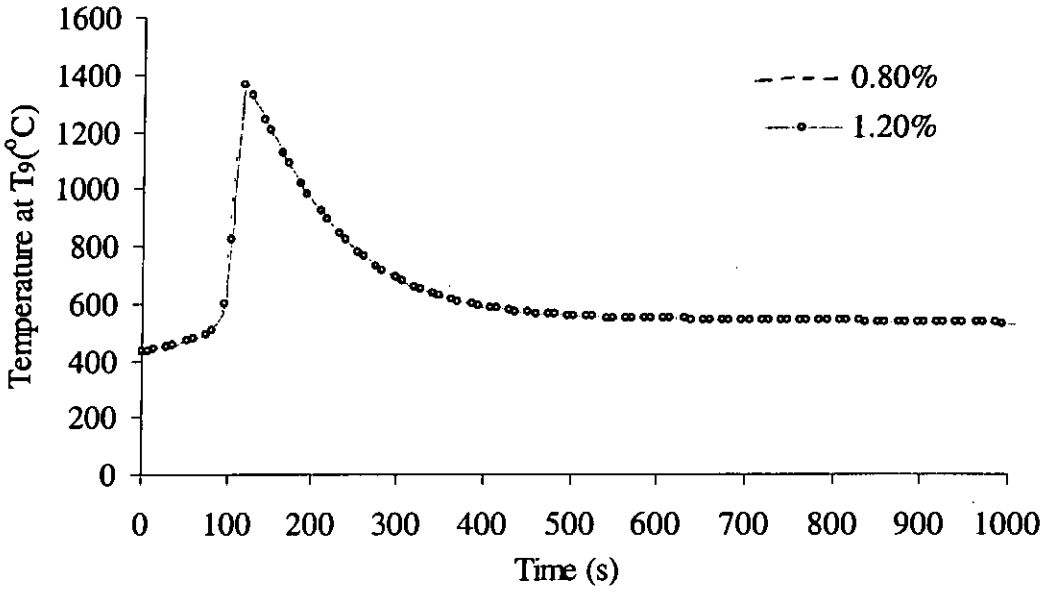

Figure 5.13 Effect of packing density on filter temperature

Operation conditions:

Inlet air flowrate : 90 l/min, Initial particulate loading : 10g
Oxygen concentration: 21%, Filtering element thickness: 150mm
Packing density: 0.8% and 1.2%

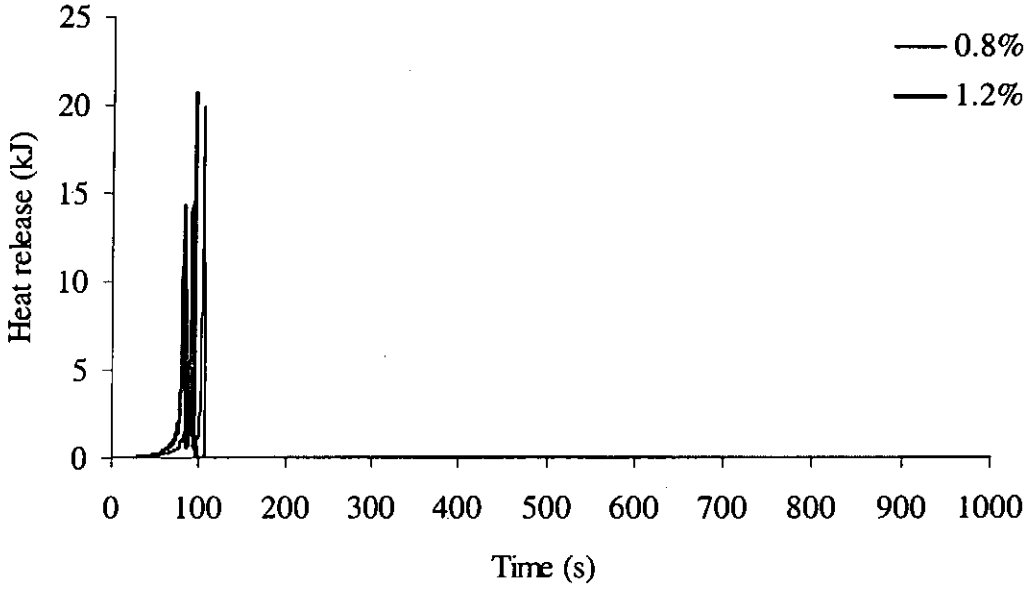

Figure 5.14 Effect of packing density on heat release

5.4.5.4 Effect of thickness of filtering element

Effect of thickness of the filtering element on the regeneration temperature and heat release is shown in Figure 5.15 and Figure 5.16 respectively. Oxidation of diesel particulate commenced at about the same time. The regeneration temperature was much lower when thickness of the filtering element was 50mm. The instantaneous and total heat release are also smaller in this case. This is mainly due to the amount of diesel particulate captured in the filter of 50mm thick is less than that of the 150mm thick filter. The initial particulate loading in the filter of 50mm was only 3.3g. Oxidation of such a small amount of diesel particulate results in a small amount of heat release. Thus, temperature of the filter increases slightly and slowly so that the reaction rate is low. This low reaction rate again gives a small heat release. As a result, both the regeneration temperature and the heat release are low.

Operation conditions:
Inlet air flowrate: 90 l/min, Oxygen concentration : 13%
Packing density : 1.2%, Initial particulate loading: 3.3g and 10g
Filtering element thickness: 50mm and 150mm

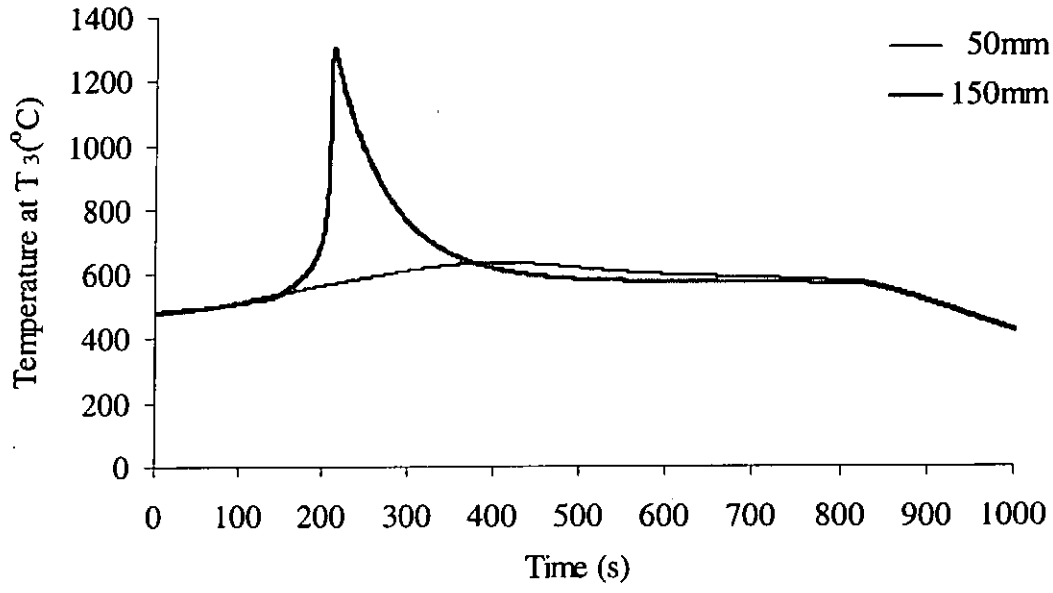

Figure 5.15 Effect of filter thickness on filter temperature

Operation conditions:

Inlet air flowrate: 90 l/min, Oxygen concentration : 13%

Packing density : 1.2%, Initial particulate loading: 3.3g and 10g

Filtering element thickness: 50mm and 150mm

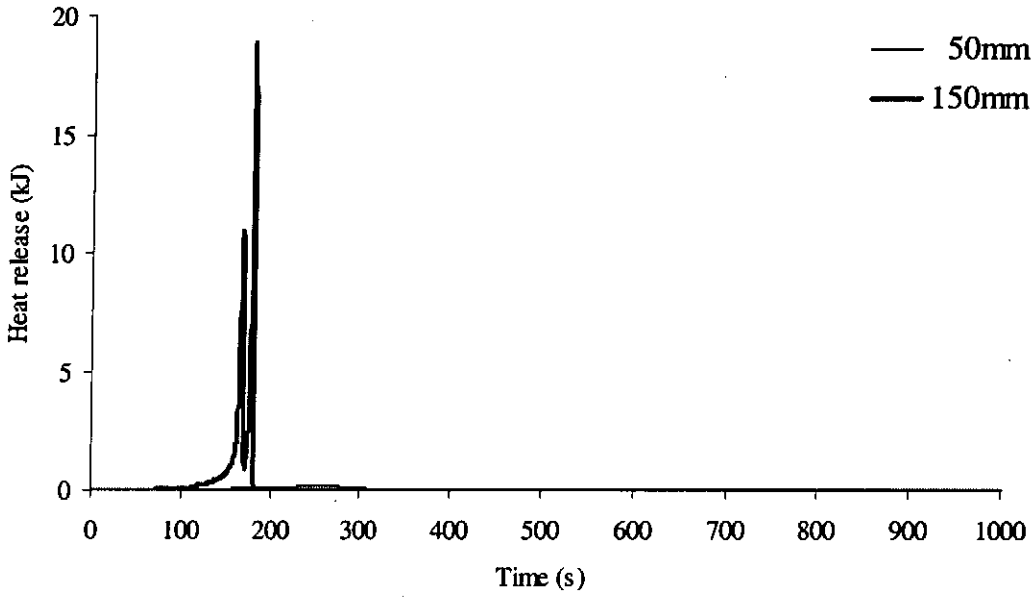

Figure 5.16 Effect of filter thickness on heat release

5.4.5.5 Effect of initial particulate loading in filtering element

Particulate acts as the fuel for the regeneration process. The effects of initial particulate loading of the filter are presented in Figure 5.17 and Figure 5.18. Garner and Dent [33] predicted that regeneration occurred later at a higher initial particulate loading but the peak temperature was much higher. The results are slightly different in this study. In this study, at higher initial particulate loading, regeneration occurred earlier and the peak temperature was also higher.

Operation conditions:

Inlet air flowrate: 90 l/min, Filtering element thickness: 150mm
Packing density : 1.2%, Oxygen concentration : 13%
Initial particulate loading : 8g and 10g

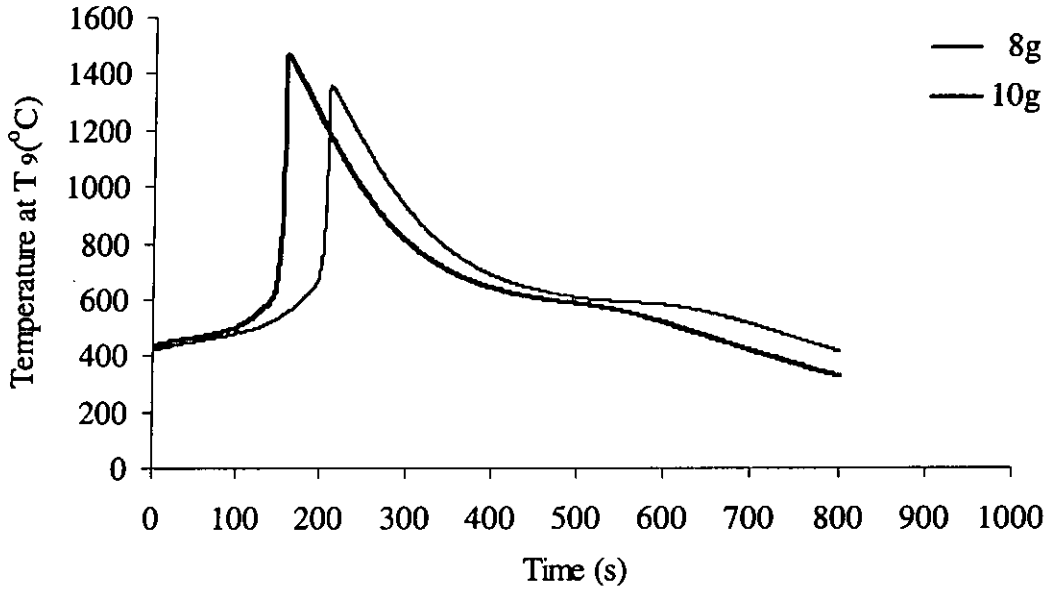

Figure 5.17 Effect of initial particulate loading on filter temperature

Operation conditions:

Inlet air flowrate: 90 l/min, Filtering element thickness: 150mm
Packing density : 1.2%, Oxygen concentration : 13%
Initial particulate loading : 8g and 10g

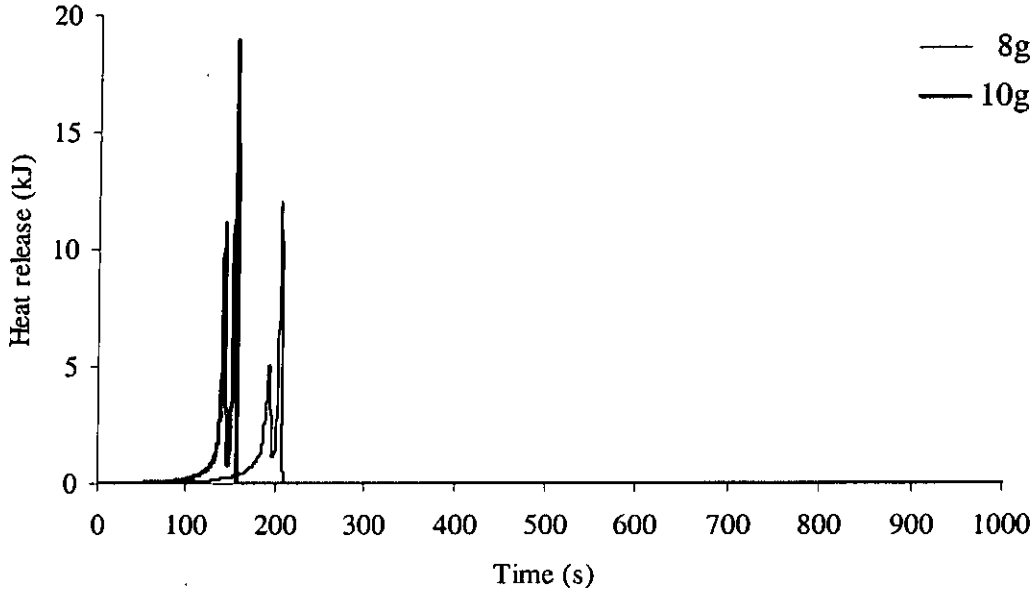

Figure 5.18 Effect of initial particulate loading on heat release

The peak filter temperature and the peak heat release increased as the initial particulate loading increased because more fuel was available for thermal regeneration. In Figure 5.18, the instantaneous peak heat release for the case of 10g was higher than that of 8g. In addition, intensive oxidation starts earlier at the higher initial particulate loading.

5.4.6 Summary of numerical study

A mathematical model was established for the thermal regeneration of diesel particulate in a metallic fibrous filter. The model consists of two sub-models. The first sub-model is on the reaction between diesel particulate and oxygen, while the second sub-model is on the subsequent heat transfer processes.

The reaction between oxygen and diesel particulate was assumed kinetically controlled and hence the rate coefficient was expressed in the Arrhenius form. Three rate coefficients were considered and the most appropriate one was chosen for further study.

The energy equations for the solid-phase and the gas-phase, taking into consideration of convective heat transfer were first considered and found not in appropriate in this study. It was the assumed that the gas-phase and solid-phase in a particular zone would reach the same temperature in a very short period of time. Hence, the change of internal energy was considered instead.

Using the model established, it was possible to compute the temperature profiles for the filter, the particulate consumption rate and the heat release during the thermal

regeneration process; and to study the effect of different parameters on the regeneration process.

CHAPTER 6 DISCUSSIONS

6.1 Introduction

Comprehensive investigations had been made experimentally on the thermal regeneration of a metallic fibrous particulate filter and the corresponding results and discussions had been presented in Chapter 4. Moreover, a numerical model had also been established to simulate the corresponding regeneration process and the predicted results had been presented in Chapter 5. The effects of the regeneration parameters had been studied experimentally and numerically in Chapter 4 and Chapter 5 respectively. Therefore, this chapter is aimed to compare the experimental and the predicted results, with concentration on the effects of the regeneration parameters. In this chapter, the simulated temperatures T_u and T_d, were compared with the experimentally temperatures, T_3 and T_9, respectively.

6.2 Comparison between experimental and predicted results

The experimental and simulated temperature profiles at the downstream zone of the filter are plotted in Figure 6.1, for the same operation conditions. Even though there are deviations between the experimental and predicted results, they can clearly reflect the regeneration behaviour of the filter.

Both of them can be divided into three periods: heating up period, heat released period and cooling down period, as stated in chapters 4 and 5. It can be observed from Figure 6.1 that the simulated temperature is slightly higher in the heating up and cooling down

periods and significantly higher than its counterpart in the heat release period. There is a sharp turning point, that is the peak filter temperature exist, this sharp turning, however had not been observed in any of the experimental results. The simulated model performs better in the heating up and cooling down periods, but is not able to fully simulate the heat release period. The deficiency of the model is discussed as below.

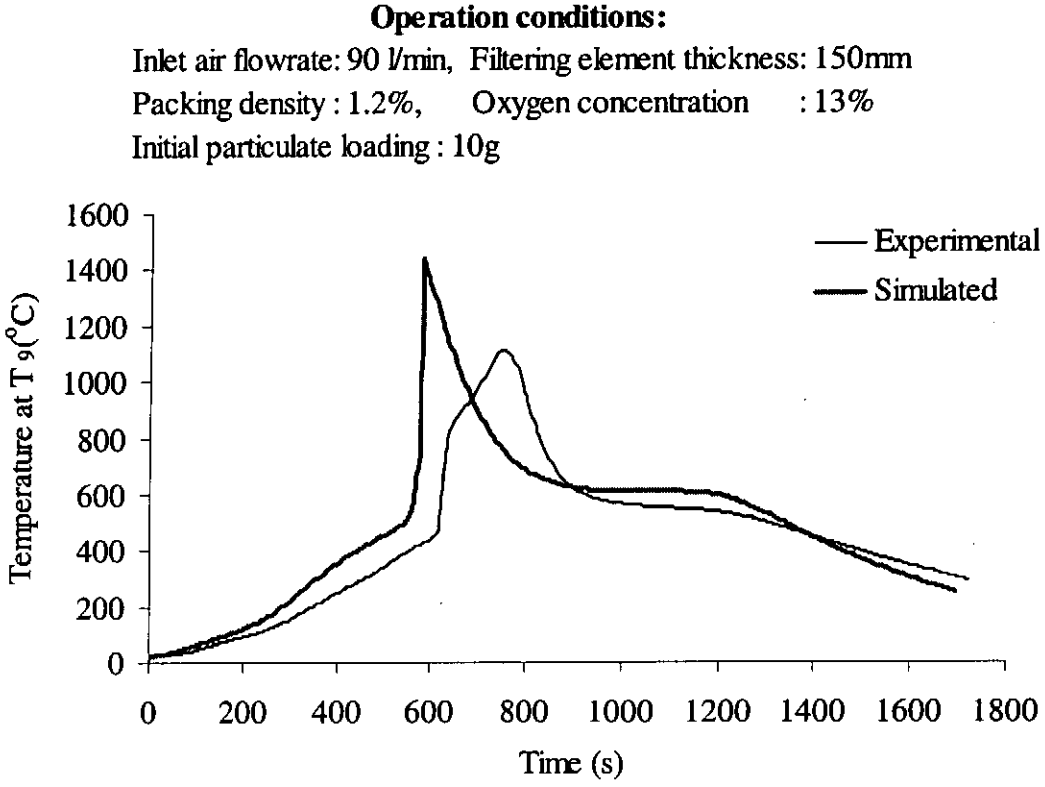

Figure 6.1 Comparison of experimental and predicted results

The deviations between the predicted and the experimental results can be explained qualitatively with the aid of the overall heat transfer model formed with the following governing equation:

$$(m_a c_{p,a} + m_f c_{p,f})\frac{\partial T}{\partial t} = \dot{m}_p U + (1-\phi)k_S \frac{\partial^2 T}{\partial x^2} + \dot{m}_a \cdot \Delta h_a \quad \ldots \quad (5.23)$$

Profile of the predicted result is quite close to the experimental result in the heating up period. However, the heat up rate is slightly higher in the model leading to an earlier commencement of thermal regeneration. Heat transfer in the filter is assumed to be one-dimensional and heat loss is negligible in the model. These assumptions enhance the rate of temperature rise in the filter. Conduction may have been overestimated due to the discontinuity of the fibres. Moreover, temperatures of the gas-phase and the solid-phase are assumed to be the same. However, temperature of the solid-phase should be slightly lower than that of the gas-phase during the heating up period. This may lead to a further overestimate of the heat transfer process. One solution to this problem can be made by introducing a compensation factor to the second and last terms on the right hand side of equation (5.23), so that the heat transfer from upstream zone to downstream zone can be reduced accordingly. However, appropriate choice of the compensation factor may be difficult to make.

The rate of temperature increase in the heat release period in the predicted result is nearly constant. However, it decreases at the middle of the heat release period in the experimental result. Oxidation of diesel particulate is assumed to be purely kinetically controlled and the reaction rate is in the form of an Arrhenius expression such that it increases exponentially with particulate temperature in the numerical model. However, the reaction slowed down in the experiment after some particulate had been oxidized because diffusivity of oxygen decreased due to the existence of an ash layer. This ash layer can easily be observed in many cases. The regeneration peak temperature of the simulated result is higher than the experimental one by 29% partially due to the above

reason and partially because the particulate has not been oxidized completely in the experiment. The model can be modified by adding a correction factor to the heat release term in equation (5.23) to account for the effect of the ash layer. Again, such correction factor cannot be obtained easily. The sharp turning at the simulated peak filter temperature is not considered as the real phenomenon of regeneration as it was not observed in any experimental results but is rather due to the discontinuous of the calculation. When all the particulate is oxidized in the model, the value of heat of combustion of particulate suddenly was assigned to zero, this sudden assignment will make the calculation to be discontinuous leading to such a sharp turning.

There are no obvious deviation of the predicted result from the experimental result in the cooling down period except the rate of temperature drop in the predicted result is higher than that of the experimental result at the end of this period.

6.3 Comparison on the effect of regeneration parameters

Experimental and predicted results on the effects of different experimental parameters, including inlet air flow rate, inlet air oxygen concentration, packing density of filter, and initial particulate loading of filter, on the thermal regeneration behaviour of the filter are compared in Figure 6.2 to Figure 6.9. Thickness of filtering element will not be discussed because oxidation has not been obtained in the experiment.

The operation conditions in the simulation are the same as the corresponding experiment in each comparison. The initial temperature of the filter is the same as the experimental temperature in all cases. In each case, comparisons had been made between the experimental and predicted results with respect to the temperature-time profile and the instantaneous global heat release. The instantaneous global heat release

in the experimental result is essentially the change in internal energy of the filter while it is calculated from the oxidation rate of particulate and the calorific value in the prediction. The differences in the effects of regeneration parameters between the experimental and predicted results will be explained qualitatively based on the assumptions made in the governing equations of the numerical model.

6.3.1 Effect of oxygen concentration of inlet hot air

Figure 6.2 and Figure 6.3 show the effect of oxygen concentration of the inlet hot air. The experimental result agrees with the prediction in the sequence of regeneration but there is a significant difference in the peak regeneration temperature. Moreover, in the simulated results, the peak regeneration temperature is higher at a lower oxygen concentration, while in the experimental results, the peak regeneration temperature is higher at a higher oxygen concentration. The occurrence of the heat release in the experiments also agrees with that in the predictions but the peak instantaneous global heat release in the prediction is nearly three times that of the experimental results. The heat release period in the predictions is much shorter than that of the experiments indicating oxidation rate is much higher in the prediction. Thus, the oxidation rate of diesel particulate may have been overestimated in the numerical model.

When the oxidation rate is overestimated, most oxygen is consumed at the upstream zone leaving little oxygen available at the downstream zone of the filter for regeneration. Regeneration occurs in the upstream zone and the heat is transferred downstream, raising the temperature of the downstream zone. Regeneration does not occur in the downstream zone because little oxygen is available. When a significant portion of the particulate in the upstream zone is consumed, little oxygen would further

be consumed in the upstream zone for sustaining regeneration, leaving more oxygen available downstream. Therefore, particulate at the downstream region starts to oxidize at a temperature, which is higher than the particulate ignition temperature, and the reaction is very rapid. Such phenomenon appears during the process of simulation. This situation is exaggerated when oxygen concentration of the inlet air is low, and hence the higher peak regeneration temperature at lower oxygen concentration.

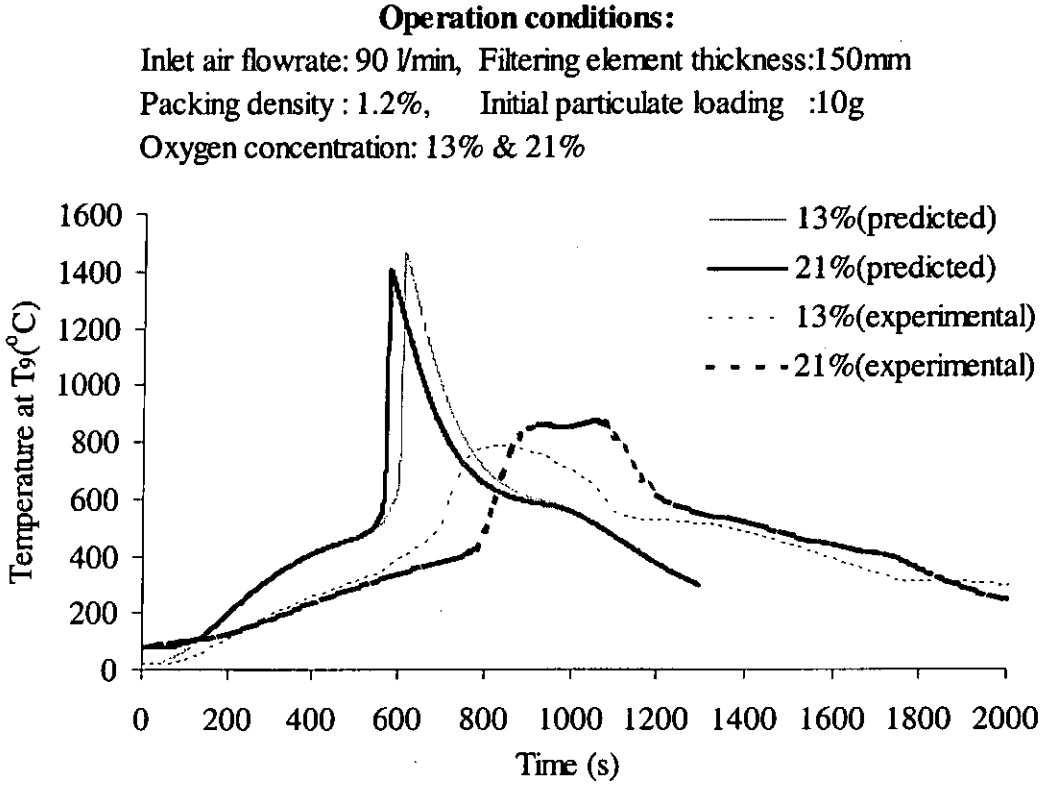

Figure 6.2 Effect of oxygen concentration on filter temperature

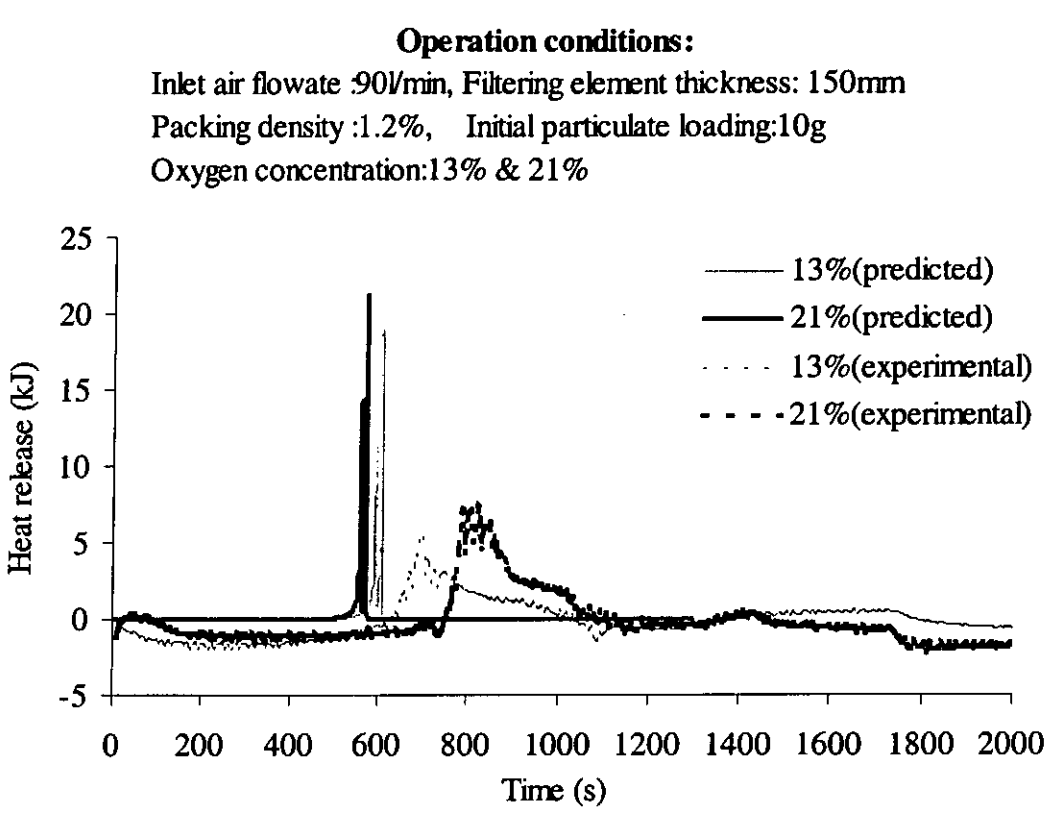

Figure 6.3 Effect of oxygen concentration on heat release

On the other hand, in the experiment, particulate oxidation rate is lower than that in the model, so that more oxygen is available at the downstream region. Experimental results indicated that the particulate at the upstream and downstream regions oxidize almost at the same temperature. The difference in the actual and predicted oxidation rate might be explained as follows. In the numerical model, the oxidation rate is assumed to be kinetically controlled. In reality, the reaction might be initially kinetically controlled when the air and particulate is evenly distributed within each other. Upon regeneration, a small quantity of ash, which is observable in the regeneration filters, is formed. The ash, coupled with the reduced amount of oxygen available upon regeneration, will reduce contact with the remaining oxygen and particulate. The reaction rate will be reduced but it has not been reflected in the numerical model.

6.3.2 Effect of flow rate of inlet hot air

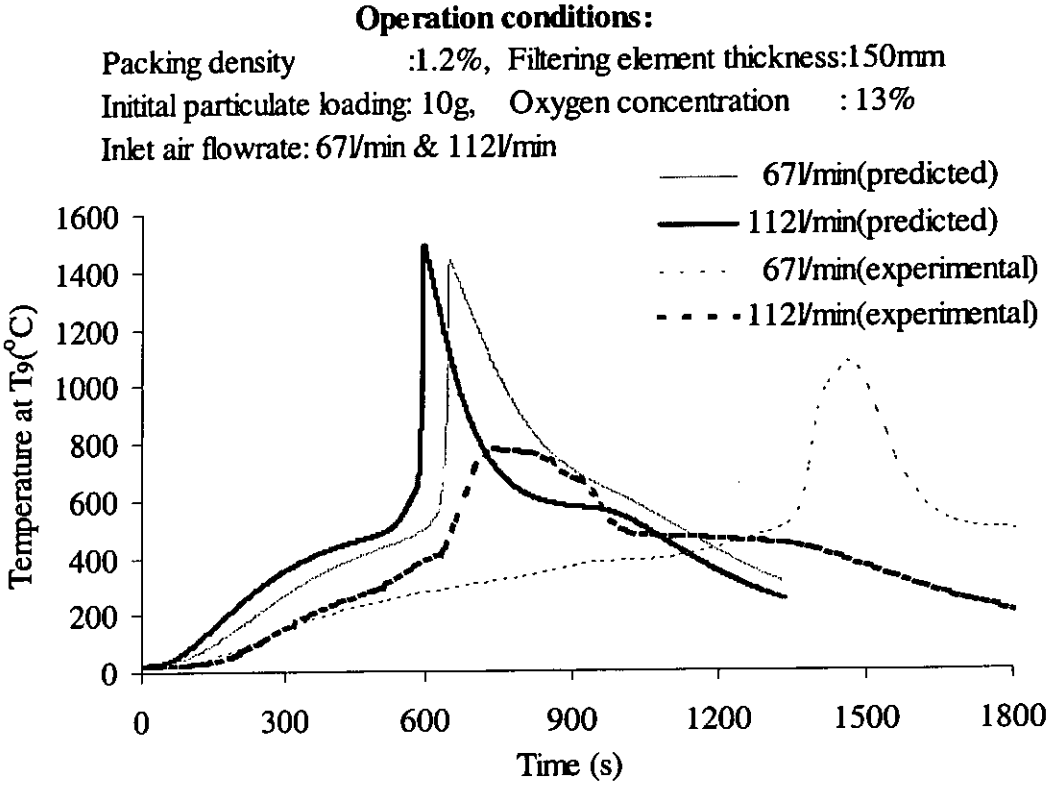

Figure 6.4 Effect of inlet air flow rate on filter temperature

Figure 6.4 and Figure 6.5 show the effect of flow rate of the inlet hot air. The flow rate of inlet hot air has the same effect on the sequence of the peak regeneration temperature and heat release in both the experimental and predicted result. However, the effect on the magnitude of the peak regeneration temperature is different between the real case and prediction. The predicted peak regeneration temperature and heat release is much higher than the experimental value when the flow rate of inlet hot air is high. However, such difference is quite small when the flow rate of inlet air is low.

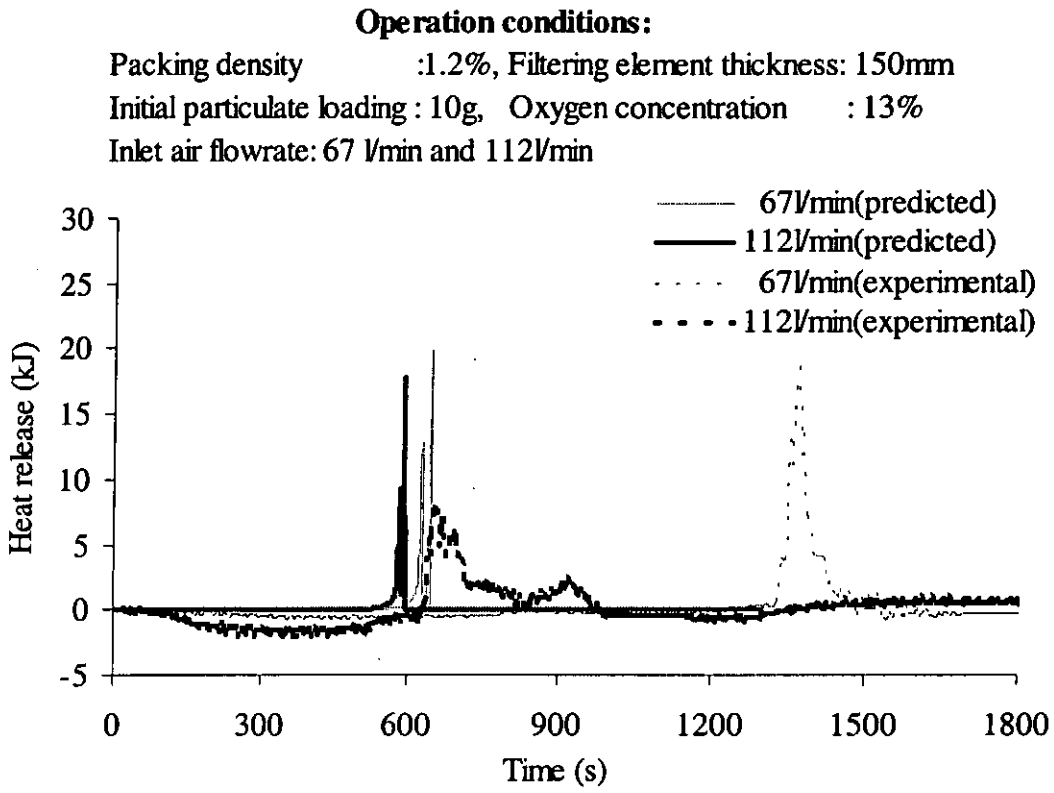

Figure 6.5 Effect of inlet air flow rate on heat release

In the prediction, temperature of particulate in the downstream region is heated up quickly due to enhanced heat transfer when the inlet air flow rate is high. Therefore, again, particulate at the downstream region starts to oxidize at a temperature higher than its ignition temperature, and the reaction is very rapid leading to a rapid heat release and high peak regeneration temperature. However, in the experiment, particulate at the upstream and downstream regions are oxidized nearly at the same temperature. Moreover, heat release from oxidation is carried away more rapidly in the case of higher inlet air flow rate, a lower regeneration peak temperature is therefore recorded.

6.3.3 Effect of packing density of filtering element

Figure 6.6 and Figure 6.7 show the effect of packing density of filtering element on the thermal regeneration. Differences in the magnitude of regeneration peak temperatures

for the cases of different packing density are small in both the experimental result and prediction but the difference in magnitude of peak heat release is large in the predicted results. Moreover, the time lag between the regeneration peak temperature and the peak heat release is negligible in the prediction but larger in the experimental result.

The difference in the heating up rate of the filters of different packing densities is large when the energy supplied from the inlet hot air is less. In the prediction, heat loss is assumed to be negligible in the prediction. However, in the real case, there should be energy loss to surroundings. Therefore difference in the heating up rate is larger in the experimental result since less energy is supplied from the inlet hot air leasing to a large time lag.

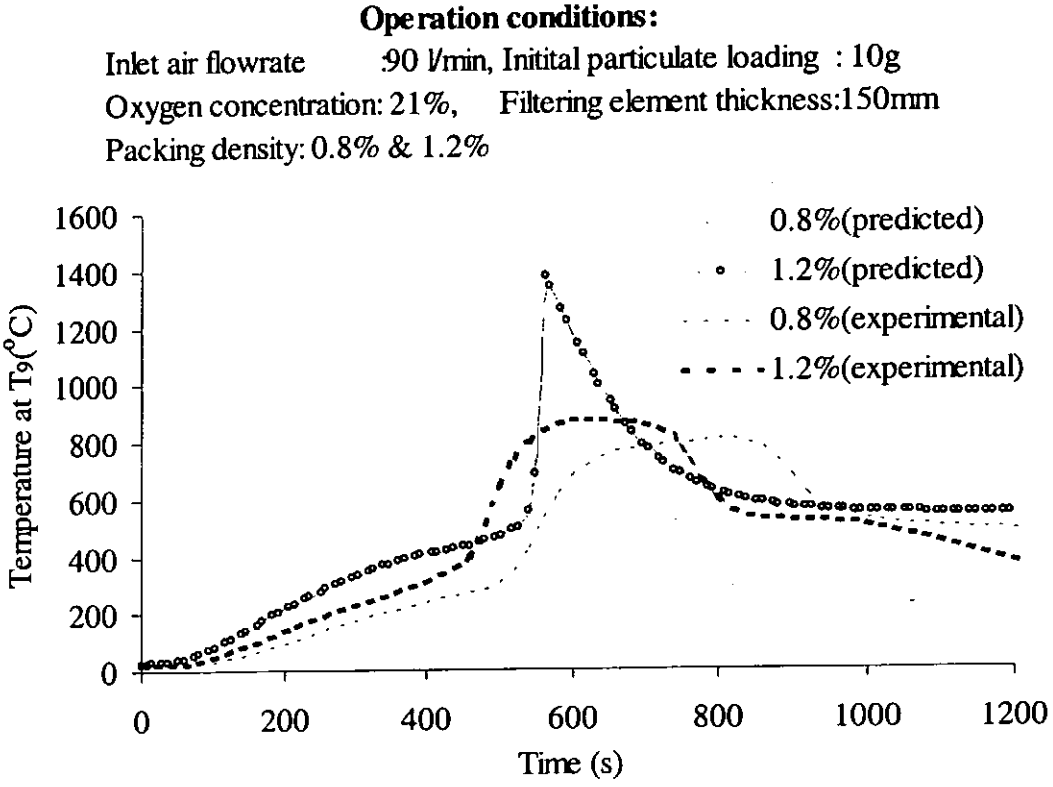

Figure 6.6 Effect of packing density on filter temperature

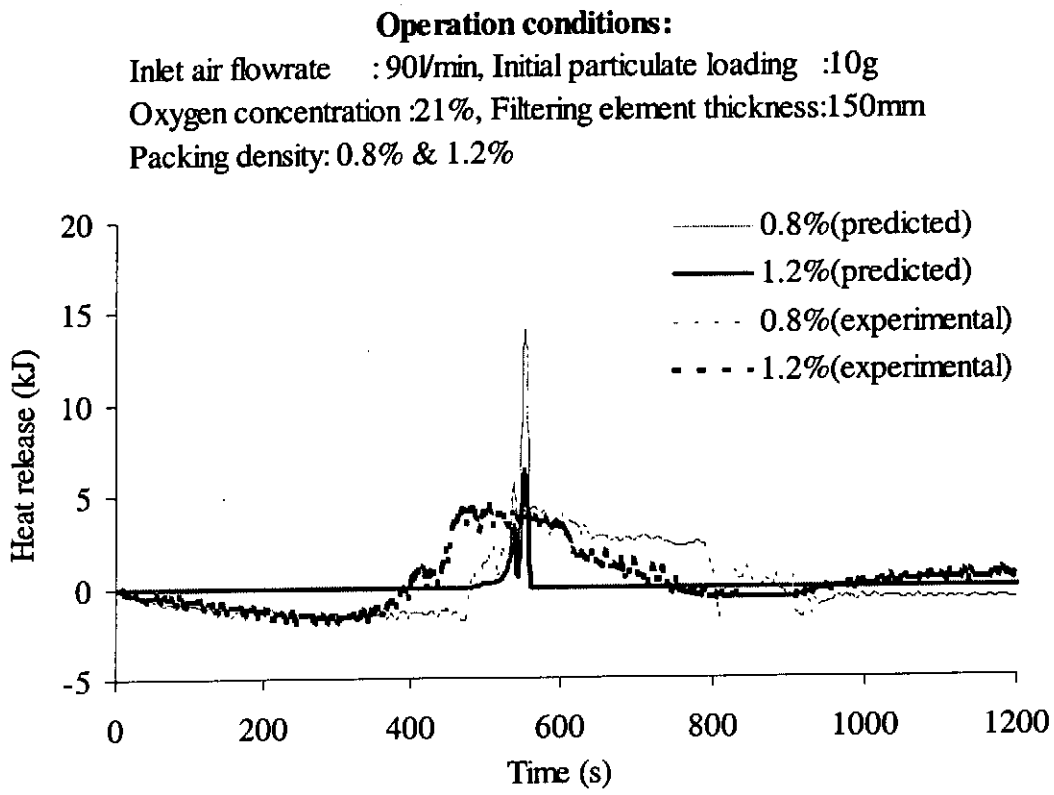

Figure 6.7 Effect of packing density on heat release

6.3.4 Effect of initial particulate loading

Figure 6.8 and Figure 6.9 show the effect of initial particulate loading on the thermal regeneration. The initial particulate loading has the same effect on the regeneration peak temperature and the peak heat release in the experimental result and the predicted result. However, the peak regeneration temperature and peak heat release are both higher in the prediction. It indicates that the initial particulate loading has more effect on the heat release in the prediction. It is because the instantaneous heat release from the model depends essentially on the particulate oxidation rate, which is hence dependent on the amount of initial particulate loading. On the other hand, the heat release in the experiments is mainly the change in internal energy of the filter and the particulate has not been oxidized completely. The difference in peak regeneration temperature is also due to the same reason as stated above.

Operation conditions:

Inlet air flowrate: 90 l/min, Filtering element thickness: 150mm
Packing density : 1.2%, Oxygen concentration : 13%
Initial particulate loading : 8g and 10g

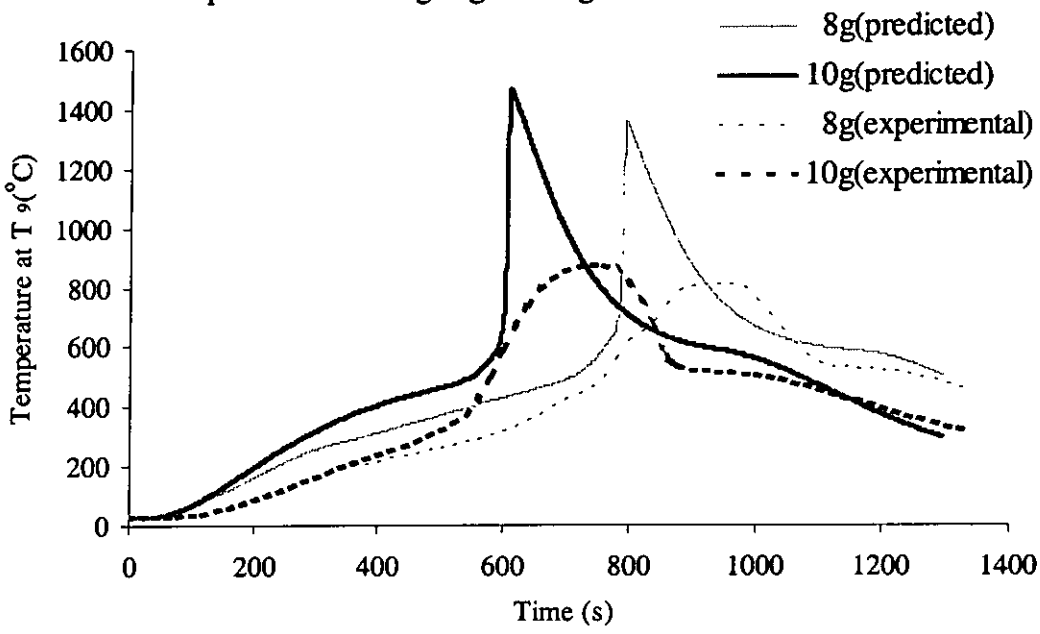

Figure 6.8 Effect of initial particulate loading on filter temperature

Operation conditions:

Inlet air flowrate: 90 l/min, Filtering element thickness: 150mm
Packing density : 1.2%, Oxygen concentration : 13%
Initial particulate loading : 8g and 10g

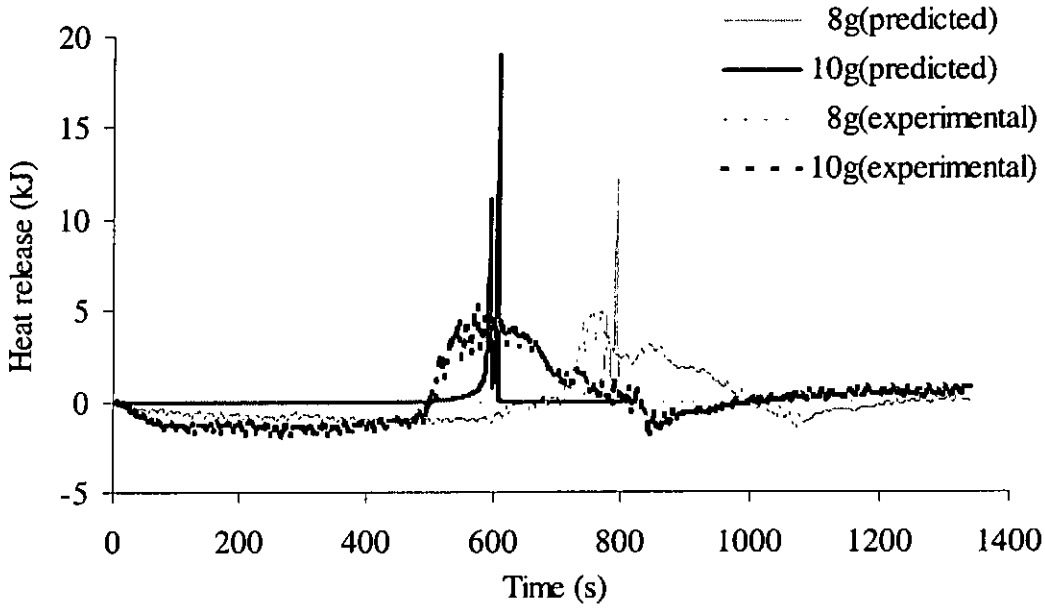

Figure 6.9 Effect of initial particulate loading on heat release

6.4 Summary of discussions

A comparison of the simulated and experimental results under different operation conditions indicated the following general results. The simulated peak regeneration temperature is higher that the measured results. During the heat release period, the simulated rate of temperature rise is higher than the measured results. A comparison of the instantaneous global heat release curves indicate that the peak instantaneous global heat release is higher in the simulated results than the ones calculated based on experimental data; but the heat release period is much shorter. Hence, heat release, or regeneration, is more even in the experiments than in the simulated conditions. Such differences are due mainly to the assumptions made in the numerical models.

CHAPTER 7 CONCLUSIONS AND RECOMMENDATIONS

This chapter summarizes the major findings and conclusions drawn from this study. Suggestions for future work in the area of thermal regeneration of metallic fibrous filter are also included.

7.1 Work accomplished

Previous investigators had studied the thermal regeneration of different kinds of particulate traps, except particulate traps using metallic fibres as the filtering element. To fill in the gap, in this project, a systematic experimental study of the thermal regeneration of metallic fibrous filters was carried out. A test rig, which enabled independent adjustment and measurement of the experimental parameters, had been designed and built for the investigation.

Again, there were a number of numerical and analytical studies on the thermal regeneration of ceramic wall-flow particulate traps, while for metallic fibrous filters, only one related literature was found. To supplement the experimental results, a numerical model, based on fundamental equations, had also been established to study the corresponding process quantitatively. The model includes two sub-models, one on the oxidation of diesel particulate and the other on the subsequent heat transfer process. Simulated results obtained from the numerical model were able to reflect the thermal regeneration process of the filter. They showed good agreement with the experimental results.

Conclusions of the present study can be drawn as follows:

1. From the experimental observation, in order to initiate the thermal regeneration, the inlet air temperature entering the filter should exceed 500°C and the filtering element should have a minimum thickness of 50mm so that sufficient surface area are provided for the particulate to absorb sufficient heat for oxidation. These conditions for regeneration to occur are obtained within the present range of parameters. However, a deficiency in the numerical model exists that thermal regeneration can still be predicted even if the thickness of the filtering element is less than 50mm.
2. The regeneration process of a metallic filter can be divided into three periods, namely, the heating up period, the heat release period and the cooling down period. This is similar to the regeneration process of other types of particulate traps.
3. The numerical model developed was able to predict the regeneration process and the three periods of the process were clearly observed in the simulated results.
4. A rate coefficient has been chosen for this study based on a comparison of the total heat release and a representative filter temperature. However, further comparison between simulated and experimental results indicated that the oxidation rate might be overestimated resulting in a shorter heat release period and higher peak filter temperatures.
5. During the regeneration, peak filter temperature inside the filter increased rapidly up to a normal value between 800°C and 1000°C in the experiments, while it increased further to 1530°C in the predictions. The peak filter temperature was mainly dependent on the oxygen concentration of the heated inlet air and initial particulate loading. In some cases, the local temperature could be as high as 1362°C in the experiment.

6. The peak filter temperature occurred in a region near the exit of the particulate filter, and the fibre of the filtering element was also found to melt at this region when the temperature was excessively high.
7. The peak filter temperature of the thermal regeneration process of a particulate filter depended on several factors, including oxygen concentration, temperature and flow rate of the inlet heated air, initial particulate loading, packing density and thickness of the filter.
8. Heavy initial particulate loading led to an earlier thermal regeneration and a higher peak temperature.
9. A higher flow rate of inlet heated air enabled the regeneration to occur earlier because of the enhanced heat transfer.
10. The total amount of heat release during the thermal regeneration of the particulate filter was found to depend slightly on the oxygen concentration of the inlet air mixture and significantly on the amount of initial particulate loading, but was rather independent of the other parameters.
11. Effects of experimental parameters obtained in the prediction and experiment were inline on the sequence of regeneration. However, the magnitude of the peak filter temperature was usually overestimated in the predicted.
12. Based on the numerical model, the particulate consumption rate, which cannot be obtained experimentally, can be calculated. This provides an additional tool for studying the thermal regeneration process of a fibrous filter.
13. The simulated results were compared with those of Garner and Dent [33] which is the only simulated results available in literature on metallic fibrous filter. The results agree with each other in most cases.

7.2 Recommendations

Several recommendations for future work arise out of this study, which involves both experimental and numerical studies.

7.2.1 Experimental work

It was assumed that the distribution of particulate was uniform in the filter. A special filter can be designed to find out if the distribution of particulate is uniform or the distribution on particulate in the filter, and how regeneration is thus affected.

The flow of air for regeneration was assumed to distribute uniformly inside the filter. A special filter may also be designed to find out the distribution of regeneration air inside the filter and how this affects the regeneration.

In this study, the distribution of temperature in the axial direction of the filter was measured. It is worthwhile to measure the distribution of temperature in the radial direction. It will provide more information on the regeneration process in the filter.

The consumption of oxygen is a reflection of the intensity of the regeneration process. Hence, in addition to the measurement of temperature, it is useful to measure the oxygen contents in different locations of the filter. Moreover, the weight of the filter can be monitored throughout the regeneration process so that the particulate oxidation rate can be measured experimentally. This will also provide information for developing the particulate oxidation model.

7.2.2 Numerical studies

It was assumed that the regeneration process was kinetically controlled. However, it was found that the oxidation rate was overestimated and hence the simulated heat release period was shorter than that derived from experimental data. Therefore, at certain stages of regeneration, especially after certain amount of oxygen has been consumed, the oxidation rate needs to be amended to take into account diffusional control of the oxidation process.

During this study, it was found that existing convective heat transfer expressions could not be applied directly to a fibrous filter using thin stainless steel fibres as the filtering element. Further search of a suitable convective heat transfer expression is required, or alternatively, experiments have to be designed to measure the convective heat transfer coefficient and be applied to the model accordingly.

Effect of radiation between the particulate, gases and fibre is suggested to take into account on the heat transfer model, especially in the heat release period, to provide a better prediction on the thermal regeneration.

PUBLICATIONS

Journal paper accepted for publication (4th September, 2002)

Chau M. W., Cheung C. S. and Leung C. W., "Thermal Regeneration of a Metallic Fibrous Diesel Particulate Filter", Heat and Mass Transfer.

Conference paper presented

Chau M. W., Cheung C. S. and Leung C. W., "Oxidation of Diesel Particulate in a Fibrous Filter", Proceedings of the 6th Asia-Pacific International Symposium on Combustion and Energy Utilization (6th APISCEU), Kuala Lumpur, Malaysia, 20-22 May, 2002, pp.460-465 (2002)

REFERENCES

1. Cheung C. S., Chan S. L., Cheun C. W., Fung H. K., Lo K. K. and Hung W. T. "A particulate trap for light duty diesel vehicles". Proceeding for Diesel Vehicle Exhaust Treatment Technology and Motorcycle Emissions Workshop (1999)

2. Oh, S.H., MacDonald, J.S., Vaneman, G.L. and Hegedus, L.L. "Mathematical modelling of fibrous for diesel particulates – theory and experiment". SAE Paper No. 810113, (1981)

3. Urban, C.M., Landman, L.C., and Wagner, R.D. "Diesel car particulate control methods". SAE Paper No. 830084, (1983)

4. Cheung C.S., Chan S.L., and Hung W.T. "Development of particulate trap for light duty diesel vehicles in hong kong". Proceedings of the 1999 Sino-Korea International Conference on Internal Combustion Engines, Korea, August 1999, pp.19-26 (1999)

5. Cheung C.S., Chan S.L., Cheun C.W., Fung H.K., Hung W.T. and Lo K.K. "Feasibility study of retrofitting low cost traps to in-use diesel vehicles below 4 tonnes gross vehicle weight". Consulting Report for the Environmental Protection Department of the Hong Kong SAR Government, July, (2000)

6. Hung W.T., Cheung C.S., Yau D., Hung A., Tsang M., Ha K. and Mok W.C. "Diesel vehicles emissions control and its emissions benefits in Hong Kong". SAE 2001 World Congress, Detroit, Michigan, 5-8 March, 2001, pp.2001-01-188 (2001)

7. Johnson J. H., Bagley S. T., Gratz L. D., and Leddy D. G. "A review of diesel particulate control technology and emissions effects-1992 horning memorial award lecture". SAE Paper 940233 (1994)

8. Ranajit S, Northrop P. S., Flagan R. C. and Gavalas G. R. "Char combustion: measurement and analysis of particle temperature histories". Combustion Science and Technology, Vol.60, pp.215-230 (1988)

9. Fedotov S. P., Tre'Yakov M. V. "Stochastic criteria for ignition of single particles". Combustion Science and Technology, Vol.78, pp.1-6 (1991)

10. Fu W. B. and Yan H. F.. "A method for analyzing the heterogeneous ignition of carbon/char particles". Combustion Science and Technology, Vol.81, pp.301-312 (1992)

11. Noirot R., Gilot P., Gadiou R. and Prado G. "Control of soot emission by filtration and post-combustion. a laboratory study of the regeneration of an organic particulate trap assisted by hydrocarbon injection". Combustion Science and Technology, Vol.85, pp.117-131 (1992)

12. Zhang G. L., Jing J. H., Ning Z., Zhao X. R., Liang L. H., Chen J. H. "Kinetic analysis on the catalytic oxidation process of diesel particulate". Transaction of CSICE, Vol. 13, No. 1, pp.46-52 (1995)

13. Mayer A., Emig G., Gmehling B., Popovska N., and Holemann K., Buck A. "Passive regeneration of catalyst coated knitted fiber diesel particulate traps". SAE Paper 960138 (1996)

14. Hawker P. and Myers N., Huthwohl G. and Vogel Th., Bates B., Magnusson L., Bronnenberg P. "Experience with a new particulate trap technology in europe". SAE Paper 970182 (1997)

15. Peterson R. C. "The oxidation rate of diesel particulate which contains lead". SAE Paper 870628 (1987)

16. Lepperhoff G. and Luders H., Barthe P. and Lemaire J. "Quasi-continuous particle trap regeneration by cerium-additives". SAE Paper 950369 (1995)

17. Pattas K., Samaras Z., and Roumbos A., Lemaire J. and Mustel W., Rouveirolles P. "Regeneration of dpf at low temperatures with the use of cerium based fuel additive". SAE Paper 960135 (1996)

18. Tan J. C., Opris C. N., Baumgard K. J., and Johnson J. H. "A study of the regeneration process in diesel particulate traps using fuel additive". SAE Paper 960136 (1996)

19. Koltsakis G. C. and Stamatelos A. M. "Modelling catalytic regeneration of wall-flow particulate filters". Ind. Eng. Chem. Res., 35, pp.2-13 (1996)

20. Koltsakis G. C.and Stamatelos A. M. "Modes of catalytic regeneration in diesel particulate filters". Ind. Eng. Chem. Res., 36, pp.4155-4165 (1997)

21. Zelenka P. and Reczek W., Mustel W., Rouveirolles P. "Towards securing the particulate trap regeneration: a system combining a sintered metal filter and ceramic fuel additive". SAE Paper 982598 (1998)

22. Stanmore B., Brilhac J. F. and Gilot P. "The ignition and combustion of cerium doped diesel soot". SAE Paper 1999-01-0115 (1999)

23. Ichikawa Y., Hattori I. and Kasai Y. "The regeneration efficiency improvement of the reverse pulse air regenerating dpf system". SAE Paper 960127 (1996)

24. Romero-Lopez A. F., Gutierrez-Salians R., and Garcia-Moreno R. "Soot combustion during regeneration of filter ceramic traps for diesel engines". SAE Paper 960469 (1996)

25. Larsen C. A., Levendis Y. A. "Filtration assessment and thermal effects on aerodynamic regeneration in silicon carbide and cordierite particulate filters". SAE Paper 1999-01-0466 (1999)

26. Konstandopoulos A. G. and Kostoglou M. "Periodically reversed flow regeneration of diesel particulate traps". SAE Paper 1999-01-0469 (1999)

27. Shadman F. "Kinetics of soot combustion during regeneration of surface filters". Engine Operation". Combustion Science and Technology, Vol.63, pp.183-191 (1989)

28. Obuchi A., Aoyama H., Ohi A. "A study of an optical temperature monitoring device sensitive in the extended region to controlled regeneration of a diesel particular filter". Combustion Science and Technology, Vol.77, pp.179-187 (1991)

29. Hoj J. W. and Sorenson S. C., Stobbe P. "Thermal loading in sic particle filters". SAE Paper 950151 (1995)

30. Okazoe H., Shimizu K., and Watanable Y., Sanitago E., Kugland P., Ruth W. "development of a full-flow burner regeneration type diesel particulate filter using sic honeycomb". SAE Paper 960130 (1996)

31. Kim J. U., Hyeon B.Y., Park D. S. and Kim E. S. "Regeneration characteristics of a burner type diesel particulate trap system in a steady-state engine operation". Combustion Science and Technology, Vol.130, pp.115-130 (1997)

32. Park D. S., Kim J. U., Cho H., and Kim E. S. "Consideration on the temperature distribution and gradient in the filter during regeneration in burner type diesel particulate trap system (II)". SAE Paper 980188 (1998)

33. Garner C.P., and Dent J.C. "A Thermal Regeneration Model for Monolithic and Fibrous Diesel Particulate Traps". SAE Paper No. 880007 (1988)

34. Wang G. H., Guo Y. N., Ji Y., Xiao Z. C., Liu X. J. "Thermal regeneration of diesel exhaust particulate trap with ceramic foam element". Transaction of CSICE, Vol. 7, No. 1, pp.7-12 (1989)

35. Opris C. N. and Johnson J. H. "A 2-D computational model describing the heat transfer, reaction kinetics and regeneration characteristics of a ceramic diesel particulate trap". SAE Paper 980546 (1998)

36. Gadde S. B. and Johnson J. H. "A computational model describing the performance of a ceramic diesel particulate trap in steady operation and over transient cycle". SAE Paper 1999-01-0465 (1999)

37. Konstandopoulos A. G. and Skaperdas E., Warren J., Allansson R. "Optimized filter design and selection criteria for continuously regenerating diesel particulate traps". SAE Paper 1999-01-0468 (1999)

38. Kojetin P. L., Kittelson D. B. "System level computer simulation for modelling electrical regeneration diesel particulate traps". SAE Paper 930127 (1993)

39. Shirk R. and Bloom R., Kitahara Y. and Shinzawa M. "Fiber wound electricitrcally regenerable diesel particulate filter cartridge for small diesel engines', SAE Paper 950153 (1995)

40. Kazushige O., Noriyuki T., Takeshi N., Hong S. T., Masaaki K. and Teruo K. "SIC diesel particulate filter application to electric heater system". SAE Paper 1999-01-0464 (1999)

41. Paul A. Baron and Klaus Willeke. *Aerosol measurement, principles, techniques, and applications, second edition.* New York (2001)

42. William C. Hinds. *Aerosol technology, properties, behavior, and measurement of airborne particles, second edition.* New York (1999)

43. Turns S. R., *An introduction to combustion*, McGraw-Hill Book Co., (1996)

44. J. P. Holman, *Experimental methods for engineers, sixth edition,* McGraw-Hill Book Co., (1994)

45. Leung C.W., Chan T.L. and Chen S. "Forced convection and friction in triangular duct with uniformly spaced square ribs on inner surfaces", Heat and Mass Transfer, Vol. 37, pp.19-25 (2001)

46. Marcuccilli F., Gilot P., Stanmore B. and Prado G. "Experimental and theoretical study of diesel soot reactivity". Twenty-Fifth Symposium (International) on Combustion/The Combustion Institute, 1994, pp.619-626 (1994)

47. J. P. Holman, *Heat Transfer, eighth edition,* McGraw-Hill Book Co., (1997)

48. D.Y. Lee, J.S. Jin and B.H. Kang "Momentum boundary layer and its influence on the convective heat transfer in porous media". International Journal of Heat and Mass Transfer, Vol. 45, p.229-233 (2002)

Appendix A Temperature profiles

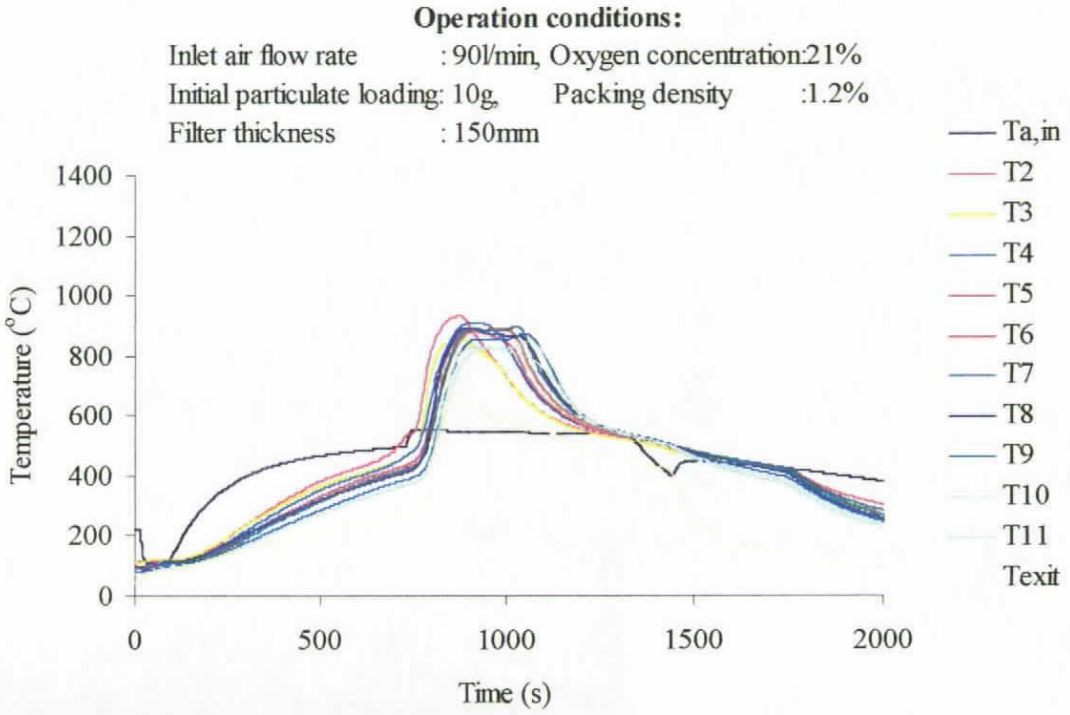

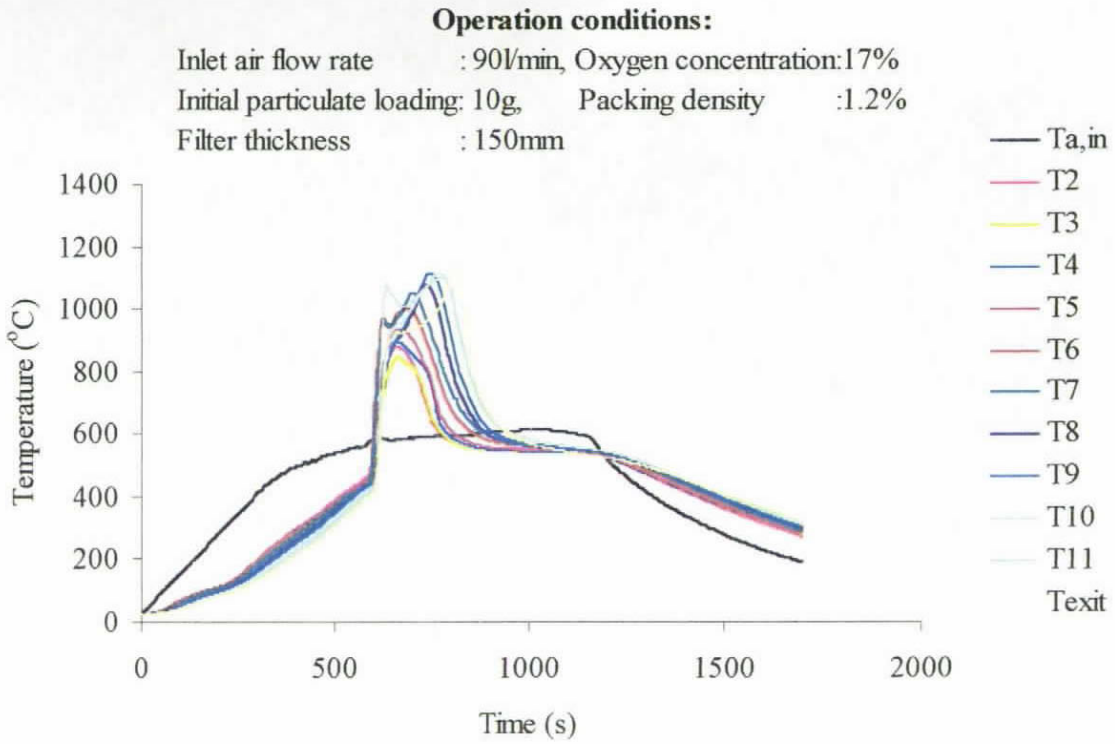

Operation conditions:

Inlet air flow rate : 90l/min, Oxygen concentration:13%
Initial particulate loading: 10g, Packing density :1.2%
Filter thickness : 150mm

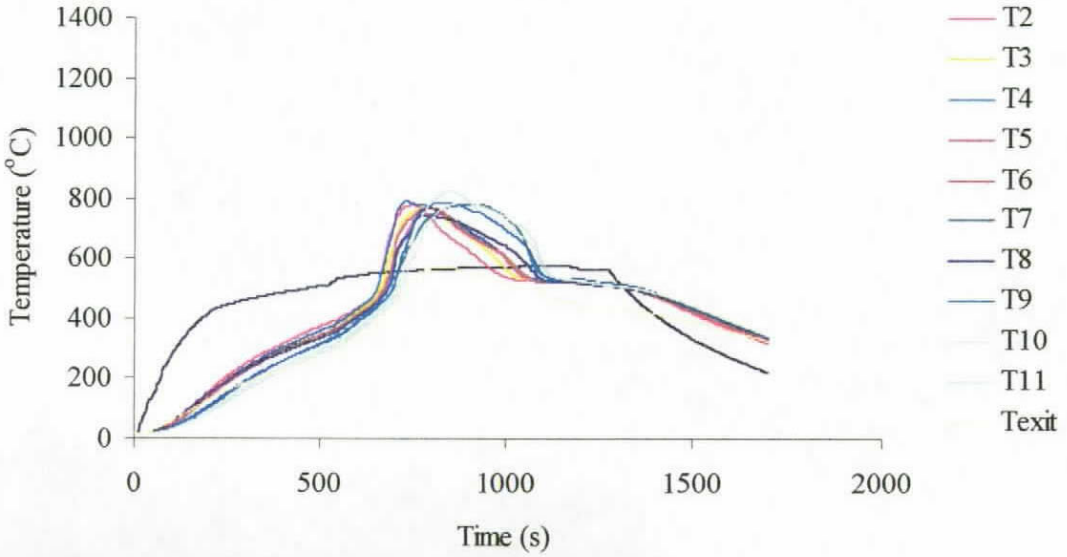

Operation conditions:

Inlet air flow rate : 67l/min, Oxygen concentration:13%
Initial particulate loading: 10g, Packing density :1.2%
Filter thickness : 150mm

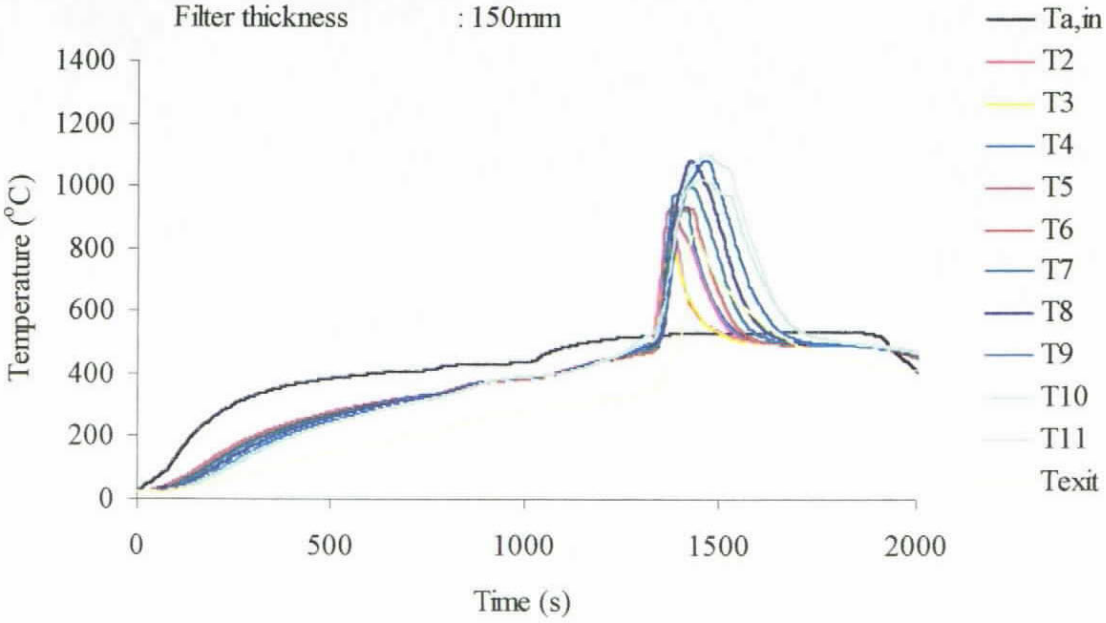

Operation conditions:

Inlet air flow rate : 90l/min, Oxygen concentration:13%
Initial particulate loading: 10g, Packing density :1.2%
Filter thickness : 150mm

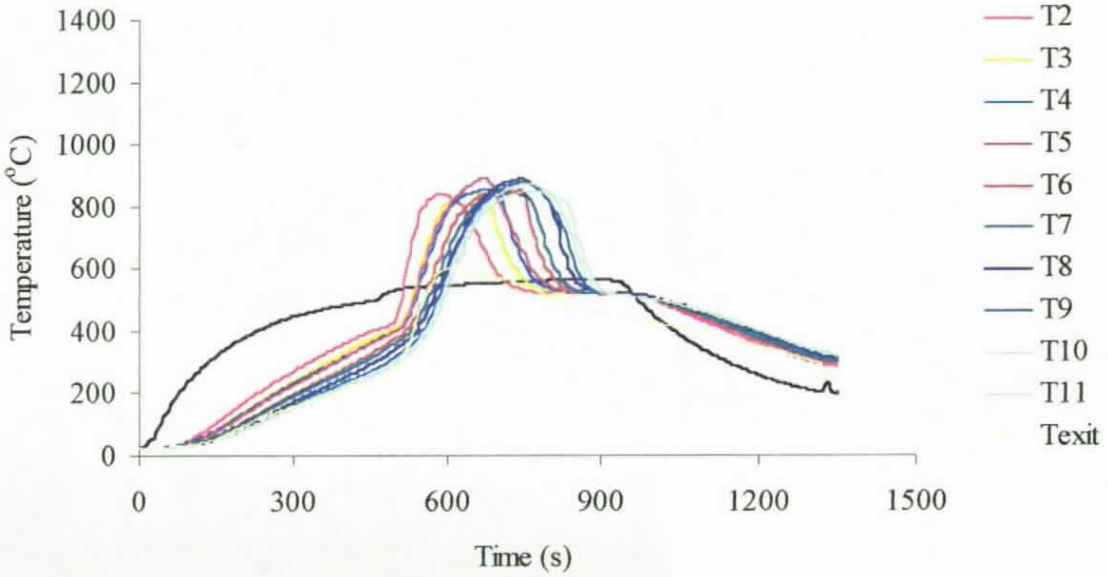

Operation conditions:

Inlet air flow rate : 112l/min, Oxygen concentration:13%
Initial particulate loading : 10g, Packing density :1.2%
Filter thickness : 150mm

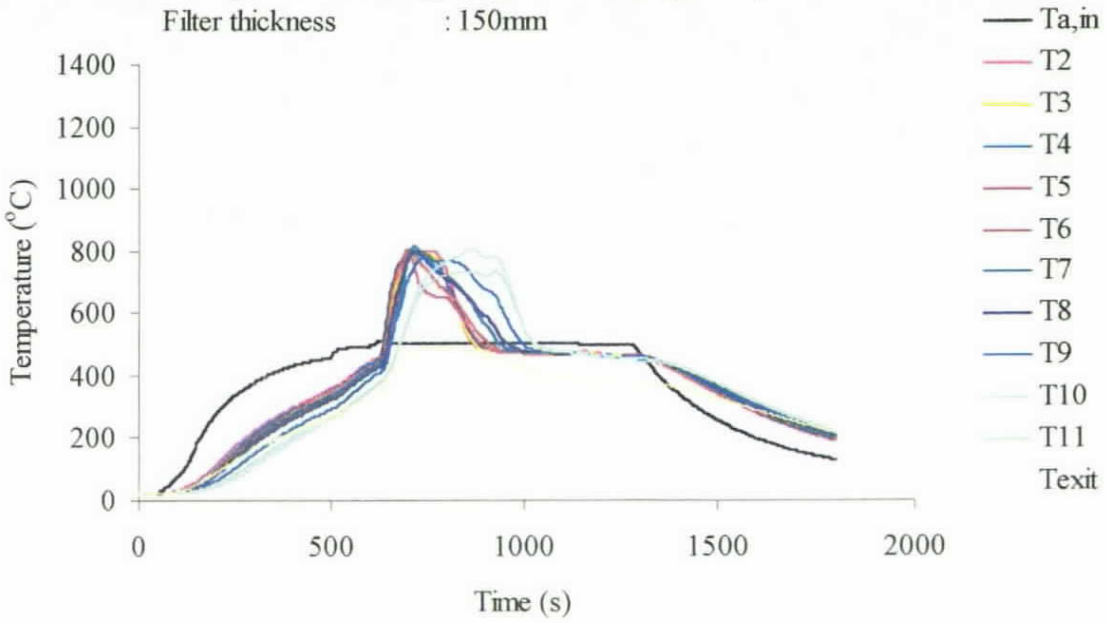

Operation conditions:

Inlet air flow rate : 90l/min, Oxygen concentration:21%
Initial particulate loading: 10g, Packing density :0.8%
Filter thickness : 150mm

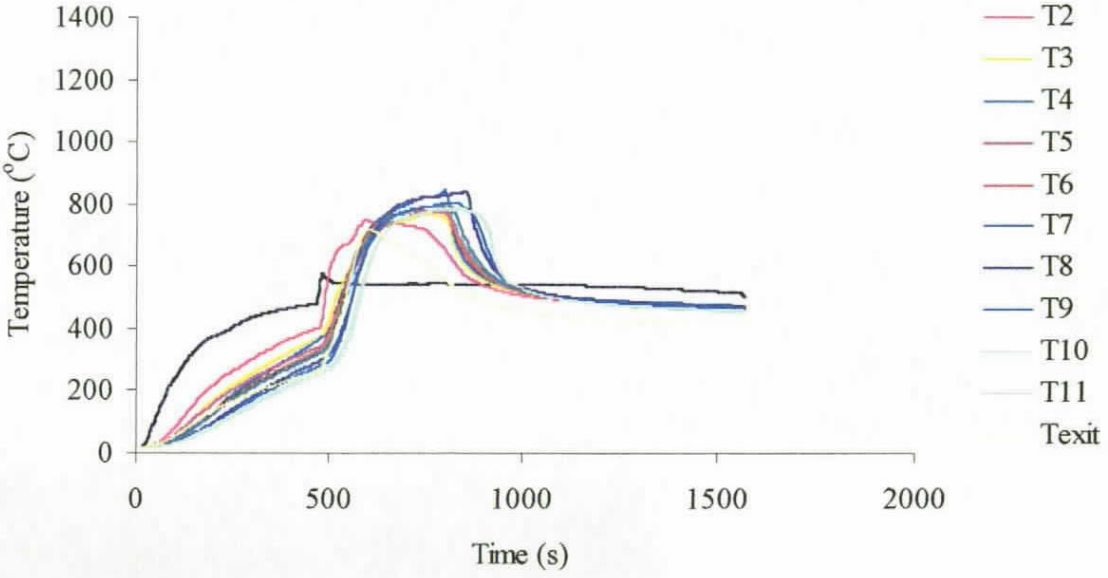

Operation conditions:

Inlet air flow rate : 90l/min, Oxygen concentration:21%
Initial particulate loading: 10g, Packing density :1.0%
Filter thickness : 150mm

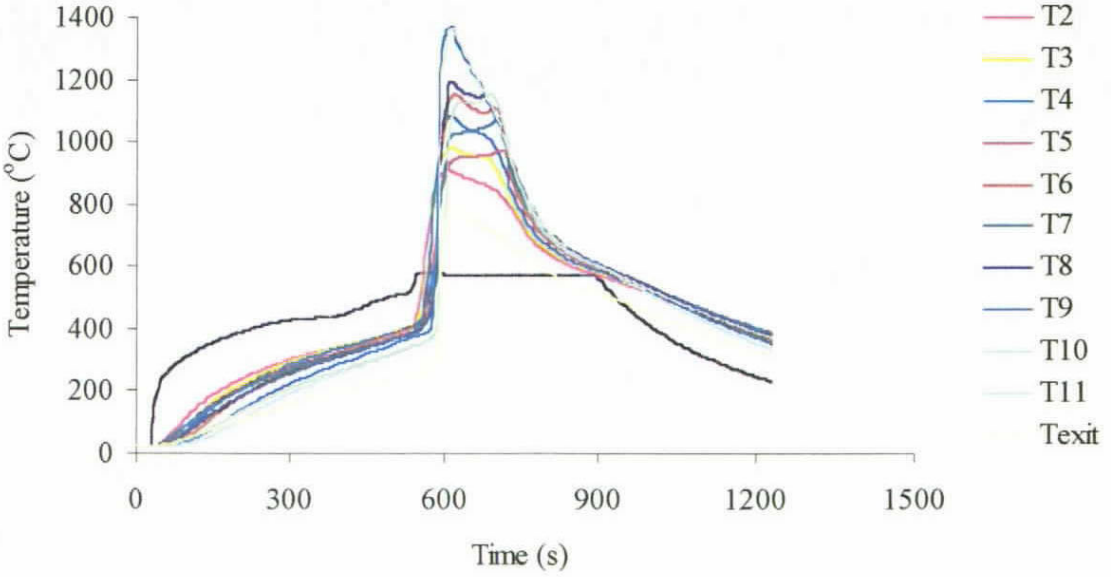

Operation conditions:

Inlet air flow rate : 90l/min, Oxygen concentration:13%
Initial particulate loading :3.3g, Packing density :1.2%
Filter thickness : 50mm

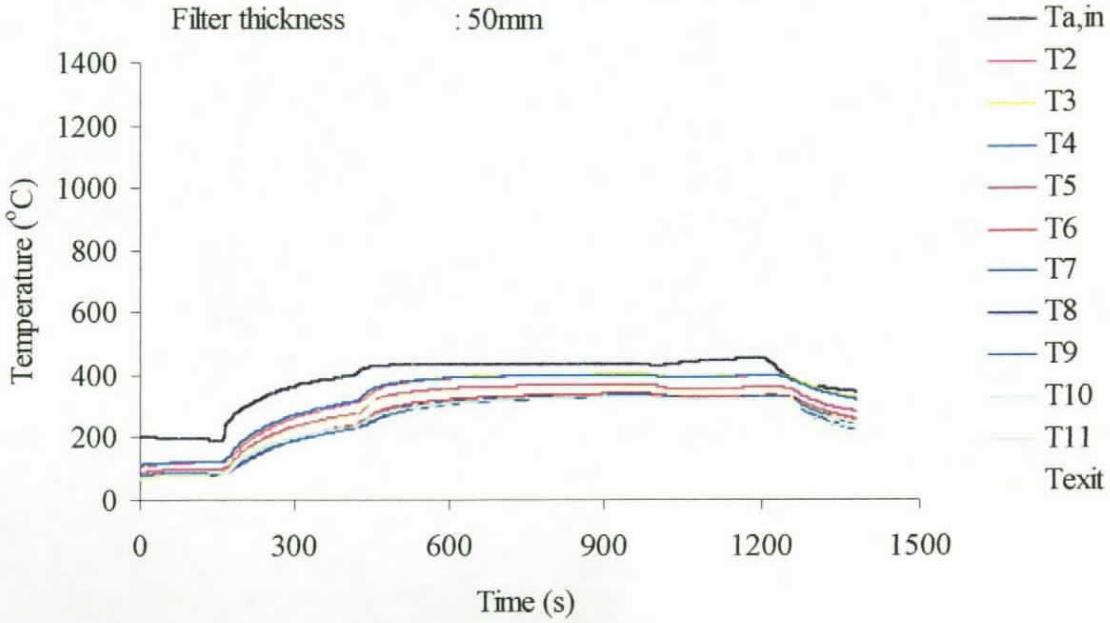

Operation conditions:

Inlet air flow rate : 90l/min, Oxygen concentration :13%
Initial particulate loading : 6.6g, Packing density :1.2%
Filter thickness : 100mm

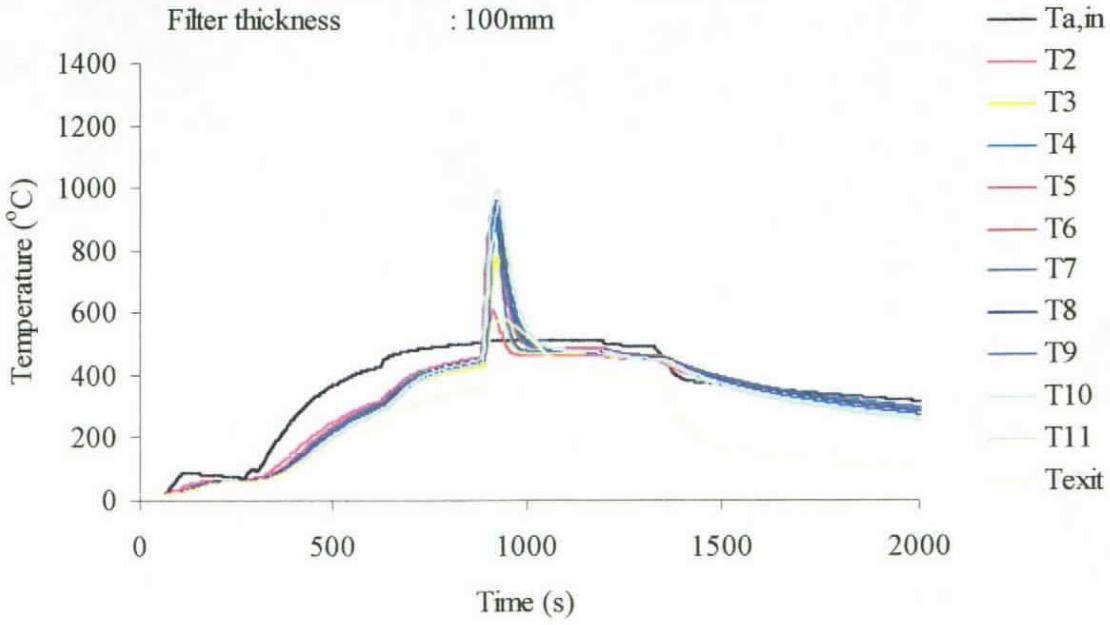

Operation conditions:

Inlet air flow rate : 90l/min, Oxygen concentration :6%
Initial particulate loading : 20g, Packing density :1.2%
Filter thickness : 150mm

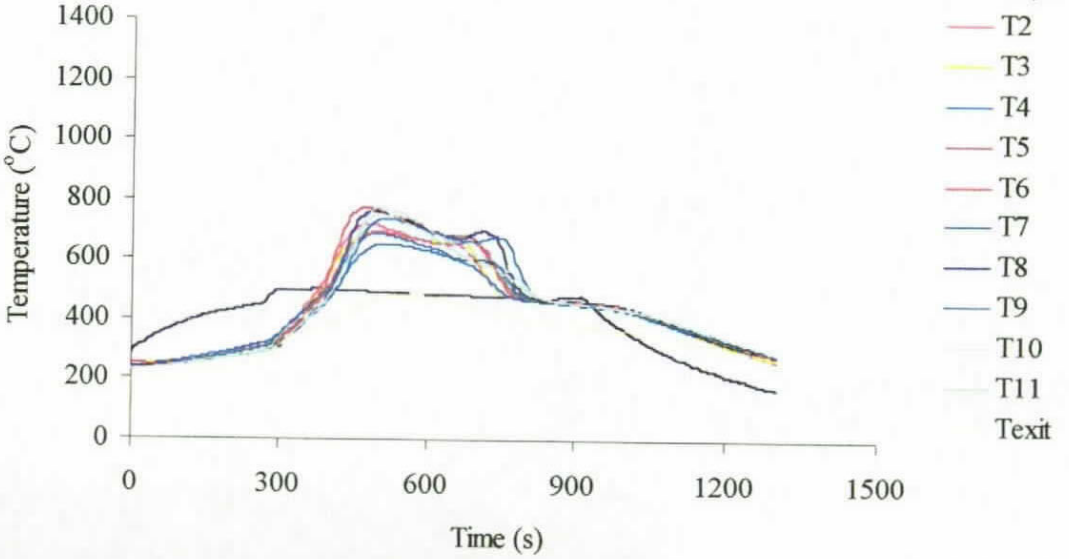

Operation conditions:

Inlet air flow rate : 90l/min, Oxygen concentration:13%
Initial particulate loading: 8g, Packing density :1.2%
Filter thickness : 150mm

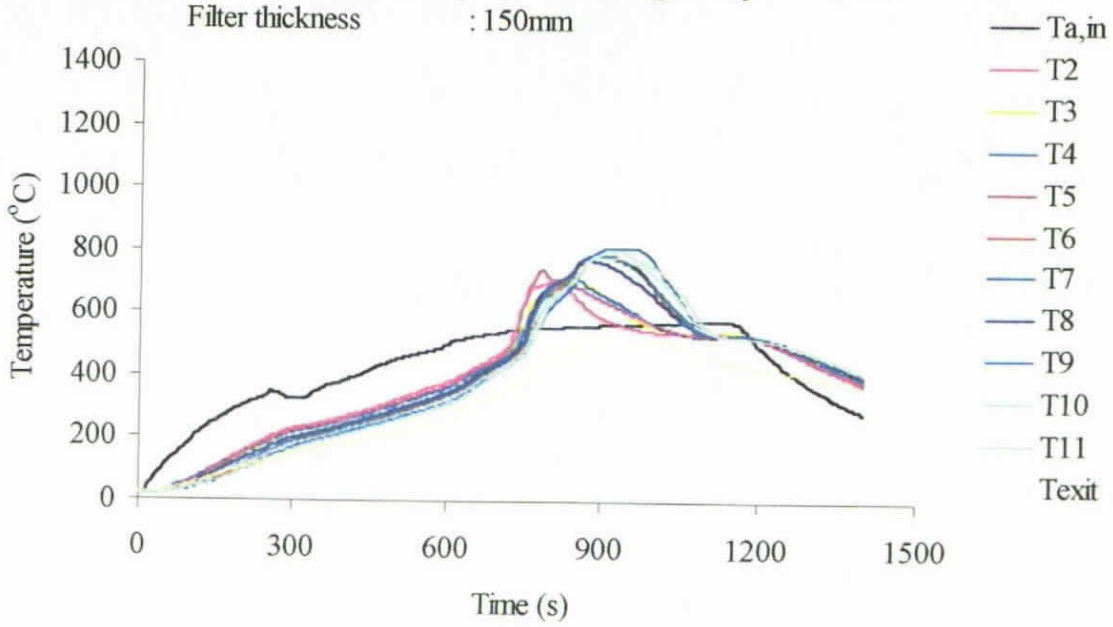

Operation conditions:

Inlet air flow rate : 90l/min, Oxygen concentration:13%
Initial particulate loading : 6g, Packing density :1.2%
Filter thickness : 150mm

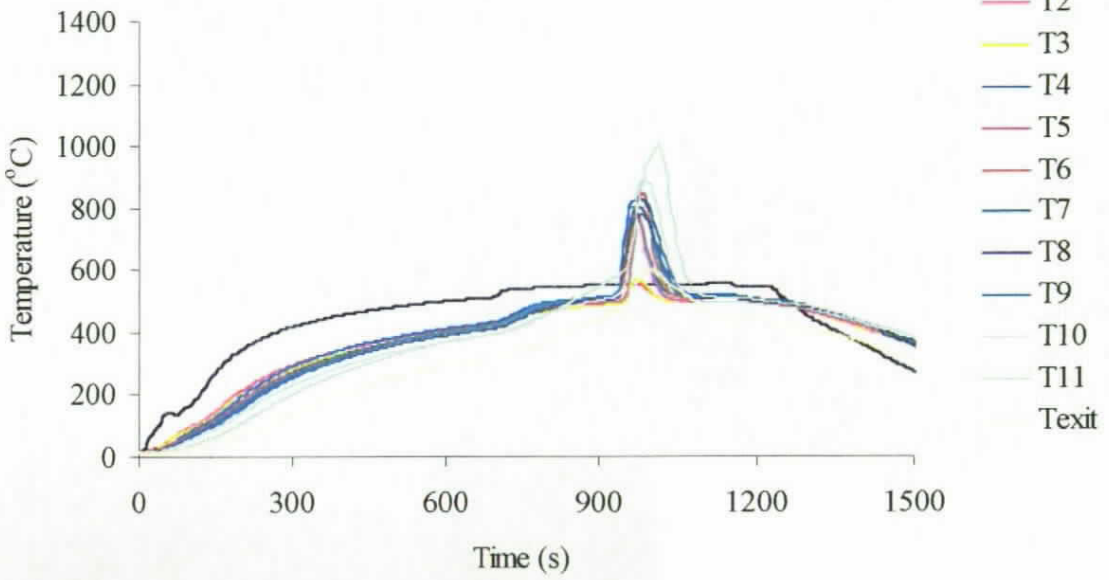

Operation conditions:

Inlet air flow rate : 90l/min, Oxygen concentration:13%
Initial particulate loading : 2g, Packing density :1.0%
Filter thickness : 150mm

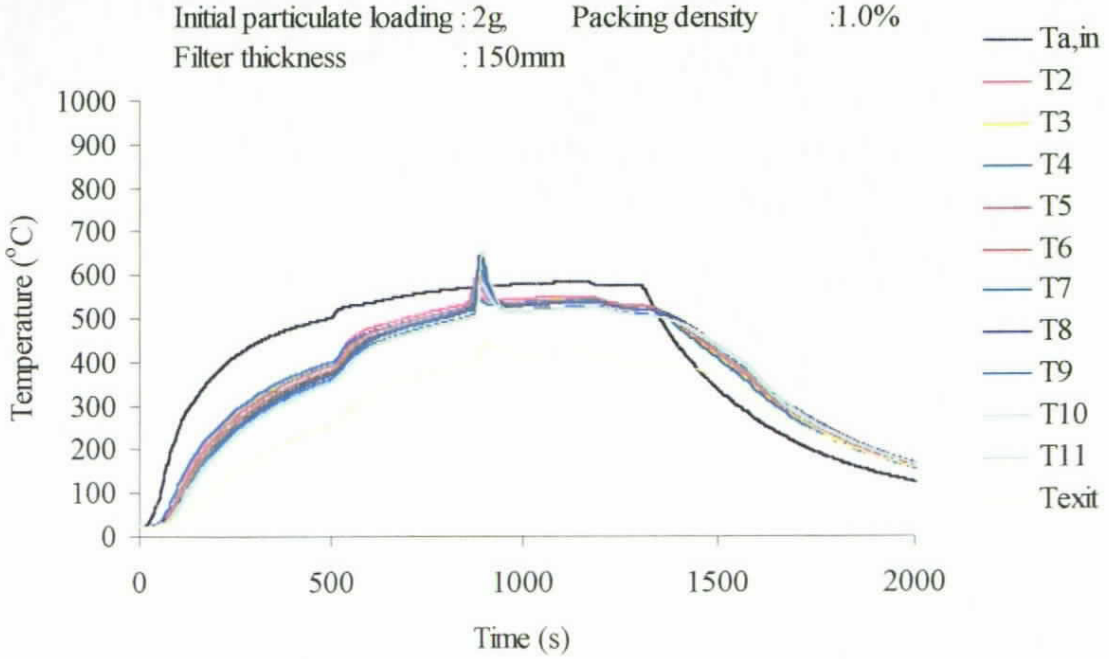

Appendix B Program listing

**The words written in italic are the remarks of the program*

Title of the MPhil project:
Thermal Regeneration of a diesel particulate filter

Start of program

```
disp(' Inlet air is assumed to consist of nitrogen air and oxygen air only.')
disp(' Please give a name for the file  which stores the result of the simulation.')

result=input('resultfile','s')
diary on
diary (result)

clear all
```

inputs by user

concentration of oxygen and nitrogen of inlet air

```
conc_O2=input('Inlet air oxygen concentration,(%)=')/100;
conc_N2=1-conc_O2;
```

input inlet air flow rate, m^3/s

```
Q=input('Inlet air flowrate,(l/min)=')*(5^0.5)/(1000*60)
```

input the initial particulate loading, kg

```
M_p1=input('Initial particulate loading on the entire filter,(g)=')
M_p=M_p1/1000;
```

no. of zones of the filter

```
nz=input('no. of zones,(nz)=')
```

packing density of the filter

```
Pd=input('packing density of the filter,%,(pd)=')
pd=Pd/100;
```

length of the filter, m

```
Le=input('length of the filter,mm,(L)=')
L=Le/1000;
```

physical numbers

density of nitrogen gas and oxygen gas at room temperature, kg/m^3
Rden_N2=1.1233;
Rden_O2=1.284;

molecular weight of oxygen and nitrogen of inlet air
mw_N2=28.013;
mw_O2=31.99;

specific heat capacity of stainless steel fibre, kJ/kg-K
cp_f=0.46;

density of stainless steel fibre, kg/m^3
Denssf=7800;

conductivity of stainless steel fibre, kW/mK
k_cond=0.05;

calculations of physical numbers

molecular weight of inlet air
mw_Air1=conc_O2*mw_O2+conc_N2*mw_N2;

mass fraction of oxygen and nitrogen of inlet air
Y_O2=mw_O2*conc_O2/mw_Air1;
Y_N2=1-Y_O2;

density of inlet air at room temperature, kg/m^3
Rden_Air1=conc_O2*Rden_O2+conc_N2*Rden_N2;

mass flow rate of inlet gas and oxygen gas, kg/s
MFR_Air1=Q*Rden_Air1;
MFR_O2=MFR_Air1*Y_O2;

physical data of the filter

diameter of the filter, m
D=0.125;

volume of filter, m^3
V_filter=((D^2)/4)*L*pi;

discrete zone volume, m^3
v_filter=V_filter/nz;

time for air flow through a discrete zone, s
t_v=v_filter/Q;

area for air flow, m^2
a_airflow=((D^2)/4)*pi*(1-pd);

space velocity of air flow, m/s
vel_air=Q/a_airflow;

length of the one zone, m
l=L/nz;

mass of stainless steel fibre of the entire filter, kg
M_f=pd*V_filter*Denssf;

mass of filter casing, kg
M_case=0.4073;

mass of spiral rod, kg
M_rod=0.074439;

mass of nuts, kg
M_nuts=0.008;

mass of washers, kg
M_washer=0.009;

mass of outlet hole plate, kg
M_ohp=0.0521;

mass of separating plates(square wire mesh), kg
M_swm=0.0053;

total mass of filter, kg
M_filter=M_case+M_rod+M_nuts+M_washer+M_ohp+M_swm;

total mass of filter per zone, kg/nz
m_filter=M_filter/nz;

mass of particulate per zone, kg/nz
m_p=M_p/nz;

mass of air in the whole filter, kg
M_air=(1-pd)*((D^2)/4)*(L)*Rden_Air1*pi;
m_air=M_air/nz

```
input the data of inlet air temperature, K
datafile=input('which exp','s')
cd('C:\research\program\Input Data\temperature')
Temp=load (datafile);

loading gas properties tables
O2_prop=load ('C:\research\program\Input Data\properties table5\O2.txt');
N2_prop=load ('C:\research\program\Input Data\properties table5\N2.txt');

loading arrhenius number
Arr=load ('C:\research\program\Input Data\properties table5\arrhenius.txt');

size of the temperature file
[m,n]=size(Temp);

total time of inlet air supplied, s
Total_time=m*5;

number of time-steps
n_t_step=(Total_time)/t_v;

open an array for filter temperature, K
T=zeros(round(n_t_step),nz);
T(1,:) =298;

open an array for inlet air temperature, K
T_a=zeros(round(n_t_step),nz);

initial value of air temperature,K
T_a(1,1)=Temp(1,2);

initialise time array, s
T_v_incr(1)=0;
t_v_incr=0;

for loop to interpolate inlet air temperature
for i=2:round(n_t_step);
   t_v_incr=t_v_incr+t_v;
   T_a(i,1)=interp1(Temp(:,1),Temp(:,2),t_v_incr);
   T_v_incr(i)=t_v_incr;
end

initial density of inlet air, kg/m^3
density_O2=interp1(O2_prop(:,1),O2_prop(:,4),T_a(1,1));
density_N2=interp1(N2_prop(:,1),N2_prop(:,4),T_a(1,1));
density_air=density_O2*Y_O2+density_N2*Y_N2;
```

```
open an array for densities of gases, kg/m^3
den_O2=zeros(round(n_t_step),nz);
den_O2(1,1)=density_O2;
den_air=zeros(round(n_t_step),nz);
den_air(1,1)=density_air;

sepecific heat capacity of oxygen, nitrogen and air, kJ/kgK
specific_heat_O2=interp1(O2_prop(:,1),O2_prop(:,3),T_a(1,1));
specific_heat_N2=interp1(N2_prop(:,1),N2_prop(:,3),T_a(1,1));
specific_heat_air=specific_heat_O2*Y_O2+specific_heat_N2*Y_N2;
cp_air=zeros(round(n_t_step),nz);
cp_air(1,1)=specific_heat_air;

enthalpy of oxygen, nitrogen and air, kJ/kg
h1_O2=interp1(O2_prop(:,1),O2_prop(:,2),T(1,1));
h1_N2=interp1(N2_prop(:,1),N2_prop(:,2),T(1,1));
enthalpy_air1=h1_O2*Y_O2+h1_N2*Y_N2;
h_air=zeros(round(n_t_step),nz);
h_air(1,:)=enthalpy_air1;

interpolation for enthalpy of inlet air, kJ/kg
for i=1:round(n_t_step);
   h1_O2=interp1(O2_prop(:,1),O2_prop(:,2),T_a(i,1));
   h1_N2=interp1(N2_prop(:,1),N2_prop(:,2),T_a(i,1));
   h_air_inlet(i)=h1_O2*Y_O2+h1_N2*Y_N2;
end;

open array for arrhenius number
K=zeros(round(n_t_step),nz);
K(1,:)=0;

open array for enthalpy of combustion,J
E_comb=zeros(round(n_t_step),nz);

open array for oxygen concentration
con_O2=zeros(round(n_t_step),nz);
con_O2(:,1)=conc_O2;

mass of oxygen gas, kg
m_O2=MFR_O2*t_v;

open array for mass of particulate, kg
M_p=zeros(round(n_t_step),nz);
M_p(1,:)=m_p;
```

main calculation

```
outer for loop for time step
for i=1:(round(n_t_step));

   initialise mass of oxygen consumed to 0
   accum_mass_O2_used=0;

   inner for loop for position
   for j=1:nz;

   inlet zone
   if j==1;

   calculation of filter temperature
   T(i+1,j)=(K(i,j)*con_O2(i,j)*den_O2(i,j)*M_p(i,j)*E_comb(i,j)+MFR_Air1*1000*
            (h_air_inlet(i)-h_air(i,j))+(k_cond*v_filter*pd*1000*(T(i,j+1)-T(i,j))/l^2))
            *t_v /(m_filter*cp_f*1000+m_air*cp_air(i,j)*1000)+T(i,j);

   calculation of heat transfer between air and fibre
   B(i,j)=MFR_Air1*1000*(h_air_inlet(i)-h_air(i,j));
   calculation of conduction
   C(i,j)=k_cond*v_filter*pd*1000*(T(i,j+1)-T(i,j))/l^2;

   outlet zone
   elseif j==nz  ;

   calculation of filter temperature
   T(i+1,j)=(K(i,j)*con_O2(i,j)*den_O2(i,j)*M_p(i,j)*E_comb(i,j)+MFR_Air1*1000*
            (h_air(i,j-1)-h_air(i,j))+(k_cond*v_filter*pd*1000*(T(i,j-1)-T(i,j))/l^2))
            *t_v /(m_filter*cp_f*1000+m_air*cp_air(i,j)*1000)+T(i,j);

   calculation of heat transfer between air and fibre
   B(i,j)=MFR_Air1*1000*(h_air(i,j-1)-h_air(i,j));
   calculation of conduction
   C(i,j)=k_cond*v_filter*pd*1000*(T(i,j-1)-T(i,j))/l^2;

   inner zones
   else;

   T(i+1,j)=(K(i,j)*con_O2(i,j)*den_O2(i,j)*M_p(i,j)*E_comb(i,j)+MFR_Air1*1000*
            (h_air(i,j-1)-h_air(i,j))+(k_cond*v_filter*pd*1000*( T(i,j+1)+T(i,j-1)-
            2*T(i,j))/l^2))*t_v /(m_filter*cp_f*1000+m_air*cp_air(i,j)*1000)+T(i,j);

   calculation of heat transfer between air and fibre
   B(i,j)=MFR_Air1*1000*(h_air(i,j-1)-h_air(i,j));
   calculation of conduction
   C(i,j)=k_cond*v_filter*pd*1000*( T(i,j+1)+T(i,j-1)-2*T(i,j))/l^2;
```

```
end;

    check if filter temperature is a number
    if isnan(T(i+1,j))>0
       error('not a numberss')
    end


    check if filter temperature reaches the ignition temperature of particulate
    if T(i+1,j) >= 773;

       T_k=(T(i,j)+T(i+1,j))/2;
       K(i+1,j)=interp1(Arr(:,1),Arr(:,3),T_k);
       E_comb(i+1,j)=28000000;

       mass of particulate in next time-step
       M_p(i+1,j)=(M_p(i,j))*exp(-(K(i+1,j)*con_O2(i,j)*den_O2(i,j)*t_v));

       mass of oxygen consumed in one zone
       mass_O2_used=(M_p(i,j)-M_p(i+1,j))*(31.999/12.01);

       accumulated mass of oxygen used
       accum_mass_O2_used=accum_mass_O2_used + mass_O2_used;

       mass of oygen available for oxidation in next zone
       mass_O2_avai=MFR_O2*t_v-accum_mass_O2_used;

       check if mass of oxygen is still available
       if mass_O2_avai >= 0,
          con_O2(i,j+1)=mass_O2_avai*mw_Air1/(mw_O2*MFR_Air1*t_v);
       else con_O2(i,j+1)=0;

       end

       check if particulate is oxidized
       if M_p(i+1,j)==M_p(i,j),
          con_O2(i,j+1)=con_O2(i,j);
       else
          con_O2(i,j+1)=con_O2(i,j+1);
       end


    else M_p(i+1,j)=M_p(i,j);
    con_O2(i,j+1)=con_O2(i,j);

    E_comb(i+1,j)=0;

    end
```

```
    if j~=nz;
       Tj=T(i,j+1);
    end

    if j~=nz;

       update gas properties
       density_O2=interp1(O2_prop(:,1),O2_prop(:,4),Tj);
       density_N2=interp1(N2_prop(:,1),N2_prop(:,4),Tj);
       den_air(i,j+1)=density_O2*Y_O2+density_N2*Y_N2;
       den_O2(i,j+1)=density_O2;

       specific_heat_O2=interp1(O2_prop(:,1),O2_prop(:,3),Tj);
       specific_heat_N2=interp1(N2_prop(:,1),N2_prop(:,3),Tj);
       cp_air(i,j+1)=specific_heat_O2*Y_O2+specific_heat_N2*Y_N2;

       h1_O2=interp1(O2_prop(:,1),O2_prop(:,2),Tj);
       h1_N2=interp1(N2_prop(:,1),N2_prop(:,2),Tj);
       h_air(i,j+1)=h1_O2*Y_O2+h1_N2*Y_N2;

    end

    end


Ti=T(i+1,1);

density_O2=interp1(O2_prop(:,1),O2_prop(:,4),Ti);
density_N2=interp1(N2_prop(:,1),N2_prop(:,4),Ti);
den_air(i+1,1)=density_O2*Y_O2+density_N2*Y_N2;
den_O2(i+1,1)=density_O2;

specific_heat_O2=interp1(O2_prop(:,1),O2_prop(:,3),Ti);
specific_heat_N2=interp1(N2_prop(:,1),N2_prop(:,3),Ti);
cp_air(i+1,1)=specific_heat_O2*Y_O2+specific_heat_N2*Y_N2;

h1_O2=interp1(O2_prop(:,1),O2_prop(:,2),Ti);
h1_N2=interp1(N2_prop(:,1),N2_prop(:,2),Ti);
h_air(i+1,1)=h1_O2*Y_O2+h1_N2*Y_N2;

end

calculation of instantaneous local heat release during combustion
for i=1:round(n_t_step);
   for j=1:nz;
      A(i,j)=K(i,j)*con_O2(i,j)*den_O2(i,j)*M_p(i,j)*E_comb(i,j);
   end;
end;
```

```
calculation of instantaneous global heat release during combustion
Aoverall=A(:,1)+A(:,2)

calculation of total heat release during combustion, kJ
AA=0
for i=1:round(n_t_step);
   for j=1:nz;
      AA=AA+A(i,j);
   end;
end;

heat=AA*t_v/1000


End of program
```